



Minnesota State University, Mankato

## Cornerstone: A Collection of Scholarly and Creative Works for Minnesota State University, Mankato

---

All Graduate Theses, Dissertations, and Other  
Capstone Projects

Graduate Theses, Dissertations, and Other  
Capstone Projects


---

2014

### Thermal Conductivity of Alumina and Silica Nanofluids

Julian Bernal Castellanos  
*Minnesota State University - Mankato*

Follow this and additional works at: <https://cornerstone.lib.mnsu.edu/etds>

 Part of the [Heat Transfer, Combustion Commons](#), and the [Nanoscience and Nanotechnology Commons](#)

---

#### Recommended Citation

Castellanos, J. B. (2014). Thermal Conductivity of Alumina and Silica Nanofluids [Master's thesis, Minnesota State University, Mankato]. Cornerstone: A Collection of Scholarly and Creative Works for Minnesota State University, Mankato. <https://cornerstone.lib.mnsu.edu/etds/371/>

This Thesis is brought to you for free and open access by the Graduate Theses, Dissertations, and Other Capstone Projects at Cornerstone: A Collection of Scholarly and Creative Works for Minnesota State University, Mankato. It has been accepted for inclusion in All Graduate Theses, Dissertations, and Other Capstone Projects by an authorized administrator of Cornerstone: A Collection of Scholarly and Creative Works for Minnesota State University, Mankato.

Thermal Conductivity of Alumina and Silica Nanofluids

By

Julian G. Bernal Castellanos

A Thesis Submitted in Partial Fulfillment of the  
Requirements for the degree of  
Master of Science in Mechanical Engineering

Minnesota State University, Mankato

Mankato, Minnesota

August 2014

Thermal Conductivity of Alumina and Silica Nanofluids

Julian Bernal

This thesis has been examined and approved by the following members of the student's committee.

---

Dr. Patrick Tebbe

---

Dr. Aaron Budge

---

Dr. Sungwon Kim

## ACKNOWLEDGEMENTS

I would like to express my sincere appreciation to my advisor, Dr. Patrick Tebbe, for his expertise, guidance and constructive input. He has been an exemplary mentor and I thank him for his guidance and insight in my project.

I also thank Dr. Sungwon Kim, Dr. Aaron Budge and Dr. Namyong Lee for being part of my committee and giving me valuable advice on my project. I would like to also thank Mr. Kevin Schull and Dr. Steven Losh for providing me assistance with the equipment needed for this project. Finally, I would like to thank my family for their unconditional support.

## Table of Contents

Signature Page .....	ii
Acknowledgements.....	iii
Abstract .....	xviii
Chapter 1: Introduction .....	1
Chapter 2: Background and Literature Review .....	3
2.1 Nanoparticles .....	3
2.1.1 Types.....	3
2.1.2 Synthesis .....	4
2.1.3 Metal Oxide Nanoparticles .....	7
2.1.4 Al <sub>2</sub> O <sub>3</sub> Properties .....	8
2.1.5 SiO <sub>2</sub> Properties .....	11
2.2 Base Fluids.....	12
2.2.1 Ethylene Glycol .....	12
2.2.2 Water.....	14
2.3 Motion of nanoparticles .....	16
2.3.1 Gravity .....	16
2.3.2 Brownian Motion.....	18
2.3.3 Thermophoresis.....	20
2.4 Thermal Conductivity .....	21
2.5 Viscosity .....	24
2.6 Density and Specific Heat.....	27
2.7 Particle Size Effects .....	27

2.8 Sonication Effect.....	28
Chapter 3: Theory .....	30
3.1 Thermal Properties.....	30
3.2 Nanoparticle Motion .....	32
Chapter 4: Experimental Approach .....	36
4.1 Thermal Conductivity Measurements.....	36
4.2 Viscosity Measurements .....	40
4.3 Sample Preparation .....	41
Chapter 5: Results and Discussion.....	44
5.1 Base Fluid Effects .....	44
5.2 Nanoparticle Type and Size Effects.....	51
5.2.1 Thermophoresis and gravity forces in opposite directions .....	51
5.2.2 Thermophoresis and gravity forces in same directions.....	55
5.3 Motion of Nanoparticles .....	58
Chapter 6: Summary and Conclusion .....	63
6.1 Summary .....	63
6.2 Recommendations and Future Studies.....	64
References.....	65
Appendix A: Nomenclature .....	70
Appendix B: Figures of thermal conductivity results over time.....	72
Appendix C: Statistical Analysis .....	96
Appendix D: Base fluid data.....	97
Appendix E: Volumetric concentration and particle size data.....	102

## List of Figures

Figure 1. Gas condensation chamber schematic .....	5
Figure 2. Variation in thermal conductivity as temperature changes for common materials .....	23
Figure 3. Viscosity visualization.....	25
Figure 4. Rheological diagram example .....	25
Figure 5. TPS 500s set up .....	36
Figure 6. Sensor .....	37
Figure 7. Thermal conductivity measurement set up.....	38
Figure 8. Viscometer diagram.....	41
Figure 9. Sonifier diagram .....	42
Figure 10. Base fluid effect on thermal conductivity, water/ $\text{Al}_2\text{O}_3$ , 10 nm.....	46
Figure 11. Base fluid effect on thermal conductivity, EG/ $\text{Al}_2\text{O}_3$ , 10 nm .....	46
Figure 12. Base fluid effect on thermal conductivity, 75%EG-25% Water/ $\text{Al}_2\text{O}_3$ , 10 nm .....	47
Figure 13. Base fluid effect on thermal conductivity, 50%EG-50% Water/ $\text{Al}_2\text{O}_3$ , 10 nm .....	47
Figure 14. Base fluid effect on thermal conductivity, 25%EG-75% Water/ $\text{Al}_2\text{O}_3$ , 10 nm .....	48
Figure 15. Base fluid effect on viscosity, water/ $\text{Al}_2\text{O}_3$ , 10 nm.....	48
Figure 16. Base fluid effect on viscosity, EG/ $\text{Al}_2\text{O}_3$ , 10 nm .....	49
Figure 17. Base fluid effect on viscosity, 75%EG-25% Water/ $\text{Al}_2\text{O}_3$ , 10 nm.....	49
Figure 18. Base fluid effect on viscosity, 50%EG-50% Water/ $\text{Al}_2\text{O}_3$ , 10 nm.....	50

Figure 19. Base fluid effect on viscosity, 25% EG-75% Water/ $\text{Al}_2\text{O}_3$ , 10 nm.....	50
Figure 20. Thermal conductivity comparison, $\text{SiO}_2$ /Water, thermophoresis and gravity in opposite direction.....	52
Figure 21. Thermal conductivity comparison, $\text{Al}_2\text{O}_3$ /Water, thermophoresis and gravity in opposite direction.....	54
Figure 22. Thermal conductivity comparison between nanofluids, thermophoresis and gravity in opposite direction .....	54
Figure 23. Thermal conductivity comparison, $\text{SiO}_2$ /Water, thermophoresis and gravity in same directions.....	57
Figure 24. Thermal conductivity comparison, $\text{Al}_2\text{O}_3$ /Water, thermophoresis and gravity in same direction .....	58
Figure 25. Velocity diagram .....	60
Figure 26. $\text{Al}_2\text{O}_3$ /Water, 10 nm, 0.2% vol. concentration, thermophoresis and gravity in opposite directions .....	72
Figure 27. $\text{Al}_2\text{O}_3$ /Water, 10 nm, 0.2% vol. concentration, thermophoresis and gravity in same directions.....	72
Figure 28. $\text{Al}_2\text{O}_3$ /Water, 10 nm, 0.5% vol. concentration, thermophoresis and gravity in opposite directions .....	73
Figure 29. $\text{Al}_2\text{O}_3$ /Water, 10 nm, 0.5% vol. concentration, thermophoresis and gravity in same directions.....	73
Figure 30. $\text{Al}_2\text{O}_3$ /Water, 10 nm, 0.7% vol. concentration, thermophoresis and gravity in opposite directions .....	74



Figure 31. Al <sub>2</sub> O <sub>3</sub> /Water, 10 nm, 0.7% vol. concentration, thermophoresis and gravity in same directions.....	74
Figure 32. Al <sub>2</sub> O <sub>3</sub> /Water, 10 nm, 1% vol. concentration, thermophoresis and gravity in opposite directions .....	75
Figure 33. Al <sub>2</sub> O <sub>3</sub> /Water, 10 nm, 1% vol. concentration, thermophoresis and gravity in same directions.....	75
Figure 34. Al <sub>2</sub> O <sub>3</sub> /Water, 10 nm, 2% vol. concentration, thermophoresis and gravity in opposite directions .....	76
Figure 35. Al <sub>2</sub> O <sub>3</sub> /Water, 10 nm, 2% vol. concentration, thermophoresis and gravity in same directions.....	76
Figure 36. Al <sub>2</sub> O <sub>3</sub> /Water, 10 nm, 3% vol. concentration, thermophoresis and gravity in opposite directions .....	77
Figure 37. Al <sub>2</sub> O <sub>3</sub> /Water, 10 nm, 3% vol. concentration, thermophoresis and gravity in same directions.....	77
Figure 38. Al <sub>2</sub> O <sub>3</sub> /Water, 150 nm, 0.2% vol. concentration, thermophoresis and gravity in opposite directions .....	78
Figure 39. Al <sub>2</sub> O <sub>3</sub> /Water, 150 nm, 0.2% vol. concentration, thermophoresis and gravity in same directions.....	78
Figure 40. Al <sub>2</sub> O <sub>3</sub> /Water, 150 nm, 0.5% vol. concentration, thermophoresis and gravity in opposite directions .....	79
Figure 41. Al <sub>2</sub> O <sub>3</sub> /Water, 150 nm, 0.5% vol. concentration, thermophoresis and gravity in same directions.....	79

Figure 42. Al <sub>2</sub> O <sub>3</sub> /Water, 150 nm, 0.7% vol. concentration, thermophoresis and gravity in opposite directions .....	80
Figure 43. Al <sub>2</sub> O <sub>3</sub> /Water, 150 nm, 0.7% vol. concentration, thermophoresis and gravity in same directions.....	80
Figure 44. Al <sub>2</sub> O <sub>3</sub> /Water, 150 nm, 1% vol. concentration, thermophoresis and gravity in opposite directions .....	81
Figure 45. Al <sub>2</sub> O <sub>3</sub> /Water, 150 nm, 1% vol. concentration, thermophoresis and gravity in same directions.....	81
Figure 46. Al <sub>2</sub> O <sub>3</sub> /Water, 150 nm, 2% vol. concentration, thermophoresis and gravity in opposite directions .....	82
Figure 47. Al <sub>2</sub> O <sub>3</sub> /Water, 150 nm, 2% vol. concentration, thermophoresis and gravity in same directions.....	82
Figure 48. Al <sub>2</sub> O <sub>3</sub> /Water, 150 nm, 3% vol. concentration, thermophoresis and gravity in opposite directions .....	83
Figure 49. Al <sub>2</sub> O <sub>3</sub> /Water, 150 nm, 3% vol. concentration, thermophoresis and gravity in same directions.....	83
Figure 50. SiO <sub>2</sub> /Water, 15 nm, 0.2% vol. concentration, thermophoresis and gravity in opposite directions .....	84
Figure 51. SiO <sub>2</sub> /Water, 15 nm, 0.2% vol. concentration, thermophoresis and gravity in same directions.....	84
Figure 52. SiO <sub>2</sub> /Water, 15 nm, 0.5% vol. concentration, thermophoresis and gravity in opposite directions .....	85

Figure 53. SiO <sub>2</sub> /Water, 15 nm, 0.5% vol. concentration, thermophoresis and gravity in same directions.....	85
Figure 54. SiO <sub>2</sub> /Water, 15 nm, 0.7% vol. concentration, thermophoresis and gravity in opposite directions .....	86
Figure 55. SiO <sub>2</sub> /Water, 15 nm, 0.7% vol. concentration, thermophoresis and gravity in same directions.....	86
Figure 56. SiO <sub>2</sub> /Water, 15 nm, 1% vol. concentration, thermophoresis and gravity in opposite directions .....	87
Figure 57. SiO <sub>2</sub> /Water, 15 nm, 1% vol. concentration, thermophoresis and gravity in same directions.....	87
Figure 58. SiO <sub>2</sub> /Water, 15 nm, 2% vol. concentration, thermophoresis and gravity in opposite directions .....	88
Figure 59. SiO <sub>2</sub> /Water, 15 nm, 2% vol. concentration, thermophoresis and gravity in same directions.....	88
Figure 60. SiO <sub>2</sub> /Water, 15 nm, 3% vol. concentration, thermophoresis and gravity in opposite directions .....	89
Figure 61. SiO <sub>2</sub> /Water, 15 nm, 3% vol. concentration, thermophoresis and gravity in same directions.....	89
Figure 62. SiO <sub>2</sub> /Water, 80 nm, 0.2% vol. concentration, thermophoresis and gravity in opposite directions .....	90
Figure 63. SiO <sub>2</sub> /Water, 80 nm, 0.2% vol. concentration, thermophoresis and gravity in same directions.....	90

Figure 64. SiO <sub>2</sub> /Water, 80 nm, 0.5% vol. concentration, thermophoresis and gravity in opposite directions .....	91
Figure 65. SiO <sub>2</sub> /Water, 80 nm, 0.5% vol. concentration, thermophoresis and gravity in same directions.....	91
Figure 66. SiO <sub>2</sub> /Water, 80 nm, 0.7% vol. concentration, thermophoresis and gravity in opposite directions .....	92
Figure 67. SiO <sub>2</sub> /Water, 80 nm, 0.7% vol. concentration, thermophoresis and gravity in same directions.....	92
Figure 68. SiO <sub>2</sub> /Water, 80 nm, 1% vol. concentration, thermophoresis and gravity in opposite directions .....	93
Figure 69. SiO <sub>2</sub> /Water, 80 nm, 1% vol. concentration, thermophoresis and gravity in same directions.....	93
Figure 70. SiO <sub>2</sub> /Water, 80 nm, 2% vol. concentration, thermophoresis and gravity in opposite directions .....	94
Figure 71. SiO <sub>2</sub> /Water, 80 nm, 2% vol. concentration, thermophoresis and gravity in same directions.....	94
Figure 72. SiO <sub>2</sub> /Water, 80 nm, 3% vol. concentration, thermophoresis and gravity in opposite directions .....	95
Figure 73. SiO <sub>2</sub> /Water, 80 nm, 3% vol. concentration, thermophoresis and gravity in same directions.....	95

## **List of Tables**

Table 1. Engineering alumina grades A1 - A9 and their characteristics .....	9
Table 2. Typical values of thermal expansion coefficient, specific heat, enthalpy and thermal conductivity at room temperature .....	9
Table 3. Typical values of dielectric breakdown voltage, loss tangent, volumetric electrical resistivity and permittivity of engineering aluminas at room temperature .....	10
Table 4. Typical values of elastic properties at room temperature for engineering alumina ceramics according to porosity level .....	10
Table 5. Mechanical properties of engineering alumina ceramics at ambient temperature .....	11
Table 6. Physical properties of silica .....	12
Table 7. Physical properties of EG .....	13
Table 8. Thermodynamic constants for phase transition of water at 101.314 kPa pressure. ....	15
Table 9. Properties of liquid water as a function of temperature .....	15
Table 10. Density of water as a function of temperature .....	16
Table 11. Settling velocity. ....	61
Table 12. Brownian diffusion coefficient. ....	61
Table 13. Mass flux due to Brownian diffusion. ....	61
Table 14. Proportionality factor. ....	61
Table 15. Thermophoresis velocity.....	62
Table 16. Mass flux due to thermophoretic effects.....	62
Table 17. Diffusion times. ....	62

Table 18. Water/ $\text{Al}_2\text{O}_3$ , 10 nm, 0.1% vol. concentration.....	97
Table 19. Water/ $\text{Al}_2\text{O}_3$ , 10 nm, 1% vol. concentration.....	97
Table 20. Water/ $\text{Al}_2\text{O}_3$ , 10 nm, 10% vol. concentration.....	97
Table 21. EG/ $\text{Al}_2\text{O}_3$ , 10 nm, 0.1% vol. concentration. ....	98
Table 22. EG/ $\text{Al}_2\text{O}_3$ , 10 nm, 1% vol. concentration. ....	98
Table 23. EG/ $\text{Al}_2\text{O}_3$ , 10 nm, 10% vol. concentration. ....	98
Table 24. 75%EG-25% Water / $\text{Al}_2\text{O}_3$ , 10 nm, 0.1% vol. concentration. ....	99
Table 25. 75%EG-25% Water / $\text{Al}_2\text{O}_3$ , 10 nm, 1% vol. concentration. ....	99
Table 26. 75%EG-25% Water / $\text{Al}_2\text{O}_3$ , 10 nm, 10% vol. concentration. ....	99
Table 27. 50%EG-50% Water / $\text{Al}_2\text{O}_3$ , 10 nm, 0.1% vol. concentration. ....	100
Table 28. 50%EG-50% Water / $\text{Al}_2\text{O}_3$ , 10 nm, 1% vol. concentration. ....	100
Table 29. 50%EG-50% Water / $\text{Al}_2\text{O}_3$ , 10 nm, 10% vol. concentration. ....	100
Table 30. 25%EG-75% Water / $\text{Al}_2\text{O}_3$ , 10 nm, 0.1% vol. concentration. ....	101
Table 31. 25%EG-75% Water / $\text{Al}_2\text{O}_3$ , 10 nm, 1% vol. concentration. ....	101
Table 32. 25%EG-75% Water / $\text{Al}_2\text{O}_3$ , 10 nm, 10% vol. concentration. ....	101
Table 33. $\text{SiO}_2$ /Water, 80 nm, 0.2% vol. concentration, thermophoresis and gravity in same directions.....	102
Table 34. $\text{SiO}_2$ /Water, 80 nm, 0.5% vol. concentration, thermophoresis and gravity in same directions.....	102
Table 35. $\text{SiO}_2$ /Water, 80 nm, 0.7% vol. concentration, thermophoresis and gravity in same directions.....	103
Table 36. $\text{SiO}_2$ /Water, 80 nm, 1% vol. concentration, thermophoresis and gravity in same directions.....	103

Table 37. SiO <sub>2</sub> /Water, 80 nm, 2% vol. concentration, thermophoresis and gravity in same directions.....	104
Table 38. SiO <sub>2</sub> /Water, 80 nm, 3% vol. concentration, thermophoresis and gravity in same directions.....	104
Table 39. SiO <sub>2</sub> /Water, 15 nm, 0.2% vol. concentration, thermophoresis and gravity in same directions.....	105
Table 40. SiO <sub>2</sub> /Water, 15 nm, 0.5% vol. concentration, thermophoresis and gravity in same directions.....	105
Table 41. SiO <sub>2</sub> /Water, 15 nm, 0.7% vol. concentration, thermophoresis and gravity in same directions.....	106
Table 42. SiO <sub>2</sub> /Water, 15 nm, 1% vol. concentration, thermophoresis and gravity in same directions.....	106
Table 43. SiO <sub>2</sub> /Water, 15 nm, 2% vol. concentration, thermophoresis and gravity in same directions.....	107
Table 44. SiO <sub>2</sub> /Water, 15 nm, 3% vol. concentration, thermophoresis and gravity in same directions.....	107
Table 45. Al <sub>2</sub> O <sub>3</sub> /Water, 150 nm, 0.2% vol. concentration, thermophoresis and gravity in same directions.....	108
Table 46. Al <sub>2</sub> O <sub>3</sub> /Water, 150 nm, 0.5% vol. concentration, thermophoresis and gravity in same directions.....	108
Table 47. Al <sub>2</sub> O <sub>3</sub> /Water, 150 nm, 0.7% vol. concentration, thermophoresis and gravity in same directions.....	109

Table 48. Al <sub>2</sub> O <sub>3</sub> /Water, 150 nm, 1% vol. concentration, thermophoresis and gravity in same directions.....	109
Table 49. Al <sub>2</sub> O <sub>3</sub> /Water, 150 nm, 2% vol. concentration, thermophoresis and gravity in same directions.....	110
Table 50. Al <sub>2</sub> O <sub>3</sub> /Water, 150 nm, 3% vol. concentration, thermophoresis and gravity in same directions.....	110
Table 51. Al <sub>2</sub> O <sub>3</sub> /Water, 10 nm, 0.2% vol. concentration, thermophoresis and gravity in same directions.....	111
Table 52. Al <sub>2</sub> O <sub>3</sub> /Water, 10 nm, 0.5% vol. concentration, thermophoresis and gravity in same directions.....	111
Table 53. Al <sub>2</sub> O <sub>3</sub> /Water, 10 nm, 0.7% vol. concentration, thermophoresis and gravity in same directions.....	112
Table 54. Al <sub>2</sub> O <sub>3</sub> /Water, 10 nm, 1% vol. concentration, thermophoresis and gravity in same directions.....	112
Table 55. Al <sub>2</sub> O <sub>3</sub> /Water, 10 nm, 2% vol. concentration, thermophoresis and gravity in same directions.....	113
Table 56. Al <sub>2</sub> O <sub>3</sub> /Water, 10 nm, 3% vol. concentration, thermophoresis and gravity in same directions.....	113
Table 57. SiO <sub>2</sub> /Water, 15 nm, 0.2% vol. concentration, thermophoresis and gravity in opposite directions. ....	114
Table 58. SiO <sub>2</sub> /Water, 15 nm, 0.5% vol. concentration, thermophoresis and gravity in opposite directions. ....	114



Table 59. SiO <sub>2</sub> /Water, 15 nm, 0.7% vol. concentration, thermophoresis and gravity in opposite directions. ....	115
Table 60. SiO <sub>2</sub> /Water, 15 nm, 1% vol. concentration, thermophoresis and gravity in opposite directions. ....	115
Table 61. SiO <sub>2</sub> /Water, 15 nm, 2% vol. concentration, thermophoresis and gravity in opposite directions. ....	116
Table 62. SiO <sub>2</sub> /Water, 15 nm, 3% vol. concentration, thermophoresis and gravity in opposite directions. ....	116
Table 63. Al <sub>2</sub> O <sub>3</sub> /Water, 150 nm, 0.2% vol. concentration, thermophoresis and gravity in opposite directions. ....	117
Table 64. Al <sub>2</sub> O <sub>3</sub> /Water, 150 nm, 0.5% vol. concentration, thermophoresis and gravity in opposite directions. ....	117
Table 65. Al <sub>2</sub> O <sub>3</sub> /Water, 150 nm, 0.7% vol. concentration, thermophoresis and gravity in opposite directions. ....	118
Table 66. Al <sub>2</sub> O <sub>3</sub> /Water, 150 nm, 1% vol. concentration, thermophoresis and gravity in opposite directions. ....	118
Table 67. Al <sub>2</sub> O <sub>3</sub> /Water, 150 nm, 2% vol. concentration, thermophoresis and gravity in opposite directions. ....	119
Table 68. Al <sub>2</sub> O <sub>3</sub> /Water, 150 nm, 3% vol. concentration, thermophoresis and gravity in opposite directions. ....	119
Table 69. Al <sub>2</sub> O <sub>3</sub> /Water, 10 nm, 0.2% vol. concentration, thermophoresis and gravity in opposite directions. ....	120

Table 70. Al <sub>2</sub> O <sub>3</sub> /Water, 10 nm, 0.5% vol. concentration, thermophoresis and gravity in opposite directions. ....	120
Table 71. Al <sub>2</sub> O <sub>3</sub> /Water, 10 nm, 0.7% vol. concentration, thermophoresis and gravity in opposite directions. ....	121
Table 72. Al <sub>2</sub> O <sub>3</sub> /Water, 10 nm, 1% vol. concentration, thermophoresis and gravity in opposite directions. ....	121
Table 73. Al <sub>2</sub> O <sub>3</sub> /Water, 10 nm, 2% vol. concentration, thermophoresis and gravity in opposite directions. ....	122
Table 74. Al <sub>2</sub> O <sub>3</sub> /Water, 10 nm, 3% vol. concentration, thermophoresis and gravity in opposite directions. ....	122
Table 75. SiO <sub>2</sub> /Water, 80 nm, 0.2% vol. concentration, thermophoresis and gravity in opposite directions. ....	123
Table 76. SiO <sub>2</sub> /Water, 80 nm, 0.5% vol. concentration, thermophoresis and gravity in opposite directions. ....	123
Table 77. SiO <sub>2</sub> /Water, 80 nm, 0.7% vol. concentration, thermophoresis and gravity in opposite directions. ....	124
Table 78. SiO <sub>2</sub> /Water, 80 nm, 1% vol. concentration, thermophoresis and gravity in opposite directions. ....	124
Table 79. SiO <sub>2</sub> /Water, 80 nm, 2% vol. concentration, thermophoresis and gravity in opposite directions. ....	125
Table 80. SiO <sub>2</sub> /Water, 80 nm, 3% vol. concentration, thermophoresis and gravity in opposite directions. ....	125

## ABSTRACT

Title of Thesis: Thermal Conductivity of Alumina and Silica Nanofluids

Degree candidate: Julian G. Bernal Castellanos

Degree: Master of Science in Mechanical Engineering.

Minnesota State University, Mankato. Mankato, MN. 2014.

This thesis studies the effects of the base fluid, particle type/size, and volumetric concentration on the thermal conductivity of Alumina and Silica nanofluids. The effects of base fluid were observed by preparing samples using ethylene glycol (EG), water, and mixtures of EG/water as the base fluid and  $\text{Al}_2\text{O}_3$  (10 nm) nanoparticles. The particles type/size and volumetric concentration effects were tested by preparing samples of nanofluids using  $\text{Al}_2\text{O}_3$  (10nm),  $\text{Al}_2\text{O}_3$  (150nm),  $\text{SiO}_2$  (15 nm), and  $\text{SiO}_2$  (80 nm) nanoparticles and ionized water as base fluid at different volumetric concentrations. All samples were mixed using a sonicator for 30 minutes and a water circulator to maintain the sample at room temperature. The thermal conductivity was measured using a Thermtest Transient Plane Source TPS 500S. The effects of gravity, Brownian motion and thermophoresis were also studied. EG produced the highest thermal conductivity enhancement out of all base fluids tested. Smaller particle size produced a higher enhancement of thermal conductivity, while the volumetric concentration did not have a significant effect in the thermal conductivity enhancement. Finally, gravity, Brownian diffusion and thermophoresis effects played a role in the total enhancement of the thermal conductivity. The nanoparticles were observed to settle rapidly after sonication suggesting gravity effects may play a significant role.

## **Chapter 1**

### **Introduction**

The use of nanoparticles to enhance the thermal properties of fluids has become an increasing area of interest among researchers across the world. When nanoparticles are introduced into a base fluid, creating a nanofluid, they are believed to affect the thermal properties of such fluid. Nanofluids are potentially important to applications like automobile transmission, drilling fluids, HVAC, and others if an economical and effective alternative of using them is developed. Extensive research on this area shows that nanoparticles do affect some of the thermal properties of the fluid; although it is not clear how significant these effects are since there are contradictory experimental results. These properties include thermal conductivity, density, viscosity, and specific heat. It is observed that thermal conductivity and density affect the heat transfer coefficient of the fluid positively, while viscosity and specific heat have a negative effect. Therefore, the best combination of nanoparticle and base fluid must be selected in order to obtain the optimal thermo physical properties for a desired application. An optimization process is necessary to make nanofluids capable of improving the performance and reduce cost of current applications.

This research studied the effects of the base fluid, particle size, and volumetric concentration on the thermal conductivity of selected nanofluids. Aluminum oxide and silica nanoparticles mixed on ethylene glycol (EG) and water were used; these nanoparticles were selected because of their promising potential found in previous studies, good physical properties, and their relative low price. In order to study the effects of the base fluid, five different base fluids were tested: water, EG, 75%EG-25%water,

50%EG-50%water, and 25%EG-75%water. Each base fluid is mixed with Aluminum Oxide nanoparticles with a particle size of 10 nm at 3 different volumetric concentrations: 0.1%, 1%, and 10%. Six samples were prepared for each base fluid at every volumetric concentration. The thermal conductivity of every sample was then measured using a Thermtest Transient Plane Source TPS 500S instrument at room temperature. To study the particles size and volumetric concentration, four different nanoparticles were used:  $\text{Al}_2\text{O}_3$  (10 nm),  $\text{Al}_2\text{O}_3$  (150 nm),  $\text{SiO}_2$  (15 nm), and  $\text{SiO}_2$  (80 nm). Each nanoparticle was mixed with ionized water at volumetric concentration of 0.2%, 0.5%, 0.7%, 1%, 2%, and 3%. The thermal conductivity was measured with the thermophoretic force in the same and opposite direction of gravity using the TPS 500s at room temperature. Measurements were taken every minute for a certain amount of time for each sample. Finally, the effects of gravity, Brownian motion, and thermophoresis were analyzed.

## **Chapter 2**

### **Background and Literature Review**

#### **2.1 Nanoparticles**

##### **2.1.1 Types**

Particles with a diameter of 1 to 100 nanometers are considered nanoparticles, regardless of the material. Nanoparticles can be metals, alloys, semiconductors, ceramics, glasses, polymers, and inorganics carbon-based materials [1]. Ceramics are a mixture of metallic and nonmetallic elements. Examples include aluminum oxides ( $\text{Al}_2\text{O}_3$ ), titania ( $\text{TiO}_2$ ), zirconia ( $\text{ZrO}_2$ ), silica ( $\text{SiO}_2$ ), sodium oxide ( $\text{Na}_2\text{O}$ ) as well as metal carbides (silicon carbide ( $\text{SiC}$ ), titanium carbide ( $\text{TIC}$ ), boron carbide ( $\text{BC}$ )), nitrides (silicon nitride ( $\text{Si}_3\text{N}_4$ ), titanium nitride ( $\text{TiN}$ ), boron nitride( $\text{BN}$ )), and borides (titanium boride ( $\text{TiB}_2$ )) [1]. Properties used to classify ceramics include hardness, temperature resistance, compression resistance, and strength. Ceramics display brittleness and they can easily fracture under tensile, shear, or impact stresses [1]. Nanoparticles made out of ceramic materials are commonly used as catalysts, photoconductors, and template materials. Metals have unique characteristics like high electrical conductivity, thermal conductivity, tensile strength, high modulus of elasticity, and toughness that make them highly desirable in many industries [1]. Often, metals are mixed with ceramics to create high-performance composite materials. Semiconductors include silicon, oxides, and other complex semiconductors like copper-indium-gallium-selenide (CIGS) [1]. Nanoparticles made out of semiconductors are widely used on the computer industry, electronics, optical applications, and the next generation of solar cells [1]. Polymers are lightweight materials and they are widely popular in many industries. Polymers can be separated in three different classes: thermosets (polyurethanes, phenolic resins, epoxy resins,

polyesters, and vinyl esters), thermoplastics (polyethylene, nylon, ABS, PI, PP, PC, and PEEK), and elastomers (silicones and EPDM) [1]. Polymers have high strength-to-mass ratio and are easy to fabricate; however, they have long-term instability under loads. Inorganics carbon-based materials include graphite, carbon blacks, fullerenes, carbon nanotubes, and diamondoids [1].

### **2.1.2 Synthesis**

Particle size, shape, crystal structure and crystallinity are key characteristics for the study of nanoparticles. In order to have control over these properties the synthesis of nanoparticles must be done carefully. The synthesis of nanoparticles is commonly categorized into two broad techniques: physical methods and chemical methods [2].

Several physical methods are employed for the synthesis of nanoparticles depending on the application and industry. The most popular physical method is the inert-gas evaporation technique used for the synthesis of single-phase metals and ceramic oxides [3]. This method involves the evaporation of a desired material, like a single metal or a compound, in a gas at low pressure, usually less than 1atm, inside a gas condensation chamber, Fig. 1.

Once the evaporated material is inserted in the chamber, the atoms or molecules strike gas atoms or molecules making them undergo a homogenous condensation to form atom clusters. These collisions take place near a cold-powder collection surface. Once the clusters are formed, they are removed from the chamber by natural convection of the gas or by force gas flow. The cluster must be removed from the chamber as soon as they are formed in order to avoid aggregation and coalescence [2]. Another physical method is the sputtering technique, in which an accelerated and highly focused beam of inert gas,

usually argon or helium, is aimed at the desired material in order to eject the atoms or clusters [2]. Another popular method involves mechanical deformation of the desired material. In this method nanoparticles are synthesized by the application of high mechanical energy, like high-energy ball mill or a high energy shear process, to degrade the coarser-grain structures into an ultrafine powder [2].

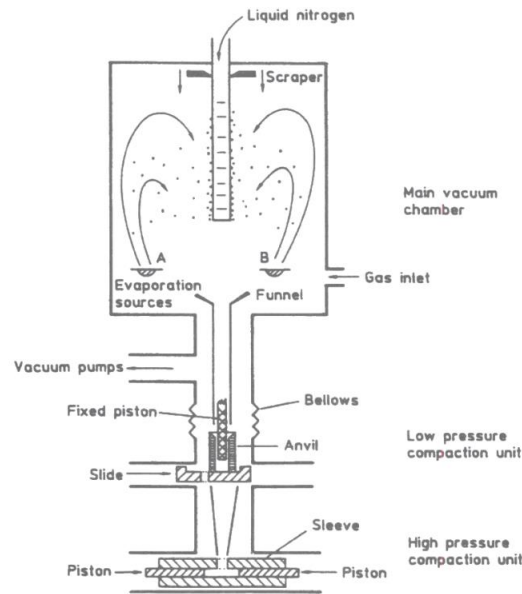


**Figure 1.** Gas condensation chamber schematic [2].

Chemical synthesis of metals and intermetallics can be categorized into two broad groups: thermal and ultrasound decomposition methods and reduction methods [2]. Thermal and ultrasound decomposition methods consist on the decomposition of organometallics precursors to yield the desired elements or alloys [2]. Reduction methods consist in the reduction of inorganic materials, like salts, by reducing agents. For the production of nanoparticles, inorganic salts are decomposed using several types of



reducing agents to produce fine metal particles. Common reducing agents used for the production of nanoparticles include  $\text{NaBEt}_3\text{H}$ ,  $\text{LiBEt}_3\text{H}$ , and  $\text{NaBH}_4$  [2].

The chemical synthesis of semiconductors is often done by preparing clusters in the form of dispersed colloids or that can be contained and stabilized inside colloids/micelles, polymers, zeolites, or glasses [2]. Generally the chemical synthesis of semiconductors is grouped depending of the material in which the semiconductors are created. When colloids/micells are employed, the use of an agent that can bind to the cluster surface is required to guarantee stabilization of the colloid in the small-cluster size regime and, therefore, prevent uncontrolled growth into larger particles [2]. Major drawbacks of using colloids/micells are irreproducibility and colloidal instability [2]. These problems can be minimized by using polymers as a matrix for semiconductors. An advantage of using polymers is that the size of the clusters can be adjusted precisely by controlling the phase-separated hydrophilic and hydrophobic regions of the polymer [2] [4]. The main advantage of chemical techniques for the synthesis of nanoparticles is the chemical homogeneity of the final product, which often is the most important characteristic; however, these methods can also be complex, produce agglomeration, and the byproducts may be hazardous.

Sol-gel is another method for the synthesis of nanocomposites materials. Typically this method is used for the fabrication of metal oxides via hydrolysis and condensation methods. The metal oxides are prepared by the hydrolysis of precursors, usually alcoxides in alcoholic solution, which result in the corresponding oxo-hydroxide [2]. Then metal hydroxide is produced by condensation. After appropriate drying and calcinations, ultrafine porous oxides are formed [5]. This method is popular because the

gel products often have the ideal properties for the desired application, the conversions occur readily with a wide variety of precursors, and it can be conducted at near room temperature [2].

### 2.1.3 Metal Oxide Nanoparticles

Oxide nanoparticles are used in a large number of applications such as sensors, fuel cells, circuits, and more. J.A. Rodriguez and M. Fernandez-Garcia presented a detailed summary of metal oxide nanoparticles [5]. A key point that was addressed on this study is that metal oxide nanoparticles exhibit unique physical properties due to their limited size and a high density of corner or edge surface sites [5].

The mechanical properties of interest when studying oxide nanoparticles usually include yield stress, hardness, and superplasticity. Typically, the yield stress ( $\sigma$ ) and hardness(H) follows the Hall-Petch (H-P) equation:

$$\sigma/H = \frac{\sigma_0}{H_0} + k_h d^{-1/2} \quad (1)$$

where  $d$  is the particle size and  $k_h$  is the corresponding slope. The particle boundaries act as obstacles for slip transfer or dislocations. When the particle size decreases so does the H-P slope; however, once the particles reach a size of a few nanometers this dislocation mechanism stops and a reversal H-P mechanism would be more dominant [6] [7] [8]. Additionally, these mechanical properties are also strain-rate dependent. It is observed that with decreasing particle size at room temperature, the strain rate sensitivity is enhanced for  $\text{TiO}_2$  and  $\text{ZrO}_2$ . Superplasticity is the capacity of oxides to undergo tensile deformation without necking or fracture [5] and it is defined as:

$$\varepsilon = A \frac{DGb}{kT} \left(\frac{b}{d}\right)^P \left(\frac{\sigma}{G}\right)^n \quad (2)$$

where  $\varepsilon$  is the strain rate,  $D$  is the diffusion coefficient,  $G$  is the shear modulus,  $b$  is the Burger's vector,  $\sigma$  is the yield strength, and  $p/n$  the particles size and yield strength exponents. This equation implies an increase in the superplasticity rate as the particle size decreases at a constant temperature. However, studies on  $ZrO_2$  and  $TiO_2$  have shown that nanocrystalline oxides do not have exhibit increment of ductibility compared to the bulk materials at room temperatures [5].

#### **2.1.4 $Al_2O_3$ Properties**

Alumina ( $Al_2O_3$ ) is a white oxide with a total of seven phases, although only four are usually used in industrial processes: alpha ( $\alpha$ ), delta ( $\delta$ ), theta ( $\theta$ ), and gamma ( $\gamma$ ). The  $\gamma$ -  $Al_2O_3$  is the most commonly obtained phase using synthetic methods. When the temperature of the gamma phase is increased, it suffers a complex phase excursion in reaching the alpha phase. The delta phase is observed at a temperature between 973-1273 K which then evolves into the theta phase and finally yields the alpha phase at temperatures between 1273 – 1373 K. During the  $\gamma$ -  $\delta$ -  $\theta$  transformation aluminum atoms migrate while oxygen atoms remain essentially fixed [5] [9]. The  $\alpha$  phase is reached by a nucleation growth mechanism which is achieved by reordering the anion packing from a cubic structure to a hexagonal structure [5] [10] [11] [12]. The temperature for the  $\theta$ -  $\alpha$  transformation is dependent of the size and presence of impurities or surface stabilizers [5] [13] [14].

**Table 1.** Engineering alumina grades A1 - A9 and their characteristics [15].

<b>Grade</b>	<b>Al<sub>2</sub>O<sub>3</sub> min %</b>	<b>Porosity %</b>	<b>Density g/cm<sup>3</sup></b>
<b>A1</b>	99.6	0.2-3	3.75 - 3.95
<b>A2</b>	99.8	<1	3.97 - 3.99
<b>A3</b>	99.5	<1	3.90 - 3.99
<b>A4</b>	99.6	3 - 6	3.75 - 3.85
<b>A5</b>	99	1 - 5	3.76 - 3.94
<b>A6</b>	96.5-99.0	1 - 5	3.71 - 3.92
<b>A7</b>	94.5-96.5	2 - 5	3.60 - 3.90
<b>A8</b>	86.0-94.5	2 - 5	3.40 - 3.90
<b>A9</b>	80.0-86.0	3 - 6	3.30 - 3.60

**Table 2.** Typical values of thermal expansion coefficient, specific heat, enthalpy and thermal conductivity at room temperature [15].

<b>Grade</b>	<b>Thermal expansion coefficient 10<sup>-6</sup> m/m K</b>	<b>Specific heat J/gK</b>	<b>Enthalpy from 25°C J/g</b>	<b>Thermal Conductivity W/mK</b>
<b>A1</b>	5.4	0.775	0	30 - 40
<b>A2</b>	5.4	0.775	0	30 - 40
<b>A3</b>	5.4	0.775	0	30 - 40
<b>A4</b>	5.4	0.775	0	25 - 35
<b>A5</b>	5.4	0.780	0	30 - 40
<b>A6</b>	5.1 - 5.4	0.780	0	25 - 30
<b>A7</b>	5.1 - 5.4	0.760 - 0.780	0	20 - 30
<b>A8</b>	4.9 - 5.5	0.755 - 0.785	0	15 - 20
<b>A9</b>	4.5 - 5.5	0.750 - 0.785	0	15 - 20

**Table 3.** Typical values of dielectric breakdown voltage, loss tangent, volumetric electrical resistivity and permittivity of engineering aluminas at room temperature [15].

Grade	Breakdown voltage gradient (9ac), kV/mm at thickness of 0.3 mm 5 mm		Loss tangent $\tan \delta$	Volumetric resistivity $\Omega\text{m}$	Relative permittivity $k'$
A1 - A4	~30	10 - 15	$10^{-4} - 10^{-3}$	$10^{-14} - 10^{-16}$	9 - 10
A5 -A6	25 - 35	10	$3 \cdot 10^{-5} - 10^{-3}$	$10^{-14} - 10^{-16}$	8.4 - 10.5
A7	~25	10	$10^{-4} - 10^{-2}$	$10^{-14} - 10^{-16}$	8.6 - 10.1
A8 - A9	27 - 30	8 - 12	$10^{-4} - 10^{-2}$	$10^{-13} - 10^{-16}$	7.1 - 10.0

**Table 4.** Typical values of elastic properties at room temperature for engineering alumina ceramics according to porosity level [15].

Grade	Al <sub>2</sub> O <sub>3</sub> /Porosity %	Young's modulus Gpa	Shear modulus Gpa	Poisson's ratio
A1	$\geq 99.6 / 0 - 2$	140 - 380	164 - 150	0.27 - 0.24
A2	$\geq 99.8 / < 1$	405 - 380	164 - 161	0.25 - 0.22
A3	$\geq 99.5 / < 1$	400 - 398	163- 161	0.26 - 0.23
A4	$\geq 99.6 / 3 - 6$	380 - 340	150 - 140	0.26 - 0.24
A5	$\geq 99.0 / 1 - 5$	380 - 340	145 - 130	0.26 - 0.24
A6	96.5 - 99.0 / 1 - 5	375 - 340	140 - 120	0.25 - 0.24
A7	94.5 - 96.5 / 1 - 5	370 - 300	140 - 110	0.25 - 0.23
A8	86.0 - 94.5 / 2 - 5	330 - 260	130 - 100	0.25 - 0.22
A9	80.0 - 86.0 / 3- 6	330 - 260	130 - 100	0.25 - 0.22

**Table 5.** Mechanical properties of engineering alumina ceramics at ambient temperature [15].

<b>Grade</b>	<b>Avg. flexural/ compressive strength MPa</b>	<b>Weibull modulus m</b>	<b>Fracture toughness MPa√m</b>	<b>Hardness HV1.0</b>
<b>A1</b>	210 - 500/ >4000	5 - 10	3.0 - 6.0	1500 - 2000
<b>A2</b>	150 - 450/ >4000	6 - 12	3.5 - 6.0	1500 - 1900
<b>A3</b>	300 - 600/ >3000	na	4.0 - 5.0	na
<b>A4</b>	150 - 450/ >4000	na	4.5 - 4.9	na
<b>A5</b>	150 - 500/ >4000	na	3.5 - 5.5	1300 - 1700
<b>A6</b>	150 - 450/ >3000	na	3.0 - 5.0	1200 - 1600
<b>A7</b>	180 - 360/ >3000	6 - 16	2.5 - 6.0	1200 - 1400
<b>A8</b>	150 - 350/ >2500	5 - 15	3.0 - 4.1	900 - 1200
<b>A9</b>	200 - 300/ >2000	na	2.5 - 3.5	800 - 1000

### 2.1.5 SiO<sub>2</sub> Properties

Silica (SiO<sub>2</sub>) is commonly found in crystalline state and very rarely in an amorphous state. Crystalline silica is grouped into three main forms: quartz, tridymite, and cristobalite [16]. Quartz is subdivided into two groups: alpha for temperatures of <573 °C and beta for temperatures of >573 °C. Tridymite is formed at 870 °C and cristobalite is formed at 1470 °C. Silica has good electrical insulation, high thermal stability and good abrasion resistance. It is insoluble in all acids except hydrogen fluoride (HF) [16].

**Table 6.** Physical properties of silica [17].

<b>Mechanical</b>	<b>Unit of Measure</b>	<b>SI/Metric</b>	<b>(Imperial)</b>
Density	gm/cc (lb/ft <sup>3</sup> )	2.2	(137.4)
Porosity	% (%)	0	0
Color	-	clear	-
Flexural Strength	Mpa (lb/in <sup>2</sup> x10 <sup>3</sup> )	-	-
Elastic Modulus	Gpa (lb/in <sup>2</sup> x10 <sup>6</sup> )	73	(10.6)
Shear Modulus	Gpa (lb/in <sup>2</sup> x10 <sup>6</sup> )	31	(4.5)
Bulk Modulus	Gpa (lb/in <sup>2</sup> x10 <sup>6</sup> )	41	(6)
Poisson's Ratio	-	0.17	(0.17)
Compressive Strength	Mpa (lb/in <sup>2</sup> x10 <sup>3</sup> )	1108	(160.7)
Hardness	Kg/mm <sup>2</sup>	600	-
Fracture Toughness K <sub>ic</sub>	MPa•m <sup>1/2</sup>	-	-
Maximum Use Temperature (no load)	°C (°F)	1100	(2000)
<b>Thermal</b>			
Thermal Conductivity	W/m•°K (BTU•in/ft <sup>2</sup> •hr•°F)	1.38	(9.6)
Coefficient of Thermal Expansion	10 <sup>-6</sup> /°C (10 <sup>-6</sup> /°F)	0.55	(0.31)
Specific Heat	J/Kg•°K (BTU/lb•°F)	740	(0.18)

## 2.2 Base Fluid

### 2.2.1 Ethylene Glycol

Ethylene Glycol (EG) is part of the glycols group along with Diethylene Glycol and Triethylene Glycol. Ethylene glycols are dihydric alcohols composed of an aliphatic carbon chain with a hydroxyl group at both ends. The two hydroxyl groups make them highly soluble in water and with a tendency to absorb moisture from air [18] [19].

Ethylene glycols reactions are similar to monohydric alcohol reactions. Mono and diesters are produced by the reaction of organic acids with EG. By the same token, polybasic acids react with EG to form polyesters. Because of its two hydroxyl groups, EG can be used to produce mono and diethers as well. Some of the most important reactions to industrial applications include esters, ethers, and oxidation derivatives [18].

EG is clear, colorless, and odorless. The first person to prepare EG was Wurtz in 1859 by saponifying ethylene glycol diacetate with potassium hydroxide. The following year he used the hydration of ethylene oxide technique to prepare EG, a technique that turned into the basis of modern industrial production of EG [19]. Due to its chemical composition, EG can easily mix with many polar solvent like water, alcohols, glycol ethers, and more; however, it has low solubility in nonpolar solvents such as benzene, toluene, and chloroform. Table 7 shows some of the physical properties of the EG [19].

**Table 7.** Physical properties of EG.

Boiling point at 101.3 kPa	197.60°C
Freezing point	-13.00°C
Density at 20°C	1.1135 g/cm <sup>3</sup>
Refractive index, $n_D^{20}$	1.4318
Heat of vaporization at 101.3 kPa	52.24 kJ/mol
Heat of combustion	19.07 MJ/kg
Critical temperature	372 °C
Critical pressure	6515.73 kPa
Critical volume	0.186 L/mol
Flash point	111°C
Ignition temperature	410°C
Lower explosive limit	3.20 vol%
Upper explosive limit	53 vol%
Viscosity at 20°C	19.83 mPa.s
Cubic expansion coefficient at 20°C	$0.62 \times 10^{-3} \text{ K}^{-1}$



EG is commonly used as an automotive engine coolant due to its low volatility, water solubility, and freeze point characteristics [19]. EG based coolants are popular because they protect during summer, prevent freeze in winter and they don't affect finishes, rubber parts, gaskets or other engine components [19]. Additionally, aqueous EG used in closed loop systems acts as an effective heat transfer, useful for the removal of ice/snow from highways and sidewalks. This is achieved by circulating a heated EG solution through coils placed under the surface. Similarly, EG based solutions are used for the removal of ice/snow from fuselages. This is done by spraying the surface to be cleaned with the solution. Some of the advantages of using EG based products include their stability in long-term storage, noncorrosiveness, high flash point, and ease of application. Other applications of glycols include: conditioning agents in adhesive, manufacturing of polyester fibers, natural gas dehydration, emulsifiers for creams and ointments, and more.

### **2.2.2 Water**

Water is the most abundant liquid on earth [20]. It is odorless, tasteless, and transparent. Water is a compound consisting of two hydrogen atoms covalently bonded to a single oxygen atom ( $\text{H}_2\text{O}$ ). It can exist as gas, liquid, or solid depending on the temperature and pressure. Table 8 shows the thermodynamic constant for phase transition of pure water [20].

Liquid water contains three different molecule populations. Single molecules are typical at high temperatures resulting in little hydrogen bonding due to the high thermal energy of the molecules. There is more hydrogen bonding forming in the middle range of temperatures where clusters of molecules start forming. At lower temperatures clusters

also form, below 15 °C these clusters are the most common arrangement [20]. The average kinetic of molecules increases as temperature increases affecting the physical properties of water. Table 9 shows typical physical properties of water for a temperature range of 0 °C - 100 °C.

**Table 8. Thermodynamic constants for phase transition of water at 101.314 kPa pressure [20].**

Temperature K	Fusion (melting)	Vaporization	
	273.15	Boiling	Sublimation
$\Delta H \text{ kJ mol}^{-1}$	6.01	40.66	51.06
$\Delta S \text{ J mol}^{-1}\text{K}^{-1}$	22	108.95	186.92
$\Delta E \text{ kJ mol}^{-1}$	6.01	37.61	48.97
$\Delta V \text{ L mol}^{-1}$	-1.621	30.1	-
Energy change of phase transition: $\Delta H$ , enthalpy; $\Delta S$ , entropy; $\Delta E$ , internal energy. $\Delta V$ : volume change of phase transition.			

**Table 9. Properties of liquid water as a function of temperature [20].**

Temperature (°C)	Heat Capacity ( $\text{J g}^{-1} \text{K}^{-1}$ )	Viscosity (mPa s)	Thermal conductance ( $\text{W K}^{-1}\text{m}^{-1}$ )	Dielectric constant	surface tension ( $\text{mN m}^{-1}$ )
0	4.2176	1.793	561	87.9	75.64
10	4.1921	1.307	580	83.96	74.23
20	4.1818	1.002	598.4	80.2	72.75
30	4.1784	0.797	615.4	76.6	71.2
40	4.1785	0.653	630.5	73.17	69.6
50	4.1806	0.547	643.5	69.88	67.94
60	4.1843	0.466	654.3	66.73	66.24
70	4.1895	0.404	663.1	63.73	64.47
80	4.1963	0.354	670	60.86	62.67
90	4.205	0.315	675.3	58.12	60.82
100	4.2159	0.282	679.1	55.51	58.91

Water possesses the largest heat capacity per unit mass of all substances. This characteristic makes water an excellent reservoir and transporter of energy [20]. The

viscosity of water changes significantly as temperature increases, it decreases from 1.793 to 0.282 cps as temperature increases from 0 °C - 100 °C. This makes the flow rate of water inside a pipe increase as the temperature increases. The density of water also varies according to temperature and it is shown in Table 10.

**Table 10. Density of water as a function of temperature [21].**

Temperature (°C)	Density (g/mL)	Temperature (°C)	Density (g/mL)
4	1	18	0.99862
5	0.99999	19	0.99843
6	0.99994	20	0.99823
7	0.99989	21	0.99801
8	0.99983	22	0.99779
9	0.99978	23	0.99756
10	0.99973	24	0.99732
11	0.99961	25	0.99707
12	0.99949	26	0.9968
13	0.99937	27	0.99653
14	0.99925	28	0.99625
15	0.99913	29	0.99596
16	0.99896	30	0.99567
17	0.99979	31	0.99536

## 2.3 Motion of Nanoparticles

Nanoparticles can develop a motion with respect of the base fluid by several mechanisms. Some of these mechanisms include gravity, Brownian diffusion and thermophoresis.

### 2.3.1 Gravity

The effect of gravity on nanoparticles is obtained through the understanding of the principles of uniform particle motion. Steady, straight-line motion is a very common type of particle motion and it is the result of external forces and the resistance that particles experience when passing through a fluid [67]. Originally, the force resisting the motion

of a sphere passing through a gas was described by Newton. Newton used the example of a cannonball travelling through air to derive what is now known as Newton's Resistance Law [67]. He realized that as the ball is traveling, air has to be pushed aside to let the ball pass through. The acceleration from the air being pushed is what produced the resistance force experienced by the ball. The volume of the gas being pushed aside equals the projected area of the sphere times its velocity. The mass of the gas is given as [67]:

$$\dot{m} = \rho_g \frac{\pi}{4} d^2 V \quad (3)$$

The acceleration of air being push is proportional to the relative velocity between the sphere and the air and is expressed as [67]:

$$\dot{m} V = \rho_g \frac{\pi}{4} d^2 V^2 \quad (4)$$

Eq. 4 describes the rate of change in momentum, which by definition is equal to the force required to move the sphere through the air, drag force given by [67]:

$$F_D = k_c \rho_g \frac{\pi}{4} d^2 V^2 \quad (5)$$

In eq. 5,  $k_c$  is a constant of proportionality that Newton thought was independent of velocity for a particular shape. This equation only applies when the Reynolds number is greater than 1000 where the viscous effects of the gas can be neglected compared with the inertial effects [67]. A more general form of this equation is obtained by replacing  $k_c$  with the coefficient of drag,  $C_D$ . This form is considered the general form of Newton's resistance equation in which the coefficient of drag remains constant for spheres having a Reynolds number greater than 1000 but changes value for spheres with a Reynolds number smaller than 1000[67]. Since eq. 5 only applies to particle motion where the

inertial effects are much greater than the viscous effects, Stokes derived an expression for particle motion where the inertial effects of the gas could be neglected compared with the viscous effects. This was done in order to examine small particles with a low Reynolds number and laminar flow, a condition in which most nanoparticle motion fall under.

### **2.3.2 Brownian Motion**

Brownian motion was first observed in 1827 by Robert Brown, a botanist, when he noticed a continuous wiggling motion of pollen grains in water [67]. Five decades later, a similar behavior was observed in smoke particles in air. This time a connection between the smoke particles' motion and the kinetic theory of gases was made. Years later, in the early 1900s, Einstein derived the relationships characterizing Brownian motion. Thermal diffusion along with convection are the main transport and deposition mechanisms for particles with a diameter of less than 0.1  $\mu\text{m}$  in diameter [67].

Brownian motion is the motion of particles suspended in a fluid. This motion is attributed to fluctuating forces that are the results of collisions with molecules of the fluid [67]. Diffusion of particles is the net transport of the particles in a concentration gradient. This transport occurs when a system is not in equilibrium and random molecular motion causes the system to become uniform. The transport always occurs from a higher concentration region to a lower concentration region. Both Brownian motion and diffusion are characterized by the particle diffusion coefficient ( $D$ ) [67]. This coefficient is a constant of proportionality relating the flux ( $J$ ) of the particles to the concentration gradient ( $dn/dx$ ). This relationship is known as Fick's first law of diffusion, eq. 6. As  $D$

increases, Brownian motion becomes more vigorous and the mass transfer in a concentration gradient is faster [67].

$$J = -D \frac{dn}{dx} \quad (6)$$

The diffusion coefficient can also be expressed in term of particle properties by the Stoke-Einstein derivation. In this case, the diffusion force on the particles is equal to the force exerted by the fluid resisting the motion of the particles. This is given by [67]:

$$\text{diffusion force} = F_{diff} = \frac{3\pi\eta V d}{C_c} \quad (7)$$

where  $C_c$  is the Cunningham correction factor. The key conclusions shown by Einstein in 1905 were: kinetic energy of a particle undergoing Brownian motion is the same as that of the fluid molecules it is suspended in and diffusion force on a particle is the net osmotic pressure force on that particle [67].

Van't Hoff's law describes the osmotic pressure for  $n$  suspended particles per unit volume as:

$$p_o = k_B T n \quad (8)$$

where  $k_B$  is the Boltzmann's constant and  $T$  is the absolute temperature. Imagine a cylinder containing a fluid with particles in it. Assuming a higher concentration region is located in the left of the cylinder and a lower concentration region is on the right, the diffusion of particles takes place from left to right. A very thin cross sectional layer is formed at some point across the length of the cylinder where the osmotic pressure differs slightly at the two surfaces of the layer. This difference is the net osmotic pressure that

creates the diffusion force pushing the particles through the thin layer. Considering only a unit cross-sectional area of the two surfaces of the layer, the volume of the fluid contained within the layer is equal to its thickness  $dx$ , and the number of particles in that volume is  $n dx$ . The diffusion force acting on an individual particle can then be given by [67]:

$$F_{diff} = -\frac{k_B T}{n} \frac{dn}{dx} \quad (9)$$

as mentioned before, the diffusion force on the particles is equal to the force exerted by the fluid resisting the motion of the particles. Substituting eq. 7 into eq. 9 gives:

$$nV = -\frac{k_B T C_c}{3\pi\eta d} \frac{dn}{dx} \quad (10)$$

in eq. 10, the left term is multiplying the number of particles per unit volume  $n$  by the velocity of the particles due to diffusion,  $V$ . The result of this multiplication is the flux of particles per unit area per second,  $J$ . Eq. 10 then takes the form of eq. 6 [67]:

$$D = \frac{k_B T C_c}{3\pi\eta d} \quad (11)$$

### 2.3.3 Thermophoresis

Thermophoresis is a force experienced by particles when a temperature gradient is established in a fluid. This force occurs in the direction of decreasing temperature and it comes from asymmetrical interactions of a particle with the surrounding fluid molecules coming from the hot and cold sides of the fluid [67]. Thermophoresis effects are dependent on the physical properties of the particles and fluid as well as the temperature gradient. This phenomenon was first observed when researchers noticed that a heated

metal rod immersed in smoke developed a dust-free layer around it [67]. This layer had a well-defined boundary and it was usually less than 1 mm thick. After careful measurements on its thickness, it was concluded that this layer was independent of the particle material and proportional to the square root of the difference in temperature between the object and the gas [67]. The particles experiencing thermophoretic force also experience a drag force. A balance of these two forces results in a particle migration velocity known as thermophoretic velocity and it is given by [67]:

$$V_t = -K_{th} \frac{\mu_g}{\rho_g} \frac{\nabla T}{T_g} \quad (12)$$

where  $K_{th}$  is the thermophoretic diffusion coefficient

For the thermophoretic velocity of nanofluids, McNab and Meisen [68] introduced a similar equation, eq. 13, where the thermophoretic diffusion coefficient is replaced by a proportionality factor  $\beta$ .

$$V_t = -\beta \frac{\mu_f}{\rho_f} \frac{\nabla T}{T_g} \quad (13)$$

where

$$\beta = 0.26 \frac{k}{2k + k_p} \quad (14)$$

## 2.4 Thermal conductivity

Thermal conductivity ( $k$ ) is the ability of a material to conduct heat. It represents the rate of conduction heat transfer per unit area for a temperature gradient of 1°C/m of the conducting medium [1]. The units for  $k$  are W/(m °C). The thermal conductivity for



different materials ranges from hundreds for good conductors like metals and diamonds to less than  $0.01 \text{ W/(m } ^\circ\text{C)}$ . Usually materials with a thermal conductivity of less than  $1 \text{ W/(m } ^\circ\text{C)}$  are considered insulators [1]. Generally the solid phase of a material has higher thermal conductivity than the liquid phase.

Temperature plays an important role in the thermal conductivity of some materials. The thermal conductivity of some substances varies by a factor of 10 or more for an order of magnitude change in temperature. However, some materials experience very little variation in the thermal temperature with temperature. Substances affected by temperature have exceedingly high thermal conductivities under low-temperature conditions, these materials are usually refer to as super-conductors. Fig. 2 shows the variation of  $k$  for several common materials as temperature changes.

Researches across the world have extensively investigated the thermal conductivity of numerous nanofluids. Experimental results have determined that nanofluids display higher thermal conductivity and it increases as the nanoparticle concentration increases. Although the increase on the thermal conductivity varies among different types of nanofluids, experimental data suggest that smaller particle size produce higher thermal conductivity. Additionally, cylindrical nanoparticles enhance the thermal properties of fluids better than spherical nanoparticles [23].

Lee et. al. [24] obtained a maximum enhancement of 1.44% in the thermal conductivity of  $\text{Al}_2\text{O}_3$ /water nanofluids with volume concentrations from 0.01% to 0.3% and a particle size of 30 nm. It was also concluded that the thermal conductivity increased almost linearly with volume concentration. For higher volume concentrations,

Chandrasekar et al [25] conducted an experiment measuring the thermal conductivity of  $\text{Al}_2\text{O}_3/\text{water}$  nanofluids with volume concentrations of 0.33%, 0.75%, 1%, 2% and 3% and a particle size of 43nm. The thermal conductivity increased as the volume concentration increased with a maximum enhancement of 9.7% at 3% volume concentration.

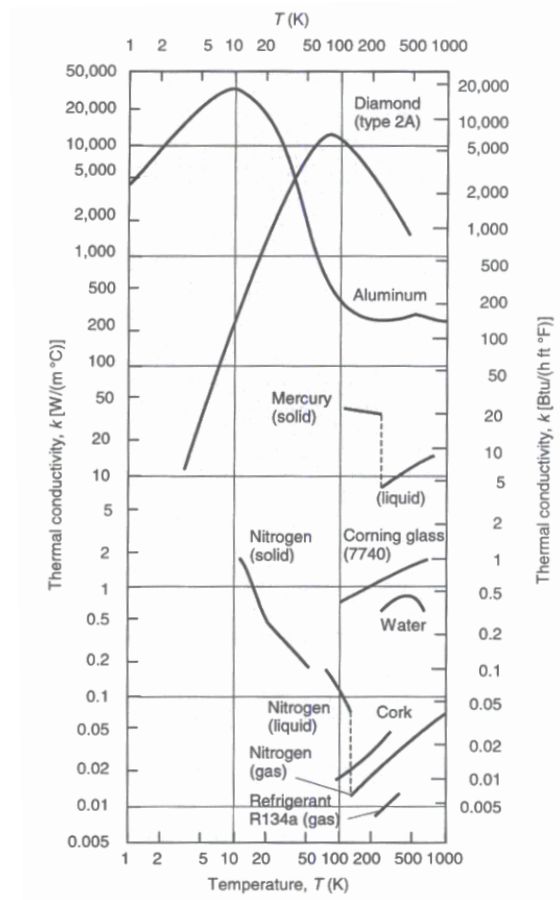


**Figure 2.** Variation in thermal conductivity as temperature changes for common materials [1].

Thermal conductivity measurements for  $\text{SiO}_2/\text{water}$  nanofluids with a volume concentration from 1% to 4% and a particle size of 12 nm were presented by Jahanshahi

et al. [26]. The results showed that the thermal conductivity increased linearly with higher volume concentration. At 1% and 4% volume concentrations, the thermal conductivity of  $\text{SiO}_2$ /water nanofluids was enhanced 3.23% and 23% respectively.

An experiment measuring the thermal conductivity of  $\text{Al}_2\text{O}_3$  nanoparticles (53nm) mixed with a base fluid consisting of 40% water and 60% EG was performed by Vajjha and Das [27]. The thermal conductivity of this nanofluid was increased by 35% with a 10% volume concentration. It was concluded that the thermal conductivity increased as the volume concentration increased. Additionally, it was observed that the thermal conductivity increases with higher temperatures. Xie et al. [28] conducted a similar experiment using  $\text{Al}_2\text{O}_3$  nanoparticles (30nm) mixed in a base fluid of 55% distilled water and 45% ethylene glycol. With a volume concentration of 1%, the thermal conductivity of the nanofluids was enhanced by 4%.

## 2.5 Viscosity

Viscosity of a fluid is defined as the fluid's resistance to motion under the action of an applied shear stress [22]. Fig. 3 helps visualize the definition of viscosity. As shown in this figure, a liquid layer with a thickness of  $\Delta y$  is between two parallel plates. The plate at the bottom is fixed while the top plate is pulled to the right by a force  $F$ . The area between the moving plate and the liquid is  $A$ , and the shear stress ( $\tau$ ) can be calculated by dividing the applied force  $F$  over the area  $A$ . As a result of the applied shear stress, the liquid deforms continuously. This deformation is the slope of the resultant linear velocity distribution within the liquid which can be expressed in terms of a strain rate. The velocity of the liquid at the fixed plate is zero while at the top it is equal to the velocity of

the plate being moved. This characteristic is known as non-slip condition where the liquid seems to adhere to the solid surface [22].

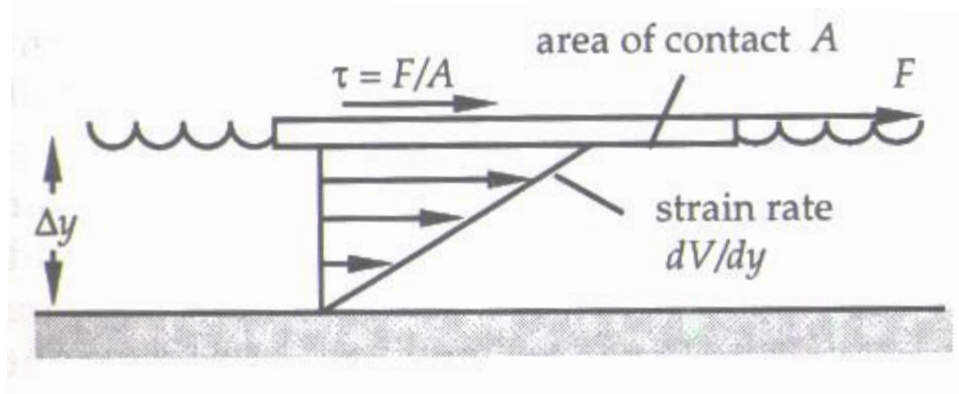


**Figure 3.** Viscosity visualization [22].

There is only one corresponding strain rate for each applied shear stress. A shear stress vs. strain rate graph can be then obtained by taking a series of measurements of forces vs. resultant strain rates. This graph is known as a rheological diagram and the slope of the line is the dynamic or absolute viscosity. Fig. 4 shows an example of a rheological diagram for various types of fluid.

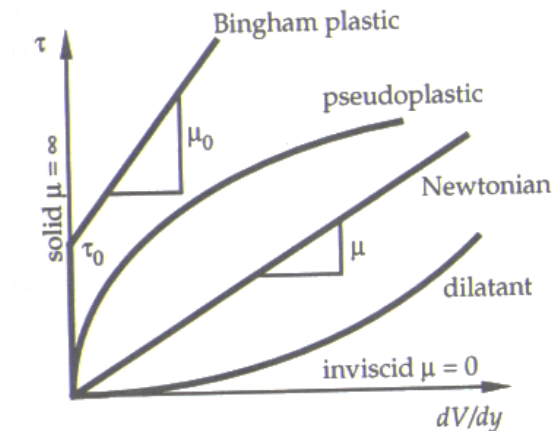


**Figure 4.** Rheological diagram example [22].

For a Newtonian fluid, the viscosity is expressed as shown in eq. 15.

$$\tau = \mu \frac{dV}{dy} \quad (15)$$

where  $\mu$  is the dynamic viscosity,  $\tau$  is the applied shear stress, and  $\frac{dV}{dy}$  is the strain rate. The dimensions of viscosity are commonly expressed as  $N \cdot s/m^2$ .

Experimental results suggest that viscosity of nanofluid increases with increasing volume concentration, this increase is significantly larger on water-based nanofluids than EG nanofluids. The viscosity also increases as the particle size decreases. Temperature also affects the viscosity of nanofluids as temperature increases the viscosity decreases [23].

Chandrasekar et. al. [25] measured the effects of volume concentration on the viscosity of  $Al_2O_3$ /water nanofluids. It was observed that the viscosity increased almost linearly as the volume concentration increased for volume concentrations of 2% or less. For volume concentrations of more than 2%, the increase of viscosity was nonlinear. The maximum enhancement of viscosity was found to be 2.36 times that of water at a volume concentration of 5%. Lee et. al. [24] measured the effects of temperature on the viscosity of  $Al_2O_3$ /water nanofluids. At low volume concentrations from 0.01% to 0.3%, the viscosity decreased significantly as the temperature increased and increased as the volume concentration increased. Dr. Lee concluded that there is a non-linear relationship between the viscosity and the volume concentration.

Annop et. al. [29] studied the effects of viscosity for  $Al_2O_3$ /EG nanofluids and  $Al_2O_3$ /water nanofluids. The results of this experiment suggest that the viscosity of these nanofluids increased as the volume concentration increased. However, the water-based nanofluid experienced a greater enhancement in viscosity than the ethylene glycol based

nanofluid. At a 6% volume concentration the viscosity of  $\text{Al}_2\text{O}_3$ /water nanofluid increased to 1.8 times that of water. At the same concentration, the viscosity of  $\text{Al}_2\text{O}_3$ /EG nanofluid increased to 1.22 times that of EG.

## **2.6 Density and Specific Heat**

There is relatively less research on the density and specific heat of nanofluids compared to that of thermal conductivity and viscosity. The density of nanofluids increases with the addition of nanoparticles. Solids have higher densities than liquids therefore when solid particles are introduced into a fluid it is expected that the density of the fluid will increase. The research done in this area suggests that the mixing theory for predicting the density of nanofluids is consistent with experimental data [23] [30].

Sommers and Yerkes [31] measured the density of  $\text{Al}_2\text{O}_3$ /propanol at room temperature. For this measurement they took a fluid sample with known volume and then weighed it using a high precision density. Their findings suggest a nearly linear relationship between the density and the volume concentration [23].

Zhou and Ni [32] measured the specific heat of  $\text{Al}_2\text{O}_3$ /water nanofluids. It was observed that the specific heat of nanofluids decreased as the volume concentration increased. The results also suggest that the model for predicting the specific heat of nanofluids based in thermal equilibrium mechanism, eq. 12, yields results that are consistent with the experimental results [26].

## **2.7 Particle Size Effects**

There have been contradictory results on the effects of the particle size on the fluid with some findings suggesting an increment in the thermal conductivity and others

suggesting the opposite [33]. The findings from a research on the effects of the particle size using  $\text{Al}_2\text{O}_3$ /water nanofluids suggest that the thermal conductivity of the nanofluid decreased as the nanoparticle size increased [34]. Particles with a nominal diameter of 20, 50, and 100 nm were used. Similar results were obtained from other experiment using  $\text{Al}_2\text{O}_3$ /water and  $\text{Al}_2\text{O}_3$ /EG nanofluids with different particle sizes [35]. It was observed that for both nanofluids the thermal conductivity decreased as the particle size increased. Water and EG based  $\text{Ag}_2\text{Al}$ ,  $\text{Al}_2\text{Cu}$ ,  $\text{TiO}_2$ , and  $\text{ZnO}$  nanofluids produced similar results [33] [36] [37] [38] [39] [40].

The findings on a study of  $\text{SiO}_2$ /water nanofluids showed opposite results to those of  $\text{Al}_2\text{O}_3$ /water [33]. An enhancement of the thermal conductivity for this nanofluid was observed as the particle size increased [41]. This behavior was also observed in  $\text{SiC}$ /water, gold/water, and  $\text{CeO}_2$ /water nanofluids [40] [42] [43]. Furthermore, a different study on  $\text{Al}_2\text{O}_3$ /water and  $\text{Al}_2\text{O}_3$ /Eg nanofluids [44] observed an increase of the thermal conductivity of these nanofluids as the particle size increased contradicting previous findings. In this case 7 different size particles were used ranging from 8nm to 282nm.

## **2.8 Sonication Effect**

The effects of sonication on the thermal properties of nanofluids have been evaluated in a few studies. In a study on  $\text{CuO}$ /water nanofluids [33] there were no changes on the thermal conductivity of the nanofluids with a sonication time of 60 minutes or less; however, after one hour the thermal conductivity started decreasing. On a different study, the effects of the sonication power rather than the sonication time were

monitored [33], [45]. Several sonication powers were applied to both alumina and copper oxide nanofluids and it was observed that a 450 W sonication power produced the highest thermal conductivity enhancement.

Findings suggest that the thermal conductivity of nanofluids like CuO/water may have a smaller enhancement as time passes after sonication [46]. After a long time the sonication effects are insignificant. An explanation to this phenomenon is due to particle agglomeration after sonication [47].



## Chapter 3

### Theory

#### 3.1 Thermal Properties

There are several models for predicting the thermal conductivity. The classical models are Maxwell [48], Hamilton-Crosser [49], and Bruggeman [50]. The Maxwell model (Eq. 16) was first proposed by J.C. Maxwell in 1881. It is used to predict the effective thermal conductivity of liquid-solid suspensions with low volumetric concentration of spherical particles [51]. This model is based on the solution of heat conduction equation through a stationary random suspension of spheres [52].

$$k_{eff} = \frac{k_p + 2k_b + 2[k_p - k_b]\phi}{k_p + 2k_b - [k_p - k_b]\phi} k_b \quad (16)$$

The Hamilton-Crosser model (Eq. 17) is a modification of the Maxwell model. This model can be used to predict the effective thermal conductivity of nanofluids containing non-spherical particles. In order to account for the shape of the particles, Hamilton and Crosser introduced a shape factor ( $n$ ). The shape factor is defined as  $n = 3/\psi$ , where  $\psi$  is the particle sphericity (the ratio of the surface area of a sphere with volume equal to the surface area of the particle). As a results, this model reduces to the Maxwell model when spherical particles are used ( $n = 3$ ).

$$k_{eff} = \frac{k_p + (n-1)k_b - (n-1)[k_b - k_p]\phi}{k_p + (n-1)k_b + [k_b - k_p]\phi} k_b \quad (17)$$

Bruggeman introduced a new model (Eq. 18) for predicting the thermal conductivity of liquid-solid suspensions. In this model, the interactions between spherical particles randomly distributed are analyzed by using the mean field approach.

This model can be used for large volumetric concentrations. This model produces similar results to the Maxwell model for low volumetric concentrations.

$$k_{eff} = \frac{(3\phi-1)\frac{k_p}{k_b} + \{3(1-\phi)-1\} + \sqrt{\Delta}}{4} * k_b \quad (18)$$

where

$$\Delta = \left[ (3\phi - 1) \frac{k_p}{k_b} + \{3(1 - \phi) - 1\} \right]^2 + 8 \frac{k_p}{k_b}$$

These classical models provide similar results that are consistent to those values obtained experimentally; however, in rare instances they may yield erroneous results [53]. A possible explanation for erroneous predictions is that these models do not take into account important factors like temperature or the size of the particles. In an effort to predict more reliable values, S.M.S. Murshed, K.C. Leong and C. Yang [54] introduced a new model (Eq. 19) that accounts for the shape and size of the nanoparticles.

$$k_{eff} = ((k_p - k_{lr})\phi_p k_{lr} [2\gamma_1^3 - \gamma^3 + 1] + (k_p + 2k_{lr}) \times \gamma_1^3 [\phi_p \gamma^3 (k_{lr} - k_f) + k_f]) (\gamma_1^3 (k_p + 2k_{lr}) - (k_p - k_{lr})\phi_p [\gamma_1^3 + \gamma^3 - 1])^{-1} \quad (19)$$

where

$$1 + \frac{h}{a} = \gamma \text{ and } 1 + \frac{h}{2a} = \gamma_1$$

$$h = \sqrt{2\pi\alpha}$$

Several models for predicting the viscosity of nanofluids have been introduced. Some of the most popular models include: Einstein [55], Classic Brinkman [56], Maïga [57], and Chamkha [58]. Einstein used the phenomenological hydrodynamic equations to determine the effective viscosity of nanofluids containing spherical particles as a function of the volumetric concentration, eq. 20, for volume concentrations lower than 5% [52], [55]. Brinkman introduced a viscosity correlation to extend Einstein's equation to

concentrated suspensions, eq. 21. However, the models proposed by Einstein and Brickman seem to underestimate the viscosity of nanofluids when compared to experimental data [52], [56]. Maiga et al. used experimental data from Wang et al. [59] to perform a least-square curve fitting including  $\text{Al}_2\text{O}_3/\text{water}$  and  $\text{Al}_2\text{O}_3/\text{Eg}$ , eq. 22, [52], [57]. Finally, Chamakha proposed another model, eq. 23.

$$\mu_{nb} = (1 + 2.5\phi)\mu_b \quad (20)$$

$$\mu_{nb} = \frac{\mu_f}{(1-\phi)^{2.5}} \quad (21)$$

$$\mu_{nb} = (123\phi^2 + 7.3\phi + 1)\mu_b \quad (22)$$

$$\log(\mu_{nb}) = Ae^{-BT} \quad (23)$$

Where

$$A = 1.837\phi^2 - 29.643\phi + 165.65$$

$$B = 4 \times 10^{-6}\phi^2 - 0.001\phi + 0.0186$$

### 3.2 Nanoparticle Motion

The velocity at which the nanoparticles settle can be found by a force balance where the drag force on the particles,  $F_D$ , is equal and opposite to the force of gravity  $F_G$ .

$$F_D = F_G \quad (24)$$

The general differential equations describing fluid motion are derived by applying Newton's second law to a fluid element on which body forces, pressure, and viscous forces are present. These differential equations are known as the Navier-Stokes equations. The Navier-Stokes equations are known to be virtually unsolvable because they are nonlinear partial differential equations. In order to provide a solution to these equations, Stokes made assumptions in order to eliminate the higher order terms from the Navier-Stokes equations. The key assumptions were that 1) The inertial forces are

negligibly small compared with the viscous forces, 2) the fluid is incompressible, 3) there are no walls or other particles nearby, 4) the motion of the particle is constant, 5) the particle is a rigid sphere, 6) the fluid velocity at the particle's surface is zero [67]. The solution to these equations is known as Stokes's law.

Stoke's law states that the total resisting force on a spherical particle moving with a velocity  $V$  through a fluid is the combination of the two resulting forces acting in the direction opposite to particle motion [67]. By integrating the normal and tangential forces over the surface of the particle, the net force acting on the particle is obtained. The two resulting forces are the form component, eq. 25, and the frictional component, eq. 26 [67].

$$F_n = \pi\mu Vd \quad (25)$$

$$F_\tau = 2\pi\mu Vd \quad (26)$$

Combining these two forces, the total resistance force is obtained, eq. 27.

$$F_D = 3\pi\mu Vd \quad (27)$$

In order to obtain the settling velocity, eq. 27 is substituted in eq. 24.

$$3\pi\mu Vd = F_G = mg \quad (28)$$

The mass is then expressed in terms of density and volume

$$3\pi\mu Vd = \frac{(\rho_p - \rho)\pi d^3}{6} g \quad (29)$$

Finally, solving eq. (29) for the settling velocity gives:

$$V_g = \frac{d_p^2(\rho_p - \rho)g}{18\mu} \quad (30)$$

Brownian motion is the random motion of nanoparticles within the base fluid. Diffusion is the net transport of these particles in a concentration gradient which always goes from a region of higher concentration to a region of lower concentration [67]. The Brownian motion is characterized by the particle diffusion coefficient,  $D_B$ , which is derived from the Einstein-Stokes's equation [67]:

$$D_B = \frac{k_B T}{3\pi\mu d_p} \quad (31)$$

The Brownian motion is more vigorous with larger values of the diffusion coefficient. Therefore, the mass transfers faster in a concentration gradient as the diffusion coefficient increases [67]. The diffusion coefficient is a constant of proportionality that relates the flux,  $j_{p,B}$ , of particles to the concentration gradient. This is known as Fick's first law of diffusion and it is typically expressed as [67]:

$$J = -D \frac{dn}{dx} \quad (32)$$

In the case of nanoparticles eq. 32 is rearranged into:

$$j_{p,B} = -\rho_p D_B \nabla \phi \quad (33)$$

A temperature gradient ( $\nabla T$ ) in a fluid can produce a force in the direction of decreasing temperature on the particles present in that fluid. The movement of the particles due to this force is called thermophoresis [67]. This thermal force is dependent on the physical properties of the particles and fluid as well as the temperature gradient.

The thermal force on a particle in a gas is given as [67]

$$F_{th} = \frac{-p\lambda d^2 \nabla T}{T} \text{ for } d < \lambda \quad (34)$$

where  $p$  is the gas pressure,  $\lambda$  is the gas mean free path,  $\nabla T$  is the temperature gradient, and  $T$  is the absolute temperature of the particle. The direction of the force is from high temperature to low temperature hence the minus sign. The velocity of thermophoresis is given as [67]

$$V_{th} = \frac{-.55\mu\nabla T}{\rho_g T} \quad (35)$$

the velocity of thermophoresis is directly proportional to the temperature gradient and independent of the size of the particles.

For nanofluids, McNab and Meisen [68] proposed a proportionality factor,  $\beta$ , that is expressed as

$$\beta = 0.26 \frac{k}{2k + k_p} \quad (36)$$

the velocity of thermophoresis is given as

$$V_T = -\beta \frac{\mu}{\rho} \frac{\nabla T}{T} \quad (37)$$

the mass flux due to thermophoresis is given as

$$j_{p,T} = -\rho_p \phi V_T \quad (38)$$

## Chapter 4

### Experimental Approach

#### 4.1 Thermal Conductivity Measurements

The thermal conductivity and specific heat of the nanofluids was measured using a Thermtest Transient Plane Source TPS 500 S instrument.



**Figure 5.** TPS 500s set up.

This method is based on the use of a transient heated plane sensor, commonly referred as the hot disk thermal constants analyzer. The hot disk sensor consists of an electrically conducting pattern in the shape of a double spiral, which has been etched out of a thin material (Nickel) foil.

The plane hot disk sensor is fitted between two pieces of the sample and then an electrical current is applied. The electrical current is high enough to increase the temperature of the sensor up to several degrees and at the same time the resistance

increment, as a function of time, is recorded. The solution of the thermal conductivity equation is based on the assumption that the disk sensor is placed in an infinite medium meaning that the transient recording must be interrupted as soon as an influence from the outside boundaries of the two sample pieces is recorded by the sensor. Typical sample sizes are between 1 and 10 cm<sup>3</sup>, although it can be reduced to 0.01 cm<sup>3</sup> in special situations. It is important to note that the size of the flat sample surface should be appreciably larger than the diameter of the hot disk sensor to allow for a transient recording [64].



**Figure 6.** Sensor design 7577 (Kapton), 2 mm radius.

The Hot Disk Thermal Constant Analyser uses a sensor element in the shape of a double spiral. The sensor serves as both the heat source and the resistance thermometer. The sensor is made of a 10 µm thick Nickel-metal double spiral. Nickel is used because of its high and well known temperature coefficient of resistivity. The double spiral is reinforced by Kapton or Mica to protect its shape, increase its strength, and keep it insulated. The Kapton layer has a thickness of 12.7 µm or 25 µm for temperatures from



30K to 500K. In special situation, Mica insulation with a thickness of around 0.1mm for temperatures from 500K to 1000K is used [64].

The sensor is placed between two halves of the sample. Next, 200 resistance readings are taken during a pre-set time from which a relation between temperature and time is set. Thermal conductivities from 0.005W/mK to 500 W/mK can be measured since key parameter like heating power, measurement time, and the size of the sensor can be changed to optimize the settings for each experiment. The accuracy of thermal conductivities is within +/- 5% and the reproducibility is within +/-2% [64].

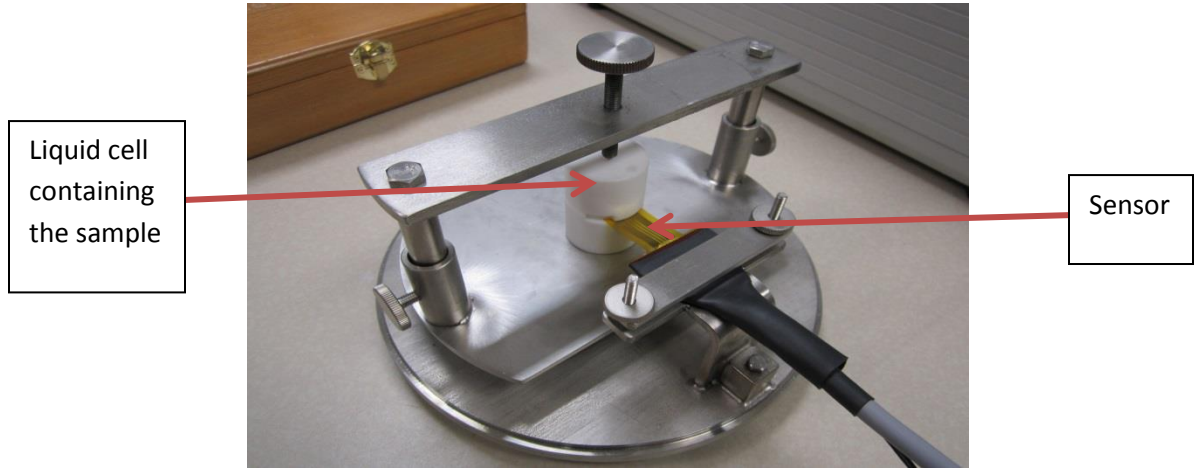


**Figure 7.** Thermal conductivity measurement set up.

To solve the thermal conductivity equation it is assumed that the Hot Disk consists of a certain number of concentric rings that act as heat sources placed in an infinitely large sample. Since the Hot Disk is electrically heated, the resistance can be expressed as a function of time using the following equation [64]:

$$R(t) = R_0 \{1 + \alpha \cdot [\Delta T_i + \Delta T_{ave}(\tau)]\} \quad (39)$$

$R_0$  is the resistance at time = 0,  $\alpha$  is the temperature coefficient of the resistivity,  $\Delta T_i$  is the constant temperature difference that is created over the two insulating layers of the Hot Disk sensor material (Usually Nickel).  $\Delta T_{ave}(\tau)$  is the temperature rise of the sample surface. Rearranging eq. (13), the temperature rise recorded by the sensor can be represented by eq. (40) [64]:

$$\Delta T_{ave}(\tau) + \Delta T_i = \frac{1}{\alpha} \cdot \left( \frac{R(t)}{R_0} - 1 \right) \quad (40)$$

$\Delta T_i$  is the measurement of the thermal contact between the sensor and the surface of the sample. After a very short time  $\Delta T_i$  becomes constant and it can be expressed using eq. (41) [64]:

$$\Delta T_i = \frac{\delta^2}{k_i} \quad (41)$$

$\delta$  is the thickness of the insulating material and  $k_i$  is its thermal diffusivity value.

$\Delta T_{ave}(\tau)$  is the time-dependent temperature increase and it can be represented by eq. (42) [64]:

$$\Delta T_{ave}(\tau) = \frac{P_0}{\pi^{3/2} \cdot a \cdot \Lambda} \cdot D(\tau) \quad (42)$$

$P_0$  is the power from the sensor,  $a$  is the radius of the disk,  $\Lambda$  is the thermal conductivity of the sample being measured and  $D(\tau)$  is a time dependent function that is dimensionless [64]:

$$\tau = \sqrt{\frac{t}{\theta}} \quad (43)$$

where  $t$  is the time recorded since the start of the transient recording, and  $\theta$  is the characteristic time expressed as [64]:

$$\theta = \frac{a^2}{k} \quad (44)$$

where  $k$  represents the thermal diffusivity of the sample [64].

Then, a plot of the recorded temperature rise vs  $D(\tau)$  is made. From this plot a straight line with an intercept of  $\Delta T_i$  and a slope of  $\frac{P_0}{\pi^{3/2} \cdot a \cdot \Lambda}$  is obtained using experimental times bigger than  $\Delta T_i$ . Because  $k$  and  $\theta$  are unknown before the experiment, the thermal conductivity is determined from the straight line obtained through a process of iteration [64].

## 4.2 Viscosity measurements

The viscosity of the nanofluids is measured using a Brookfield Digital Viscometer. This method is based on measuring the torque required to rotate an immersed element, the spindle, in a fluid [65]. The rotation of the spindle is produced by a synchronous motor through a calibrated spring. The viscosity of the fluid is proportional to the rotational speed of the spindle and its geometry (size and shape), an increase in viscosity will be indicated by an increase in the deflection of the spring. The schematic of the Brookfield Digital Viscometer is shown in Fig. 8.

This Instrument is capable of measuring a wide range of viscosities by using interchangeable spindles of various sizes and a multiple speed transmission (four or eight). The selection of the speed of the motor and size of the spindle is on a trial and error basis. The goal is to obtain a viscometer dial reading between 10 and 100. The

accuracy improves as the reading approaches 100. If a reading is above 100, a slower speed and/or smaller spindle should be selected. By the same token if a reading is below 10 then a higher speed and/or bigger spindle should be selected. Once a satisfactory reading is obtained, it is multiplied by the factor for the spindle/speed combination being used. This factor is found on the “Factor Finder” supplied with the viscometer. The Brookfield Viscometer is guaranteed to be accurate to within  $\pm 1\%$  and a reproducibility of  $\pm 2\%$  [65].

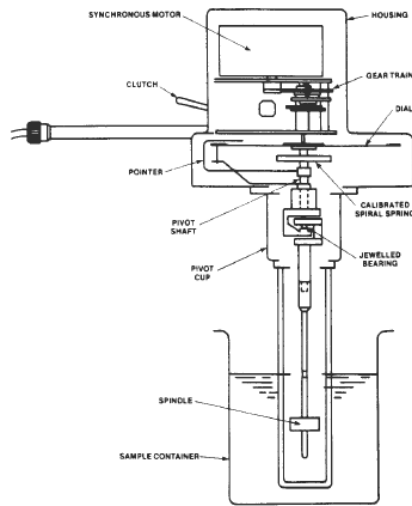


**Figure 8.** Viscometer diagram [65].

### 4.3 Sample Preparation

The preparation of the nanofluids is the preliminary step for experimentation. The proper and careful preparation of the nanofluid is required in order to obtain accurate results. Key factors to ensure correct preparation include: stable suspension, adequate durability, negligible agglomeration of particles, among others. Usually one of the major problems for the synthesis of nanofluids is agglomeration. In order to avoid this problem, two processes has been commonly adopted by researches the single-step process and the

two-step process. The single-step method produces the nanoparticles and the suspension in one step whereas in the two-step method the nanoparticles are produced first and then dispersed in the based fluid. Because nanoparticles can easily be purchased from various companies, the two-step method is more popular among researchers. The two-step method is used for the production of the nanofluids studied in this research. The nanoparticles are purchased from a supplier and then mixed with the base fluid. Then the mixture is dispersed using a digital sonifier. The mixture is dispersed by using ultrasonic vibrations for a specified amount of time.

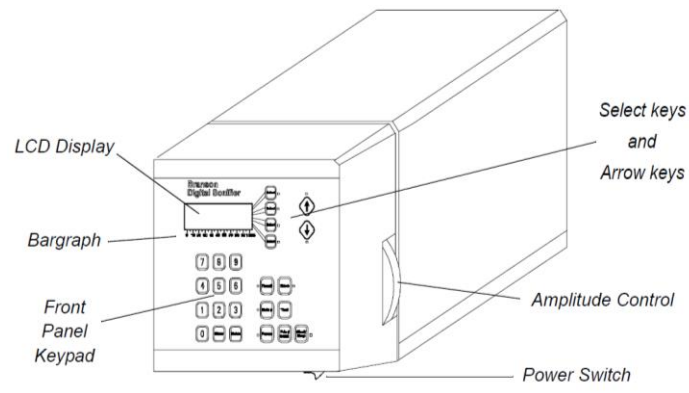


**Figure 9.** Sonifier diagram [63].

A Branson Digital Disruptor 250, Fig. 9, is used for the sonication of the nanofluids. The digital sonifier inputs high-frequency electrical energy into a converter. The converter contains a lead zirconate titanate electrostrictive element that expands and contracts when it enters in contact with alternating voltage; hence, it transforms the electrical energy received into mechanical vibrations. The converter then transmits the vibration motion to a horn tip which is immersed in the liquid sample causing cavitation. The cavitation induced by the horn tip causes the molecules in the liquid to become agitated [63].

In order to observe the effects to the base fluid, 5 different base fluids were tested: Ionized water, EG, 75%EG-25%water, 50%EG-50% water, and 25%EG-75%water. Each nanofluid was mixed in a 600 mL beaker. Each sample contained 500 mL of the base fluid and the appropriate amount of nanoparticles to create the desired volumetric concentration. The nanoparticles were measured using a high precision scale, an Ainsworth DE series model 100A scale. The beaker containing the base fluid was placed into a water circulator. Then, the nanoparticles and base fluid were mixed using a Branson digital sonifier for 30 minutes at 40% of maximum amplitude. The temperature of the water bath was adjusted to maintain the temperature of the nanofluid at 21.5 °C. The temperature of the base fluid was monitored using a J thermocouple connected to a high accuracy digital thermometer (omega HH-21A series). After 30 minutes, the sample was immediately placed in the container and the thermal conductivity reading was taken. A total of six different samples were mixed and measured at each volumetric concentration. Three samples were tested initially, and a week later three additional samples were tested. The measuring time was set for 2.5 second, the recommended time for measuring liquids. The heating power was set at 1W using a 7577 sensor with a radius of 2.001 mm.

The effects of volumetric concentration and particles size were tested using 4 different types of nanoparticles:  $\text{Al}_2\text{O}_3$  (10 nm),  $\text{Al}_2\text{O}_3$  (150 nm),  $\text{SiO}_2$  (15 nm), and  $\text{SiO}_2$  (80 nm). Each nanoparticle was mixed with ionized water at volumetric concentration of 0.2%, 0.5%, 0.7%, 1%, 2%, and 3%. The nanofluids were mixed using the same method described before. The thermal conductivity for each sample was measured every minute for 20 minutes with the sensor facing up and down.

## Chapter 5

### Results and Discussion

#### 5.1 Base Fluid Effects

In order to observe the effects of the base fluid, five different base fluids were tested: EG, Water, 75%EG/25%Water, 50%EG/50%Water, and 25%EG/75%Water.  $\text{Al}_2\text{O}_3$  nanoparticles with a diameter of 10nm were used for all base fluids. 4 different volumetric concentrations were used: 0%, 0.1%, 1%, and 10%. All tests were performed at room temperature. Each sample was tested three times and a week later three more reading were taken for a total of 6 separate readings. These reading were then averaged to obtain a final value. The results are shown in Fig. 10 – 19.

The results indicate a nonlinear behavior of the thermal properties as the volumetric concentration increases. The theoretical results were closer to the experimental results for small volumetric concentrations. Ionized water indicated a linear increase in viscosity as the volumetric concentration increased; however, the thermal conductivity and specific heat were nonlinear. The thermal conductivity decreased by 0.44% at 0.1% vol. concentration, it decreased by 2.82% at 1% vol. concentration and then it increased by 10% at 10% vol. concentration. On the other hand the specific heat of the sample increased at 0.1% and 1% vol. concentrations and then decreased at 10% vol. concentration.

EG nanofluid produced slightly different results. The viscosity actually decreased by 1.91% and 1.57% at vol. concentrations of 0.1% and 1% respectively and then it increased by 15.6% at 10% vol.concentration. The thermal conductivity increased by

0.86% and 0.5% at 0.1% and 1% vol. concentrations respectively and then it decreased by 9.85% at 10% vol. concentration. However, the specific heat increased linearly as the volumetric concentration increased. It increased by 0.27%, 2.67%, and 38.3% at vol. concentrations of 0.1%, 1%, and 10% respectively.

75%EG/25%water nanofluid showed an increment in the viscosity as the vol. concentration increased. It increased by 2.3%, 3.94%, and 20.7% at 0.1%, 1%, and 10% vol. concentrations respectively. At 0.1% vol. concentration the thermal conductivity increased by 5.38% and then it decreased by 1.1% and 29.74% at 1% and 10% vol. concentrations respectively. Inversely, the specific heat decreased at 0.1% vol. concentration and then increased at 1% and 10% vol. concentrations.

50%EG/50%water and 25%EG/75%water nanofluids resulted in the thermal conductivity decreasing in all vol. concentrations and the specific heat increasing. At low vol. concentrations the viscosity decreased or did not change significantly; however at 10% vol. concentrations the viscosity of both nanofluids increased by 12%.

Previous studies indicated a linear behavior between the thermal properties of the nanofluid and the volumetric concentration. Segregation of particles was found to be a major factor in the study of nanofluids. The particles settled rapidly and therefore the enhancement from the particles was diminished after a few minutes. In order to prevent this behavior, a combination of surfactants and sonication has been found to be effective in creating a stable mix in previous studies.

After observing the rapid settling of the particles, the slip mechanism of the particles were studied along with the effects of the particle type/size.



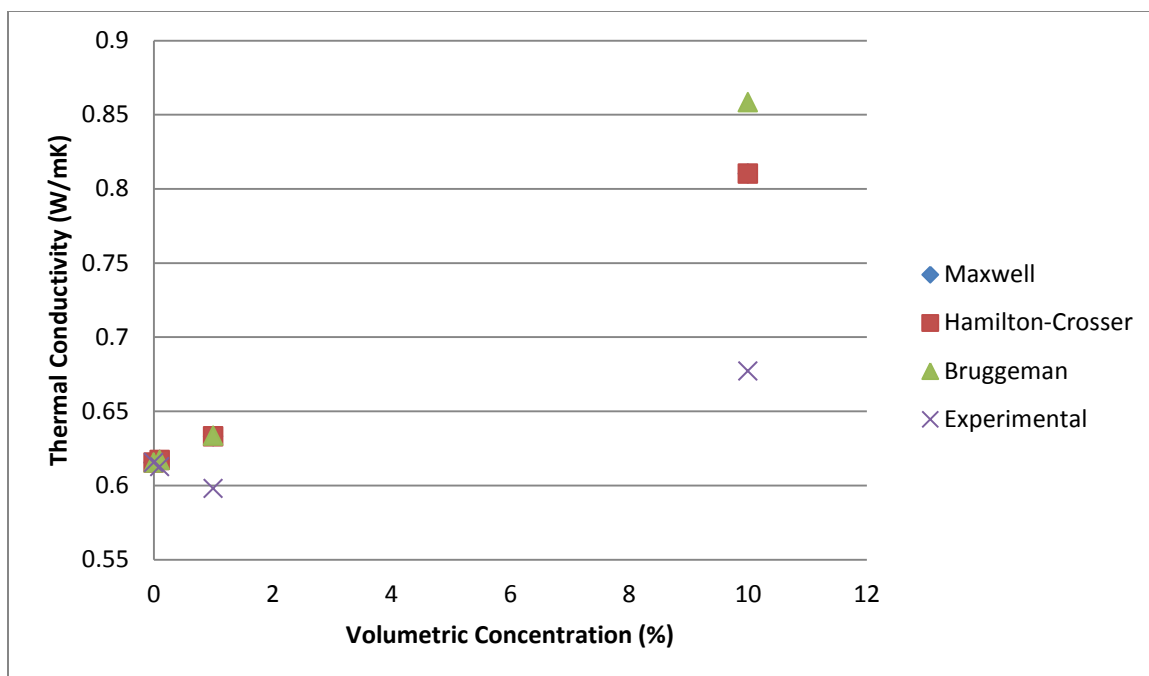


**Figure 10.** Base fluid effect on thermal conductivity, water/Al<sub>2</sub>O<sub>3</sub>, 10 nm.

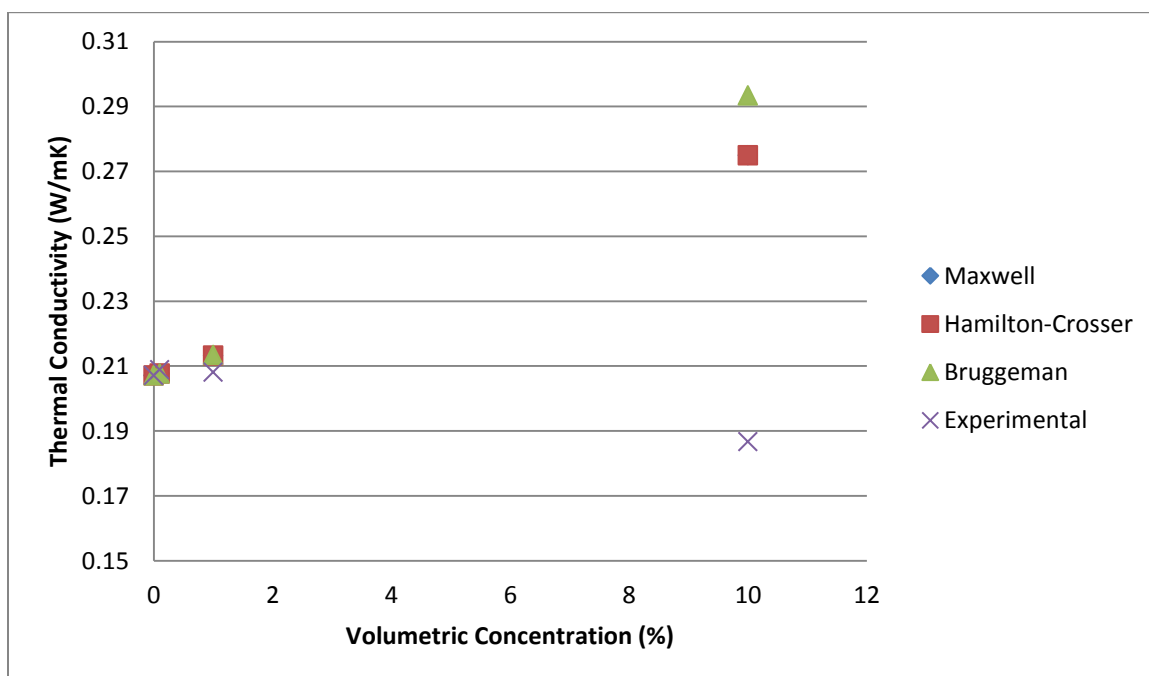


**Figure 11.** Base fluid effect on thermal conductivity, EG/Al<sub>2</sub>O<sub>3</sub>, 10 nm.

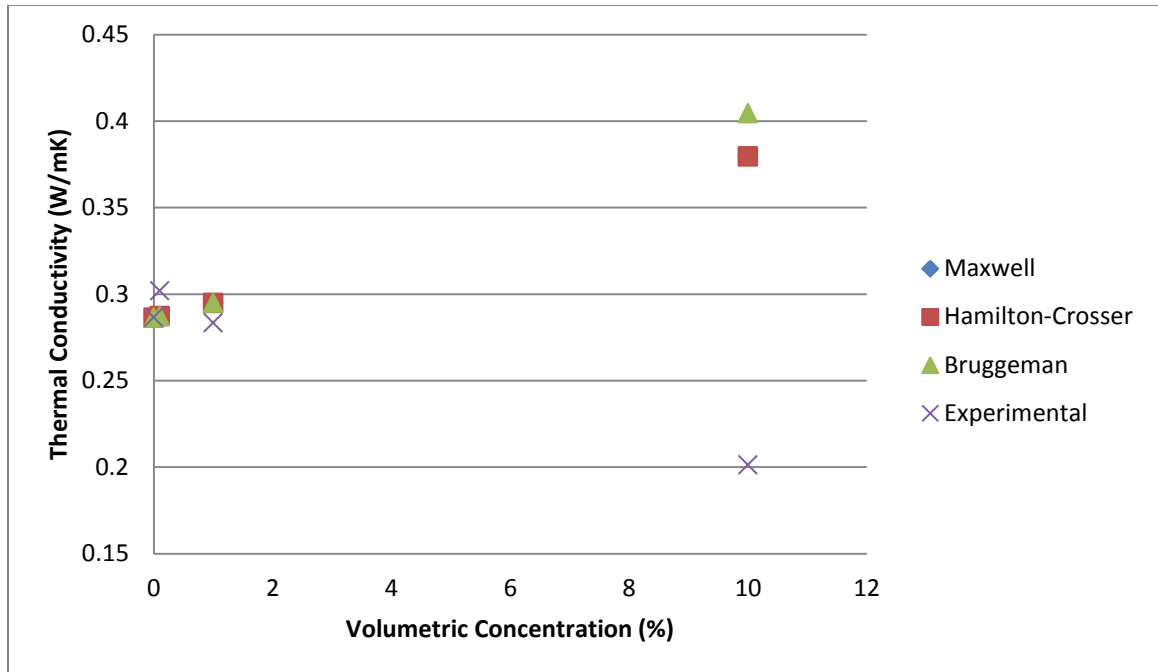


**Figure 12.** Base fluid effect on thermal conductivity, 75% EG-25% Water/Al<sub>2</sub>O<sub>3</sub>, 10 nm.

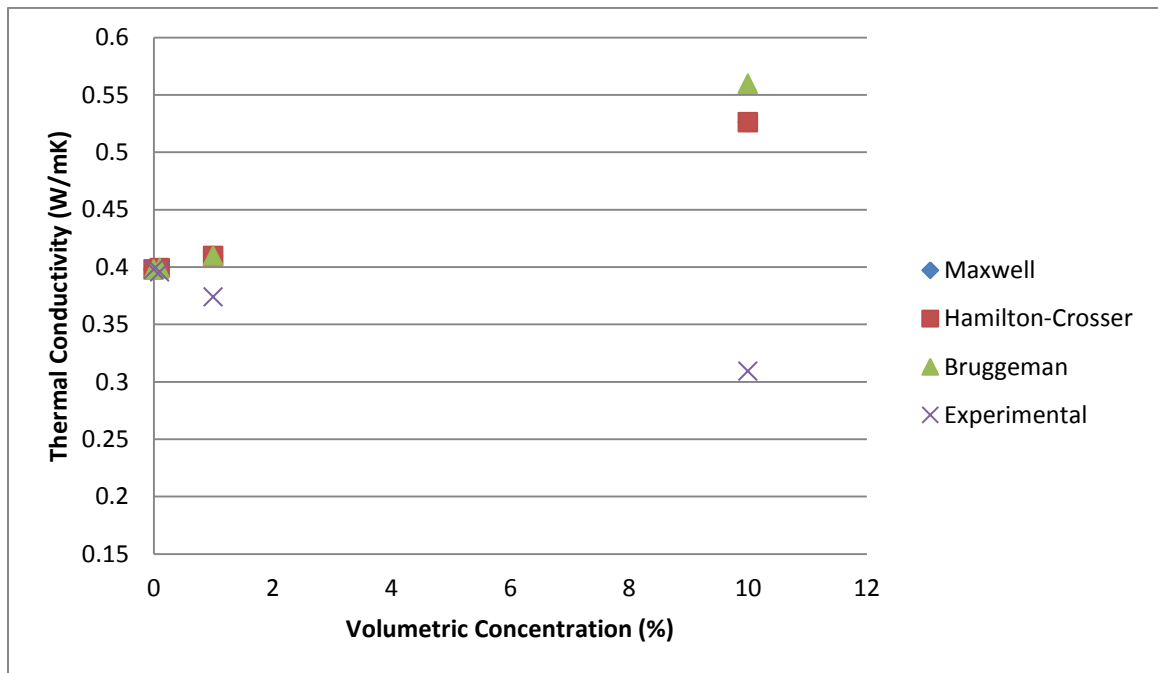


**Figure 13.** Base fluid effect on thermal conductivity, 50% EG-50% Water/Al<sub>2</sub>O<sub>3</sub>, 10 nm.

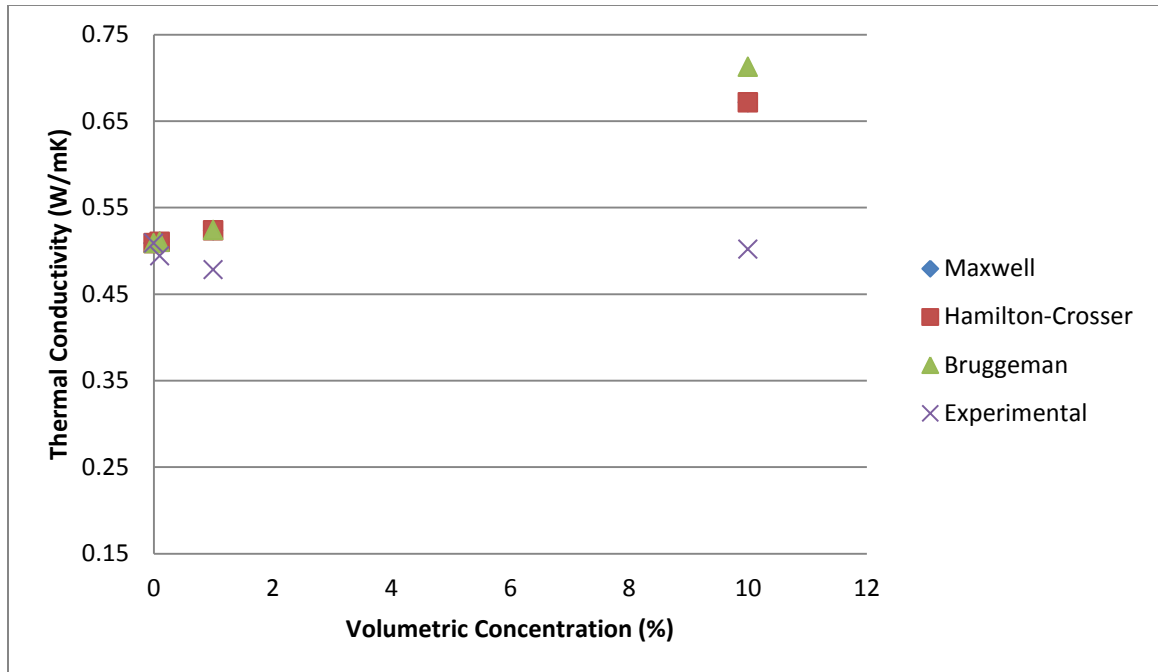


**Figure 14.** Base fluid effect on thermal conductivity, 25%EG-75% Water/ $\text{Al}_2\text{O}_3$ ,10 nm.

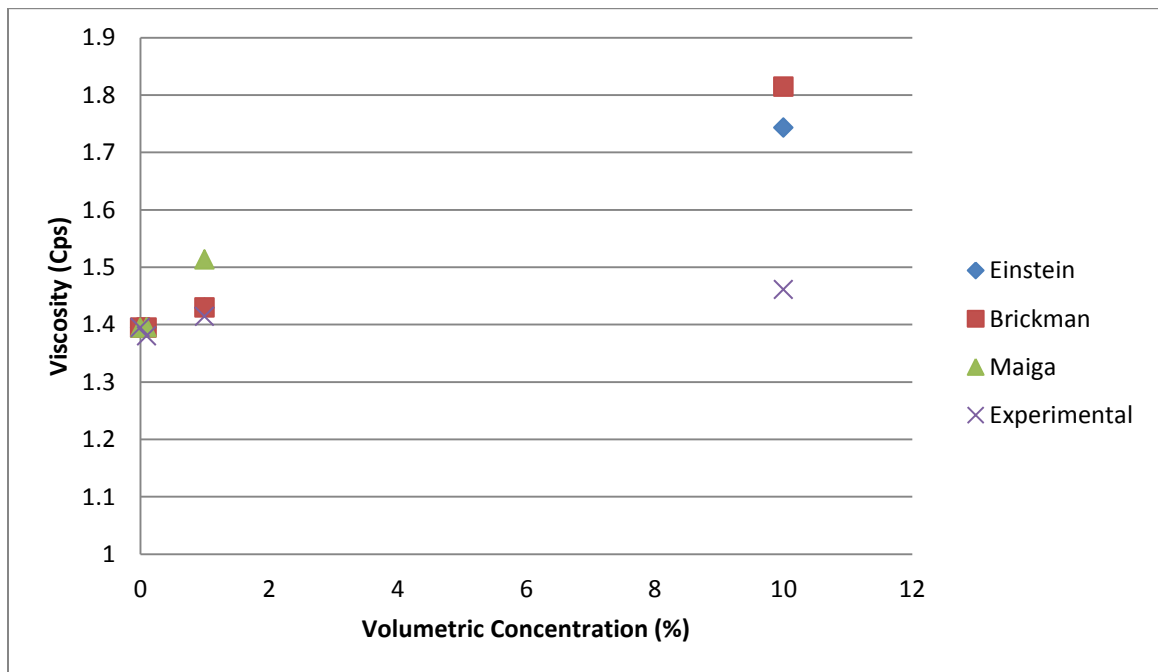


**Figure 15.** Base fluid effect on viscosity, water/ $\text{Al}_2\text{O}_3$ ,10 nm.

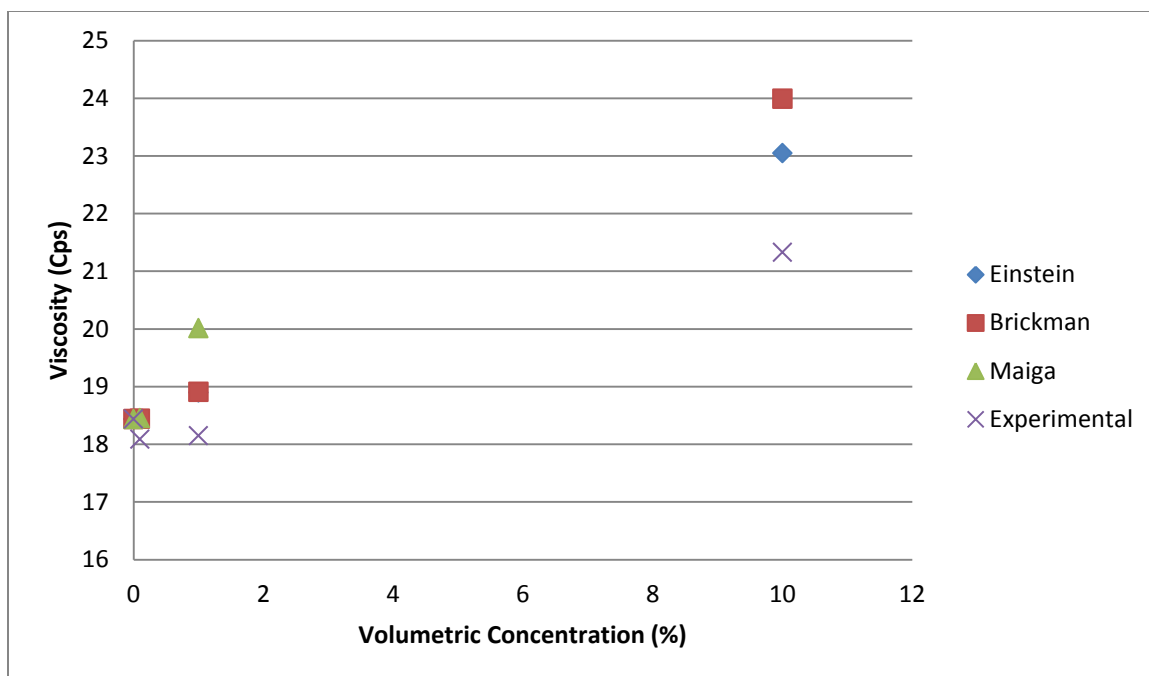


**Figure 16.** Base fluid effect on viscosity, EG/Al<sub>2</sub>O<sub>3</sub>, 10 nm.

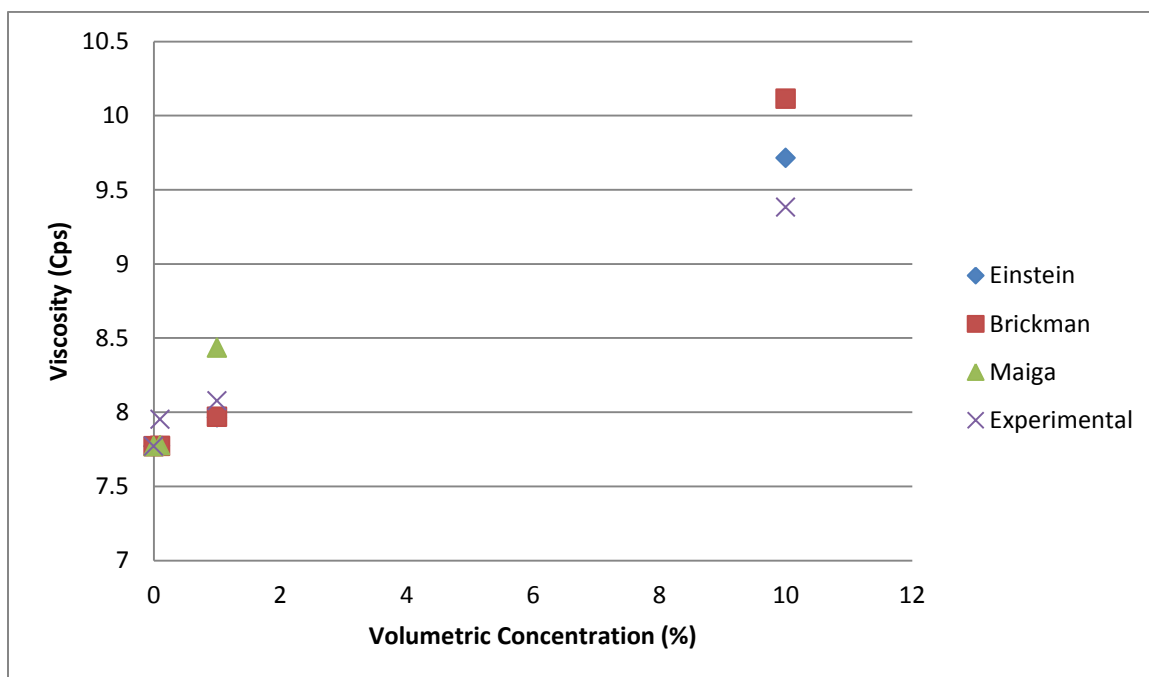


**Figure 17.** Base fluid effect on viscosity, 75% EG-25% Water/Al<sub>2</sub>O<sub>3</sub>, 10 nm.

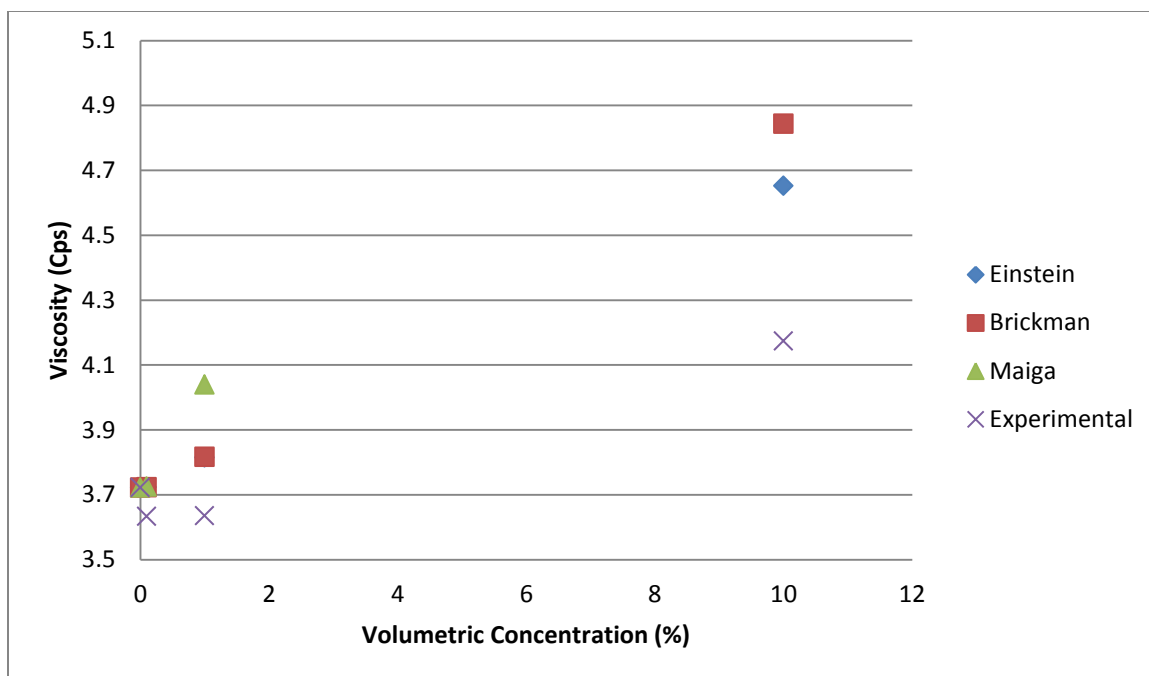


**Figure 18.** Base fluid effect on viscosity, 50% EG-50% Water/ $\text{Al}_2\text{O}_3$ , 10 nm.

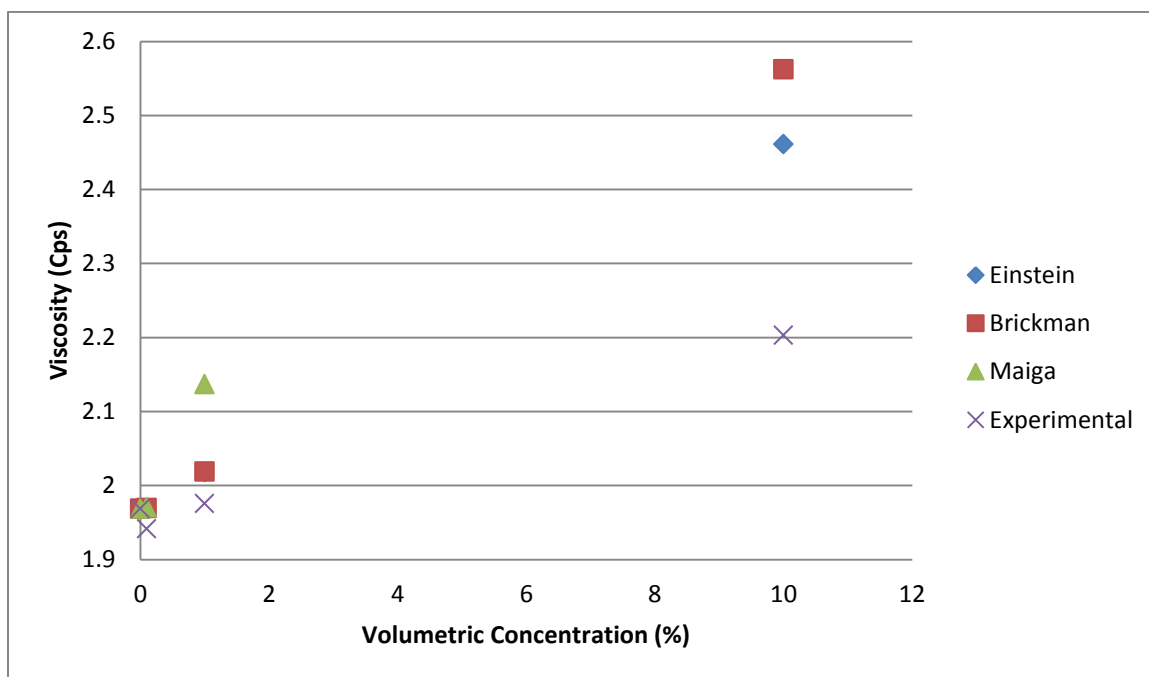


**Figure 19.** Base fluid effect on viscosity, 25% EG-75% Water/ $\text{Al}_2\text{O}_3$ , 10 nm.

## 5.2 Nanoparticle Type and Size Effects

### 5.2.1 Thermophoresis and gravity forces in opposite directions

SiO<sub>2</sub>/Water nanofluids showed significant enhancement in the thermal conductivity of the nanofluids for volumetric concentrations of 1% or less when the gravity and thermophoresis forces were in opposite directions, Fig. 20. At a volumetric concentration of 0.2%, the thermal conductivity was improved by 6.12% and 8.76% using nanoparticles of 15 nm and 80 nm in diameter respectively. These results were significantly higher than those predicted by theoretical models. Nanofluids using SiO<sub>2</sub> nanoparticles with a diameter of 80 nm produced higher thermal conductivity results than those using SiO<sub>2</sub> nanoparticles of 15 nm in diameter.

At 2% and 3% volumetric concentrations, the SiO<sub>2</sub>/water nanofluids did not produce thermal conductivity enhancement. SiO<sub>2</sub>/water nanofluid using nanoparticles with a diameter of 15 nm decrease the thermal conductivity of the fluid by 2.7% and 2.75% at 2% and 3% volumetric concentrations respectively. For the SiO<sub>2</sub>/Water nanofluid using nanoparticles with a diameter of 80 nm the enhancement was really small, 0.19% and 2.53 % for a volumetric concentration of 2% and 3% respectively. Over a period of 20 minutes, the thermal conductivity of the SiO<sub>2</sub>/Water nanofluid with particle size of 15 nm increased by a total of 3.55% from the initial reading at time zero and a volumetric concentration of 0.2%. In the same time interval the thermal conductivity increased by 3.4% and 5.13% for 0.5% and 0.7% volumetric concentrations respectively. At 1% volumetric concentration the thermal conductivity remained constant with an overall change of 0.11% after 20 minutes. For 2% and 3% volumetric

concentration the thermal conductivity decreased over a period of 20 minutes by 5.48% and 7.10% respectively. Similarly, the thermal conductivity of the SiO<sub>2</sub>/Water nanofluid using nanoparticles with a diameter of 80 nm increased by 6.60% with a volumetric concentration of 0.2% over a period of 20 minutes. At 0.5%, 0.7%, and 1% volumetric concentrations the thermal conductivity remained stable changing by 0.43%, 2.58%, and 0.5% respectively over the same time period. At higher volumetric concentrations, the thermal conductivity decreased significantly over time; at 2% and 3% volumetric concentrations the thermal conductivity decreased by 15.71% and 8.17% respectively.

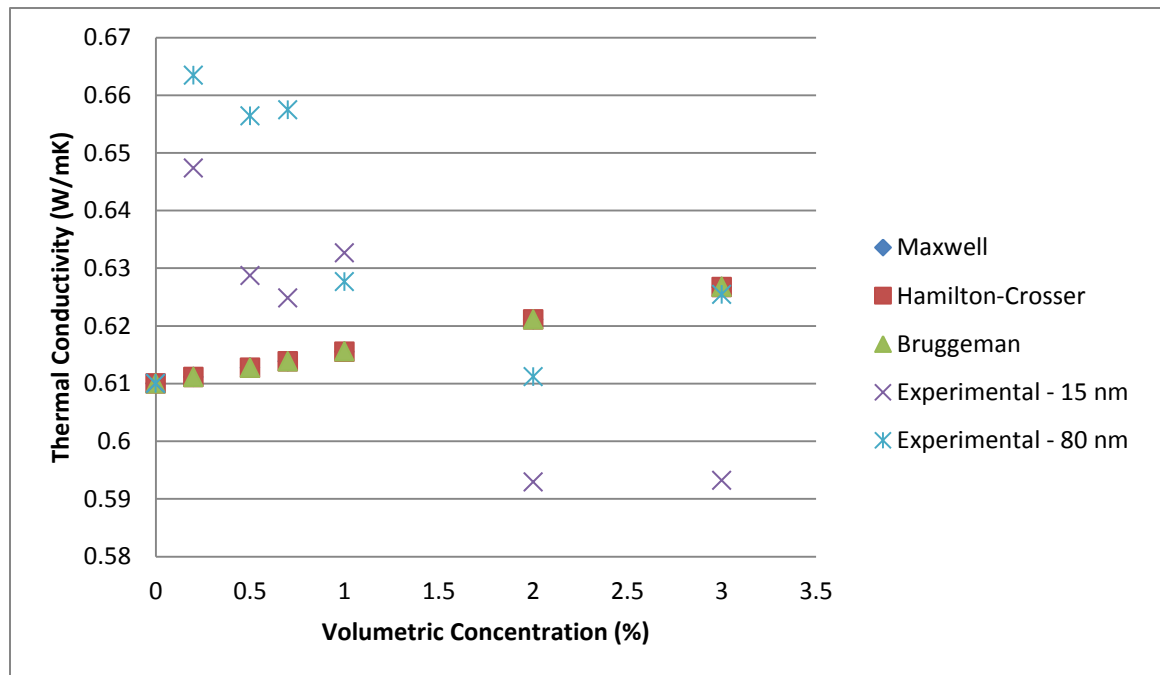


**Figure 20.** Thermal conductivity comparison, SiO<sub>2</sub>/Water, thermophoresis and gravity in opposite direction.

Al<sub>2</sub>O<sub>3</sub>/Water nanofluids did not produce thermal conductivity enhancement. This is due to the rapid settling of the particles, much faster than the settling velocity of SiO<sub>2</sub> nanoparticles, since those particles have a higher density. Al<sub>2</sub>O<sub>3</sub>/Water nanofluid using

nanoparticles with a diameter of 10 nm showed small variation in the thermal conductivity results when compared to the results obtained using nanoparticles with a diameter of 150 nm, Fig. 21. In fact, the thermal conductivity was reduced significantly as the volumetric concentration increased for nanofluids using  $\text{Al}_2\text{O}_3$  nanoparticles with a diameter of 150 nm. Over a period of 20 minutes the  $\text{Al}_2\text{O}_3$ /Water nanofluids showed an enhancement of the thermal conductivity over time. The thermal conductivity for  $\text{Al}_2\text{O}_3$ /Water nanofluid with particle size of 10 nm increased by 4.23%, 2.51%, 2.99%, and 2.79% at 0.2%, 0.5%, 0.7% and 1% volumetric concentrations after 20 minutes respectively. At a volumetric concentration of 2%, the thermal conductivity decreased by 6.18% and at a volumetric concentration of 3% the thermal conductivity increased by 4.66%. For  $\text{Al}_2\text{O}_3$ /Water nanofluid with particle size of 150 nm, the thermal conductivity increased by 2.99%, 3.75%, and 5.17% after 20 minutes for volumetric concentrations of 0.2%, 0.5%, and 0.7% respectively. At higher concentrations, the thermal conductivity decreased over time; it decreased by 0.65%, 2.57%, and 7.99% for volumetric concentrations of 1%, 2%, and 3% respectively. Fig. 22 compares the results of the thermal conductivity readings obtained for both  $\text{Al}_2\text{O}_3$ /Water and  $\text{SiO}_2$ /Water nanofluids.



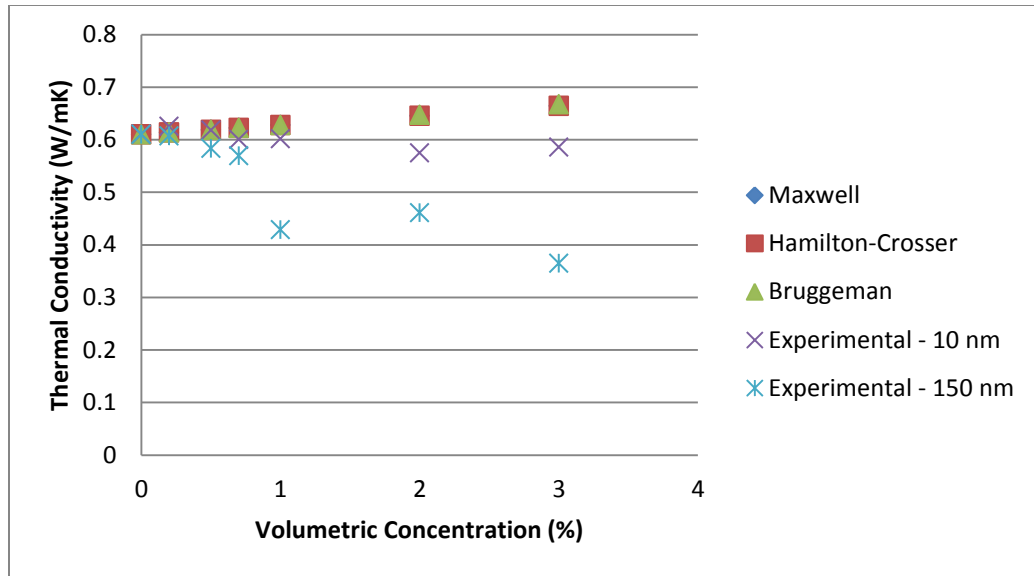


**Figure 21.** Thermal conductivity comparison,  $\text{Al}_2\text{O}_3/\text{Water}$ , thermophoresis and gravity in opposite direction.

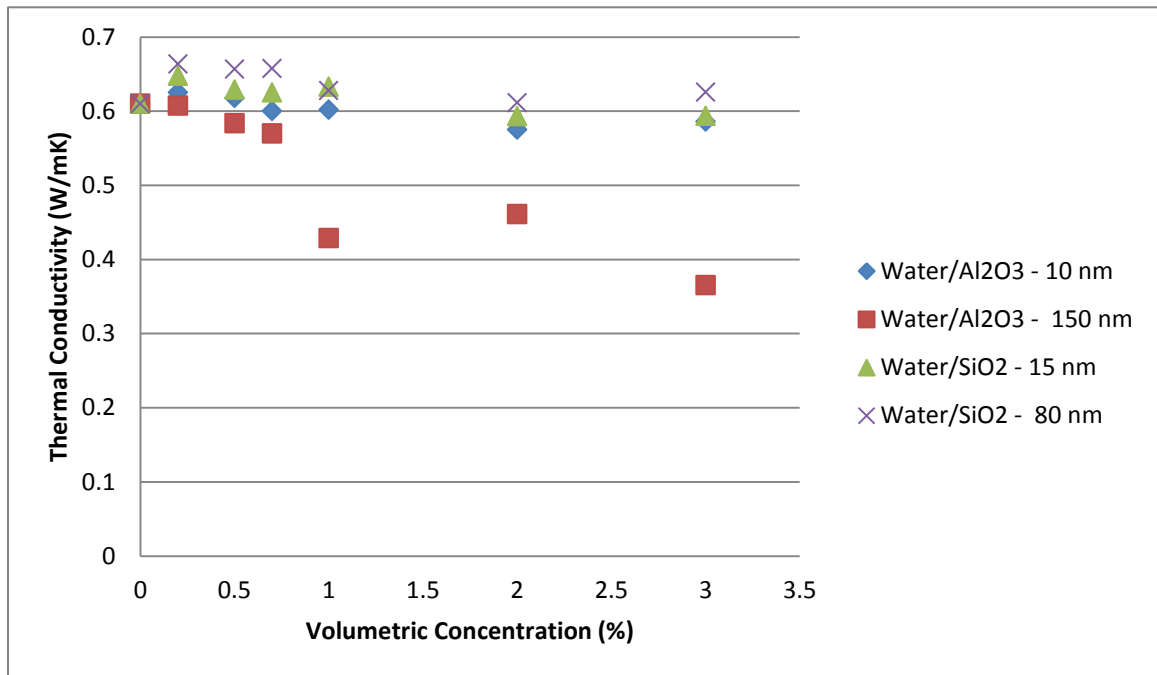


**Figure 22.** Thermal conductivity comparison between nanofluids, thermophoresis and gravity in opposite direction.

### 5.2.2 Thermophoresis and gravity forces in same directions

SiO<sub>2</sub>/Water nanofluids showed significant enhancement in the thermal conductivity of the nanofluids for all volumetric concentrations when the thermophoresis and gravity forces were in the same direction, Fig. 23. The highest thermal conductivity enhancement, 23%, was found in the SiO<sub>2</sub>/Water nanofluid with particle size of 15 nm and a volumetric concentration of 3%. SiO<sub>2</sub>/Water nanofluids using particles with a particle diameter of 15 nm showed greater thermal conductivity enhancement than SiO<sub>2</sub>/Water nanofluids using particles with a particle diameter of 80 nm. At a volumetric concentration of 0.2%, the thermal conductivity was improved by 21.7% and 11.3% using nanoparticles of 15 nm and 80 nm in diameter respectively. At a volumetric concentration of 0.5%, the thermal conductivity using particles with a 15 nm diameter showed an enhancement of 17.9% which is less than the enhancement achieved using a volumetric concentration of 0.2% but still higher than the enhancement predicted using theoretical models. At a volumetric concentration of 0.5%, the thermal conductivity using particles with an 80 nm diameter was enhanced by 14.45% which is a higher enhancement than the one found using a lower volumetric concentration. At 0.7%, 1%, 2%, and 3% volumetric concentrations using particles with a 15 nm diameter, the thermal conductivity was enhanced by 21.8%, 19.7%, 21.6%, and 23.0% respectively. These results were significantly higher than those predicted by theoretical models. SiO<sub>2</sub>/Water nanofluids using nanoparticles of 80 nm in diameter produced lower thermal conductivity enhancement. At a volumetric concentration of 0.2%, the thermal conductivity was enhanced by 11.3%. At volumetric concentration of 0.5%, 0.7%, 1%, 2%, and 3% the thermal conductivity enhancement was 14.4%, 11.5%, 9.7%, 8.1%, and 4.9%

respectively. After 20 minutes, the thermal conductivity for SiO<sub>2</sub>/Water nanofluids using nanoparticles of 15 nm changed little in most volumetric concentrations. At 0.2%, 0.5% and 0.7% volumetric concentrations, the thermal conductivity difference between the reading at time zero and the reading at time 20 minutes was just 1.12%, 1.66%, and 1.05 % respectively. The biggest difference in thermal conductivity over time was found at a volumetric concentration of 1%, after 20 minutes the thermal conductivity increased by 9.67%. At 2% and 3% volumetric concentrations, the thermal conductivity again remained almost constant after 20 minutes with a difference of 1.6% and 2.8% respectively. For SiO<sub>2</sub>/Water nanofluids using nanoparticles of 80 nm in diameter, the biggest change in thermal conductivity after 20 minutes was found at a volumetric concentration of 0.2% with an increase of 11.18%. At all other volumetric concentrations, there was minimal change in thermal conductivity over time. At 0.5% and 1% volumetric concentrations, the thermal conductivity remained constant with a change in the thermal conductivity of 0.16% and 0.13% respectively after the 20 minutes. At 0.7%, 2%, and 3%, the thermal conductivity decreased by 2.1%, 3.64%, and 3.86% respectively.

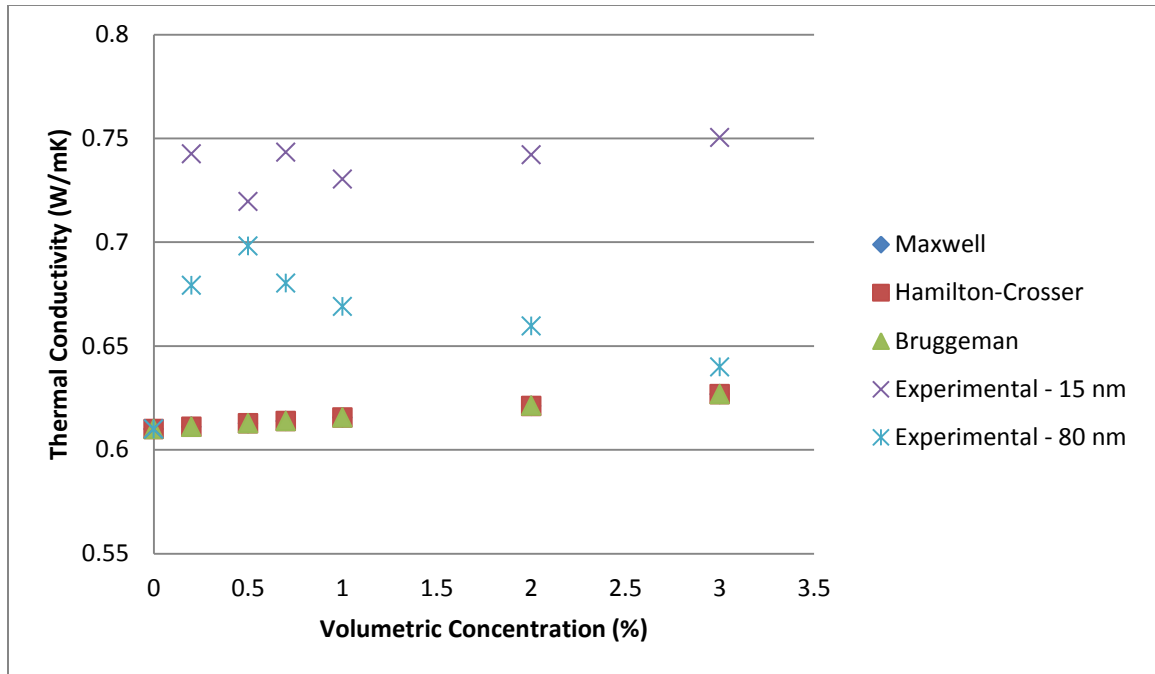


**Figure 23.** Thermal conductivity comparison, SiO<sub>2</sub>/Water, thermophoresis and gravity in same directions.

Al<sub>2</sub>O<sub>3</sub>/Water nanofluids produced similar results, Fig. 24. Al<sub>2</sub>O<sub>3</sub>/Water nanofluids containing nanoparticles with a diameter of 10 nm produced higher thermal conductivity enhancement than nanofluids using particles with a diameter of 150nm. The highest enhancement, 23%, was obtained using Al<sub>2</sub>O<sub>3</sub>/Water nanofluids with a particle diameter of 10 nm and a volumetric concentration of 0.2%. Similarly, at volumetric concentrations of 0.5%, 0.7%, 1%, 2%, and 3% the thermal conductivity for Al<sub>2</sub>O<sub>3</sub>/Water nanofluids with particle diameter of 10 nm was enhanced by 22.5%, 22.1%, 17.3%, 19.6%, and 22.4% respectively. For the Al<sub>2</sub>O<sub>3</sub>/Water nanofluid with a particle size of 10 nm, the thermal conductivity increased over time by 7.14% and 2.68% with volumetric concentrations of 0.2% and 0.5% respectively. At volumetric concentrations of 0.7% and 1%, the thermal conductivity was almost constant over time with a total change of 0.31% and 0.65% respectively. The thermal conductivity decreased by 2.57% and 7.99% after

20 minutes for volumetric concentrations of 2% and 3% respectively. Similar results were obtained using  $\text{Al}_2\text{O}_3/\text{Water}$  nanofluid using particles with a diameter of 150nm. At 0.2% and 0.5% volumetric concentrations, the thermal conductivity increased by 7.10% and 3.15% respectively. At a volumetric concentration of 0.7%, there was a negligible change in thermal conductivity with a change of 0.42% after 20 minutes. At volumetric concentrations of 1%, 2% and 3%, the thermal conductivity decreased by 4.73%, 9.44% and 3.02% respectively.

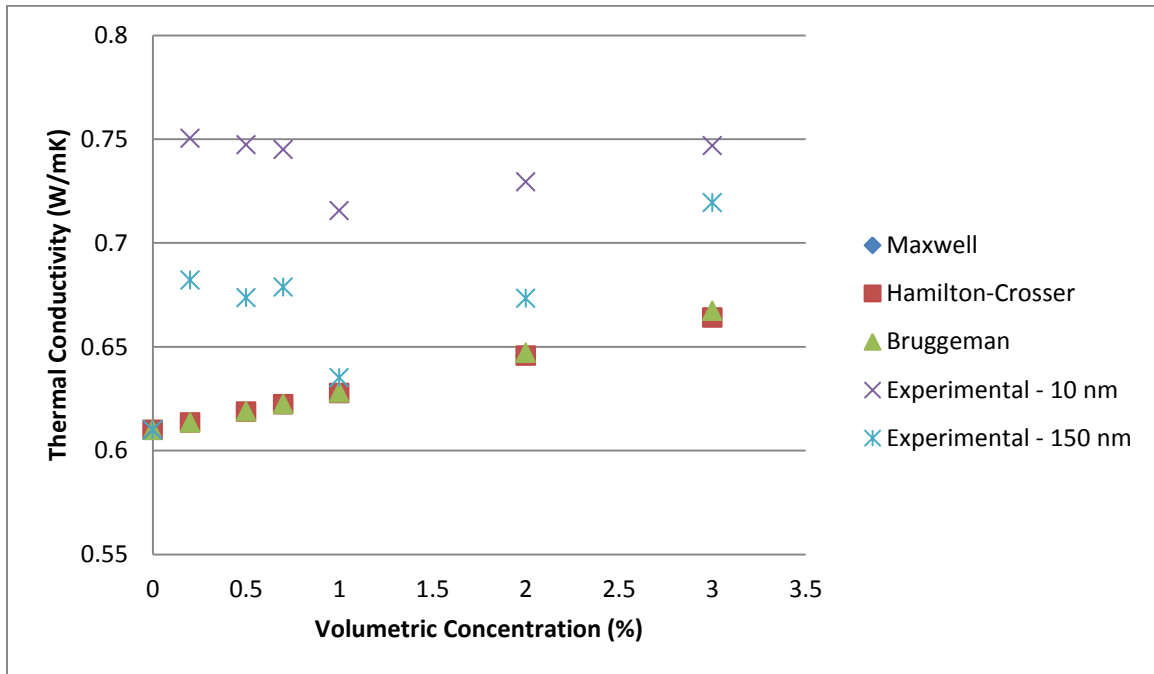


**Figure 24.** Thermal conductivity comparison,  $\text{Al}_2\text{O}_3/\text{Water}$ , thermophoresis and gravity in same direction.

### 5.3 Motion of Nanoparticles

The theoretical results show the settling velocity is higher than the velocity of thermophoresis for  $\text{Al}_2\text{O}_3/\text{Water}$  nanofluids, Table 11. The settling velocity of

Al<sub>2</sub>O<sub>3</sub>/Water nanofluids is 1.694E-10 m/s and 3.8115E-8 m/s for Al<sub>2</sub>O<sub>3</sub>/Water nanofluids with a particle diameter of 15 nm and 150 nm respectively. The velocity of thermophoresis is 7.32E-10 m/s. On the other hand, the velocity of thermophoresis for SiO<sub>2</sub>/Water nanofluids was higher than the settling velocity. The settling velocity is 1.577E-10 m/s and 4.486E-9 m/s for SiO<sub>2</sub> nanofluids with a particle diameter of 15 nm and 80 nm respectively. The velocity of thermophoresis is 1.15E-8 m/s. The higher settling velocity for Al<sub>2</sub>O<sub>3</sub>/Water nanofluids indicates most particles are settling at the sensor. As more particles accumulate at the sensor, especially at bigger volumetric concentrations, the temperature of the sample surrounding the sensor is significantly lower, affecting the final thermal conductivity reading. This is due to the much higher thermal conductivity of the Al<sub>2</sub>O<sub>3</sub> nanoparticles (40 W/mK) as opposed to the thermal conductivity of SiO<sub>2</sub> nanoparticles (1.4 W/mK). As shown is eq. 46 the higher the thermal conductivity on the particles, the lower the temperature of the fluid surrounding the sensor.

$$q = \frac{kA(T_{sensor}-T_{room})}{\Delta x} \quad (45)$$

solving for T<sub>sensor</sub> gives

$$T_{sensor} = T_{room} + \frac{qx}{kA} \quad (46)$$

this behavior was confirmed by the experimental results as Al<sub>2</sub>O<sub>3</sub>/Water had lower T<sub>sensor</sub> than SiO<sub>2</sub>/Water nanofluids and it decreased as the volumetric concentration increased. Fig. 25 shows the direction of the velocities in the experimental set up with the sensor facing up.

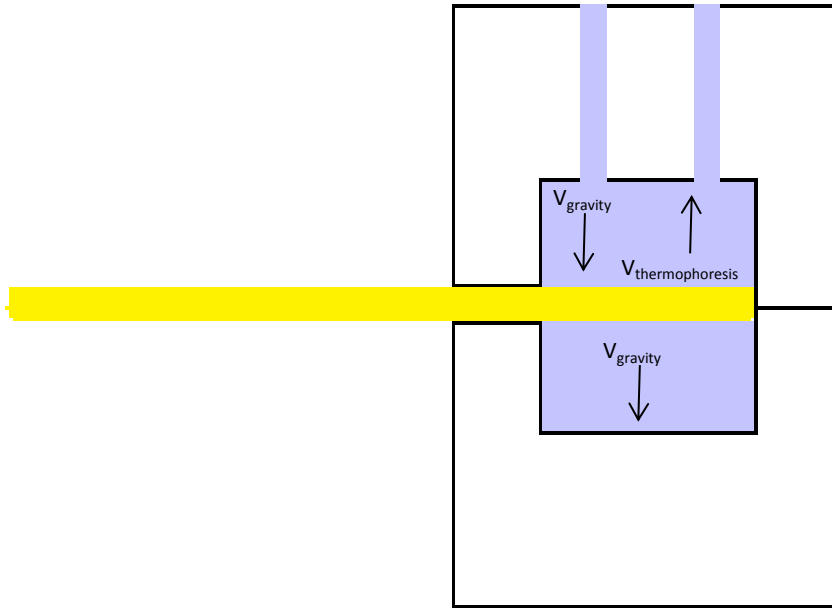


**Figure 25. Velocity diagram**

In order to observe the Brownian diffusion and thermophoretic diffusion effects, the thermal conductivity of each sample was taken every minute for a period of time, Fig. 26 - 73. The diffusion times are shown in Table 17. The overall diffusion time was significantly lower for SiO<sub>2</sub>/Water nanofluids. The thermal conductivity for Al<sub>2</sub>O<sub>3</sub>/Water nanofluids increased over time for all volumetric concentration and size. On the other hand, the thermal conductivity for SiO<sub>2</sub>/Water nanofluids increased over time for lower volumetric concentration but it decreased over time for higher volumetric concentrations. This trend was observed for both nanoparticles, 10 nm and 150 nm in diameter.

The mass flux due to thermophoretic effects was much larger than the mass flux due to Brownian diffusion, Tables 13 and 16. The overall mass flux for Al<sub>2</sub>O<sub>3</sub>/Water nanofluids was a magnitude lower than the mass flux for SiO<sub>2</sub>/Water nanofluids. The size

of the nanoparticles did not result in a significant difference in the mass flux. The mass flux increased linearly as the volumetric concentration increased.

**Table11. Settling velocity.**

<b>Settling Velocity</b>			
<b>Particle's Type/Size</b>	<b>dp (m)</b>	<b>Density (kg/m<sup>3</sup>)</b>	<b>Settling Velocity (m/s)</b>
Al <sub>2</sub> O <sub>3</sub> /10 nm	1.00E-08	3900	1.694E-10
Al <sub>2</sub> O <sub>3</sub> /150 nm	1.50E-07	3900	3.8115E-08
SiO <sub>2</sub> /15nm	1.50E-08	2200	1.57717E-10
SiO <sub>2</sub> /80nm	8.00E-08	2200	4.48617E-09

**Table 12. Brownian diffusion coefficient.**

<b>Brownian Diffusion Coefficient</b>		
<b>Particle's Type/Size</b>	<b>dp (m)</b>	<b>D<sub>B</sub> (m<sup>2</sup>/s)</b>
Al <sub>2</sub> O <sub>3</sub> /10 nm	1.00E-08	4.66E-11
Al <sub>2</sub> O <sub>3</sub> /150 nm	1.50E-07	3.11E-12
SiO <sub>2</sub> /15nm	1.50E-08	3.11E-11
SiO <sub>2</sub> /80nm	8.00E-08	5.82E-12

**Table 13. Mass flux due to Brownian diffusion.**

<b>Vol. Concentration</b>	<b>j<sub>p,B</sub></b>			
	<b>Al<sub>2</sub>O<sub>3</sub> /10 nm (kg/m<sup>2</sup>s)</b>	<b>Al<sub>2</sub>O<sub>3</sub> /150 nm (kg/m<sup>2</sup>s)</b>	<b>SiO<sub>2</sub> - 15nm (kg/m<sup>2</sup>s)</b>	<b>SiO<sub>2</sub> - 80nm (kg/m<sup>2</sup>s)</b>
0.2	-3.63E-08	-2.42E-09	-1.37E-08	2.56E-09
0.5	-9.08E-08	-6.06E-09	-3.42E-08	6.40E-09
0.7	-1.27E-07	-8.48E-09	-4.78E-08	8.97E-09
1	-1.82E-07	-1.21E-08	-6.83E-08	1.28E-08
2	-3.63E-07	-2.42E-08	-1.37E-07	2.56E-08
3	-5.45E-07	-3.63E-08	-2.05E-07	3.84E-08

**Table 14. Proportionality factor.**

<b>β (Al<sub>2</sub>O<sub>3</sub>) =</b>	<b>0.003847647</b>
<b>β (SiO<sub>2</sub>) =</b>	<b>0.060534351</b>



**Table 15. Thermophoresis velocity.**

$V_T (\text{Al}_2\text{O}_3) =$	-7.32E-10 m/s
$V_T (\text{SiO}_2) =$	-1.15E-08 m/s

**Table 16. Mass flux due to thermophoretic effects.**

Vol. Concentration	$j_{p,T}$			
	$\text{Al}_2\text{O}_3 / 10 \text{ nm (kg/m}^2\text{s)}$	$\text{Al}_2\text{O}_3 / 150 \text{ nm (kg/m}^2\text{s)}$	$\text{SiO}_2 - 15\text{nm (kg/m}^2\text{s)}$	$\text{SiO}_2 - 80\text{nm (kg/m}^2\text{s)}$
0.2	-5.71E-07	-5.71E-07	-5.07E-06	-5.07E-06
0.5	-1.43E-06	-1.43E-06	-1.27E-05	-1.27E-05
0.7	-2.00E-06	-2.00E-06	-1.77E-05	-1.77E-05
1	-2.86E-06	-2.86E-06	-2.53E-05	-2.53E-05
2	-5.71E-06	-5.71E-06	-5.07E-05	-5.07E-05
3	-8.57E-06	-8.57E-06	-7.60E-05	-7.60E-05

**Table 17. Diffusion times.**

Particle's Type/Size	Brownian Diffusion (s)	Thermophoresis Diffusion (s)
$\text{Al}_2\text{O}_3/10 \text{ nm}$	2.147E-06	1.366E+01
$\text{Al}_2\text{O}_3/150 \text{ nm}$	7.246E-03	2.049E+02
$\text{SiO}_2/15\text{nm}$	7.246E-06	1.302E+00
$\text{SiO}_2/80\text{nm}$	1.099E-03	6.946E+00

## Chapter 6

### Conclusion and Future Recommendations

#### 6.1 Conclusion

This research presents the effects of base fluids, volumetric concentration, and particle size on thermal conductivity of nanofluids. The effects of gravity, Brownian motion, and thermophoresis on the motion of the nanoparticles are also studied. Ionized water is in the only base fluid that produced a significant enhancement in thermal conductivity.

The rapid settling of the particles reduces significantly the enhancement of the thermal conductivity of nanofluids, even when the nanofluids are mixed with a sonifier. The effects of sonication do not last long, as observed in the rapid particle settling found in all samples. When the sensor was facing up, the thermal conductivity reading decreased as the particles settle at the sensor. This decrease in thermal conductivity was found almost immediately after placing the mixed nanofluid in the container for measurement. A powerful sonifier along with the use of surfactants is required to maintain the particles suspended for a significant amount of time.

The particle size is significant in the enhancement of the thermal conductivity. Smaller particles produced a higher overall thermal conductivity enhancement than bigger particles. The highest thermal conductivity enhancement, 23%, was found in  $\text{Al}_2\text{O}_3$ /Water nanofluids using particles with a diameter of 10 nm and a volumetric concentration of 0.2%. Similar enhancements were found using  $\text{SiO}_2$ /Water nanofluids with particle diameter of 15 nm and volumetric concentrations of 0.2% and 3%. The

volumetric concentration does not have a significant effect in the thermal conductivity. The thermal conductivity enhancement varied little among samples at different volumetric concentrations of same nanoparticle type and size.

Brownian motion and thermophoresis also play a significant role in the enhancement of thermal conductivity of nanofluids. Over time, the thermal conductivity increased at lower volumetric concentrations and decreased at higher volumetric concentrations. Additionally, the direction of the motion of the particles due to gravity and thermophoresis is significant. When the thermophoresis force pointed in the opposite direction of gravity, the settling velocity was higher than the thermophoresis force and thus the particles settle at the sensor producing no enhancement; however, a significant enhancement was obtained when these forces pointed in the same direction.

## **6.2 Future Studies**

During this study, it was noted that the particles settle very rapidly. In practical applications, a stable mixture is necessary in order to use nanofluids as an alternative. Therefore, it is recommended that surfactants are used along with a sonicator. A study of the effects of different surfactants may be performed if there is any evidence it may play a role in the total enhancement of the thermal conductivity.

Additionally, a significant enhancement was found when gravity and thermophoresis pointed in the same direction. An optimization process for the creation of nanofluids and the forces affecting it may be necessary in order to make use of nanofluids for commercial application possible.

## References

- [1] L. C. Thomas, Heat Transfer Professional Version, second edition. Capstone Publishing Corporation.
- [2] H. S. Nalwa, Nanostructured Materials and Nanotechnology – Concise Edition, Academic Press, 2002.
- [3] R. W. Seigel, Materials Science and Technology, Vol. 15, p. 583, VCH Publishers, 1991.
- [4] (a) T. Goto, S. Saito, and M. Tanaka, Solid State Commun. 80, 331 (1991), (b) R. F. Ziolo, E.P. Giannelis, B.A. Weinstein, M.P. O'Horo, B.N. Ganguly, V. Mehrotra, M.W. Rusell, and D.R. Huffman, Science 257, 219 (1992).
- [5] M. Fernandez-Garcia, J. A. Rodriguez, Metal Oxide Nanoparticles - Nanomaterials: Inorganic and Bioinorganic Perspectives, Brookhaven National Laboratory, Oct. 2007.
- [6] Weertman, J.R.; Averback, R.S. Mechanical properties in “Nanomaterials: synthesis, properties and applications” (Edelstein, A.S.; Cammarata, R.C.; Eds.). Inst. Physics Publishing: London, 1996.
- [7] Tjong, S.C.; Chen, H.; Mat. Sci. Eng. 2004, 45, 1.
- [8] Zhang, Z.; Seal, S.; Patil, S.; Zha, C.; Xue, Q.; J. Phys. Chem. C. 2007, 111, 11756.
- [9] Cai, S.-H.; Rashkeev, S.N.; Pantelides, S.T.; Sohlberg, K.; Phys. Rev. B 2003, 67, 224104.
- [10] Rodríguez, J.A., Fernández-García, M; (Eds.) Synthesis, Properties and Applications of Oxide Nanoparticles. Wiley: New Jersey, 2007.
- [11] Sharma, P.K.; Varadan, V.V.; Varadan, V.K.; J. European Ceramic Soc. 2003, 23, 659.
- [12] Noda, H.; Muramoto, H.K.; J. Mater. Sci. 2003, 38, 2043.
- [13] McHale, J.M.; Yureki, K.; Dabbs, D.M.; Novrotsky, A.; Sunderesan, S.; Aksay, I.A.; Chem. Mater., 1997, 9, 3096.
- [14] Mather, G.C.; Martinez-Arias; A.; Transport properties and Oxygen Handling in “Synthesis, Properties and Applications of Oxide Nanoparticles” (Rodríguez, J.A., Fernández-García, M; Eds.). Wiley: N.J., 2007. Chpt. 13.
- [15] P. Auerkari, Mechanical and Physical Properties of Engineering alumina ceramics, VTT Manufacturing Technology, 1996

- [16] Dr. Kamar Shah Ariffin (2004) EBS 425 – Mineral Perindustrian
- [17] Fused Silica Material Properties, Accuratus Ceramic Corporation. Retrieve from <http://accuratus.com/pdf/SiO2props.pdf>
- [18] Properties of Ethylene Glycol, Retrieve from [http://www.sbioinformatics.com/design\\_thesis/Ethylene\\_Glycol/Ethyleneglycol\\_Properties&uses.pdf](http://www.sbioinformatics.com/design_thesis/Ethylene_Glycol/Ethyleneglycol_Properties&uses.pdf)
- [19] Ethylene Glycol, Diethylene Glycol, Triethylene Glycol, Huntsman Corporation, 1998.
- [20] C. Chien, Fundamental Characteristics of Water, Department of Chemistry, University of Waterloo, Ontario, Canada.
- [21] Handbook of Chemistry and Physics, 76<sup>th</sup> Edition.
- [22] W.S. Janna, Design of Fluid Thermal Systems – second edition. PWS Publishing Company 1998.
- [23] M. Chandrasekara, S. Sureshb, T. Senthilkumar, Mechanisms proposed through experimental investigations on thermophysical properties and forced convective heat transfer characteristics of various nanofluids – A review, Renewable and Sustainable Energy Reviews (2011)
- [24] Lee JH, Hwang KS, Jang SP, Lee BH, Kim JH, Choi SUS, et al, Effective viscosities and thermal conductivities of aqueous nanofluids containing low volume concentrations of Al<sub>2</sub>O<sub>3</sub> nanoparticles, International Journal of Heat and Mass Transfer 2008;51:2651–6.
- [25] Chandrasekar M, Suresh S, Chandra Bose A, Experimental investigations and theoretical determination of thermal conductivity and viscosity of Al<sub>2</sub>O<sub>3</sub>/water nanofluid, Experimental Thermal and Fluid Science 2010;34:210–6.
- [26] Jahanshahi M, Hosseinizadeh SF, Alipanah M, Dehghani A, Vakilinejad GR, Numerical simulation of free convection based on experimental measured conductivity in a square cavity using Water/SiO<sub>2</sub> nanofluid, International Communications in Heat and Mass Transfer 2010;37:687–94.
- [27] Vajjha RS, Das DK, Experimental determination of thermal conductivity of three nanofluids and development of new correlations, International Journal of Heat and Mass Transfer 2009;52:4675–82.
- [28] Xie H, Li Y, Yu W, Intriguingly high convective heat transfer enhancement of nanofluid coolants in laminar flows, Physics Letters A 2010;374:2566–8.

- [29] Anoop KB, Kabelac S, Sundararajan T, Das SK, Rheological and flow characteristics of nanofluids: influence of electroviscous effects and particle agglomeration, *Journal of Applied Physics* 2009;106:034909.
- [30] Pak BC, Cho Y, Hydrodynamic and heat transfer study of dispersed fluids with submicron metallic oxide particle, *Experimental Heat Transfer* 1998;11:151–70.
- [31] Sommers AD, Yerkes KL. Experimental investigation into the convective heat transfer and system-level effects of Al<sub>2</sub>O<sub>3</sub>-propanol nanofluids. *Journal of Nanoparticle Research* 2010;12:1003–14.
- [32] Zhou SQ, Ni R. Measurement of the specific heat capacity of water-based Al<sub>2</sub>O<sub>3</sub> nanofluid. *Applied Physics Letters* 2008;92:093123.
- [33] John Philip, P.D. Shima, Thermal properties of nanofluids, *Advances in Colloid and Interface Science* (2012).
- [34] Teng TP, Hung YH, Teng TC, Moa HE, Hsu HG, The effect of alumina/water nanofluid particle size on thermal conductivity, *App Therm Eng* 2010;30:2213-8.
- [35] Patel HE, Sundararajan T, Das SK, An experimental investigation into the thermal conductivity enhancement in oxide and metallic nanofluids,. *J Nanopart Res* 2010;12:1015-31.
- [36] Chopkar M, Das PK, Manna I, Synthesis and characterization of nanofluid for advanced heat transfer applications, *Scr Mater* 2006;55:549-52.
- [37] Chopkar M, Kumar S, Bhandari DR, Das PK, Mannaa I. Development and characterization of Al<sub>2</sub>Cu and Ag<sub>2</sub>Al nanoparticle dispersed water and ethylene glycol based nanofluid. *Mater Sci Eng B* 2007;139:141-8.
- [38] Chopkar M, Sudarshan S, Das PK, Manna I. Effect of Particle Size on Thermal Conductivity of Nanofluid. *Mettal Mater Trans A* 2008;39:1535-42.
- [39] Hong J, Kim SH, Kim D, Effect of laser irradiation on thermal conductivity of ZnO Nanofluids, *J Phys: Conference Series* 2007;59:301-4.
- [40] Beck MP, Yuan Y, Warriar P, Teja AS, The thermal conductivity of aqueous nanofluids containing ceria nanoparticles, *J Appl Phys* 2010;107:066101.
- [41] Chen G, Yu W, Singh D, Cookson D, Routbort J, Application of SAXS to the study of particle size dependent thermal conductivity in silica nanofluids, *J Nanopart Res* 2008;10:1109-14.

- [42] Timofeeva EV, Smith DS, Yu W, France DM, Singh D, Routbort JL, Particle size and interfacial effects on thermo-physical and heat transfer characteristics of water-based  $\alpha$ -SiC nanofluids, *Nanotechnology* 2010;21:215703.
- [43] Shalkevich N, Escher W, Burgi T, Michel B, Ahmed LS, Poulikakos D, On the Thermal Conductivity of Gold Nanoparticle Colloids, *Langmuir* 2010;26: 663-70.
- [44] Beck MP, Yuan Y, Warriar P, Teja AS, The effect of particle size on the thermal conductivity of alumina nanofluids, *J Nanopart Res* 2009;11:1129-36.
- [45] Gowda R, Sun H, Wang P, Charmchi M, Gao F, Gu Z, et al. Effects of Particle Surface Charge, Species, Concentration, and Dispersion Method on the Thermal Conductivity of Nanofluids. *Adv Mech Eng* 2010;2010:1–10.
- [46] Meibodi ME, Sefti MV, Rashidi AM, Amrollahi A, Tabasi M, Kalal HS, The role of different parameters on the stability and thermal conductivity of carbon nanotube/water nanofluids, *Int Commu Heat Mass Transfer* 2010;37:319-23.
- [47] Karthikeyan NR, Philip J, Raj B. Effect of clustering on the thermal conductivity of nanofluids. *Mater Chem Phys* 2008;109:50-5.
- [48] J.C. Maxwell, *A Treatise on Electricity and Magnetism*, second ed. Clarendon Press, Oxford, UK, 1881.
- [49] R.L. Hamilton, O.K. Crosser, Thermal Conductivity of Heterogeneous Two Component Systems, *I&EC Fundamentals* 1 (1962) 182–191.
- [50] D.A.G. Bruggeman, Calculation of Various Physical Constants of Heterogeneous Substances, I. dielectric constants and conductivity of the substances from mischkorper isotropic, *Annals of Physics Leipzig* 24 (1935) 636–679.
- [51] Fei Duan, Thermal Property Measurement of Al<sub>2</sub>O<sub>3</sub>-Water, Nanofluids School of Mechanical and Aerospace Engineering, Nanyang Technological University Singapore
- [52] Khalil Khanafer, Kambiz Vafai, A critical synthesis of thermophysical characteristics of nanofluids, *International Journal of Heat and Mass Transfer* (2011)
- [53] Rohit S. Khedkar, Shriram S. Sonawane, Kailas L. Wasewar, Influence of CuO nanoparticles in enhancing the thermal conductivity of water and monoethylene glycol based nanofluids, *International Communications in Heat and Mass Transfer* (2012)
- [54] S.M.S. Murshed, K.C. Leong, C. Yang, Investigations of thermal conductivity and viscosity of nanofluids, *International Journal of Thermal Sciences* 47 (2008) 560–568.

- [55] A. Einstein, Eine neue bestimmung der molekuldimensionen, *Ann. Phys., Leipzig* 19 (1906) 289–306.
- [56] H.C. Brinkman, The viscosity of concentrated suspensions and solutions, *J. Chem. Phys.* 20 (1952) 571.
- [57] S. Maiga, S.J. Palm, C.T. Nguyen, G. Roy, N. Galanis, Heat transfer enhancement by using nanofluids in forced convection flows, *Int. J. Heat Fluid Flow* 26 (2005) 530–546.
- [58] E. Abu-Nada, A.J. Chamkha, Effect of nanofluid variable properties on natural convection in enclosures filled with a CuO–EG–Water nanofluid, *Int. J. Therm.Sci.* 49 (12) (2010) 2339–2352.
- [59] X. Wang, X. Xu, S.U.S. Choi, Thermal conductivity of nanoparticles–fluid mixture, *J. Thermophys. Heat Transfer* 13 (1999) 474–480.
- [60] Gardner, K.A., 1945, Efficiency of extended surface, *Trans. ASME, Journal of Heat Transfer*, no. 65: p.621-631.
- [61] Schmidt, T.E., 1949, Heat transfer calculation for extended surfaces, *Refrigerating Engineering*, vol. 57: p.351-357.
- [62] P. Wais, Fin-Tube Heat Exchanger Optimization, Cracow University of Technology, Department of Thermal Power Engineering, Poland.
- [63] Branson Ultrasonic Corporation, Digita sonifier<sup>®</sup> Models 250 & 450 User's Manual.
- [64] Therm Test inc, Thermal Constant Analyser TPS 500 S User's Manual
- [65] Brookfield Engineering Laboratories, INC, Brookfield Digital Viscometer model DV-I+ Operating Instructions.
- [66] N. Jamshidi, M. Farhadi, K. Sedighi, D. Domeiry, Optimization of Design Parameters for Nanofluids Flowing Inside Helical Clois, *International Communications in Heat and Mass Transfer*, 2011.
- [67] W. C. William, *Aerosol technology – Properties, Behavior, and Measurement of Airborne particles*, John Wiley & Sons Ins, 1999.
- [68] McNab, G. S., Meisen, A., Thermophoresis in Liquids, *J. Colloid Interface Sci.*, 442, pp. 339 (1973).



## Appendix A: Nomenclature

$\sigma$  – yield stress

H – hardness

d – diameter

$k_h$  – slope

$\varepsilon$  – strain rate

D – diffusion coefficient

G – shear modulus

b – Burger's vector

$\dot{m}$  – mass flow rate

$\rho$  – density

V – velocity

$F_D$  – drag force

$J$  – flux of particles

$C_c$  – Cunningham correction factor

$k_B$  – Boltzmann's constant

T – temperature

$K_{th}$  – thermophoretic diffusion coefficient

$\mu$  – viscosity

$\beta$  – proportionality factor

$k$  – thermal conductivity

$\tau$  – shear stress

$F$  – force

A – area

$\emptyset$  – volumetric concentration

$p$  – subscript - nanoparticle

$b$  – subscript – base fluid

$nb$  – subscript – nanofluid

$\psi$  – shape factor

## Appendix B: Figures of thermal conductivity results over time

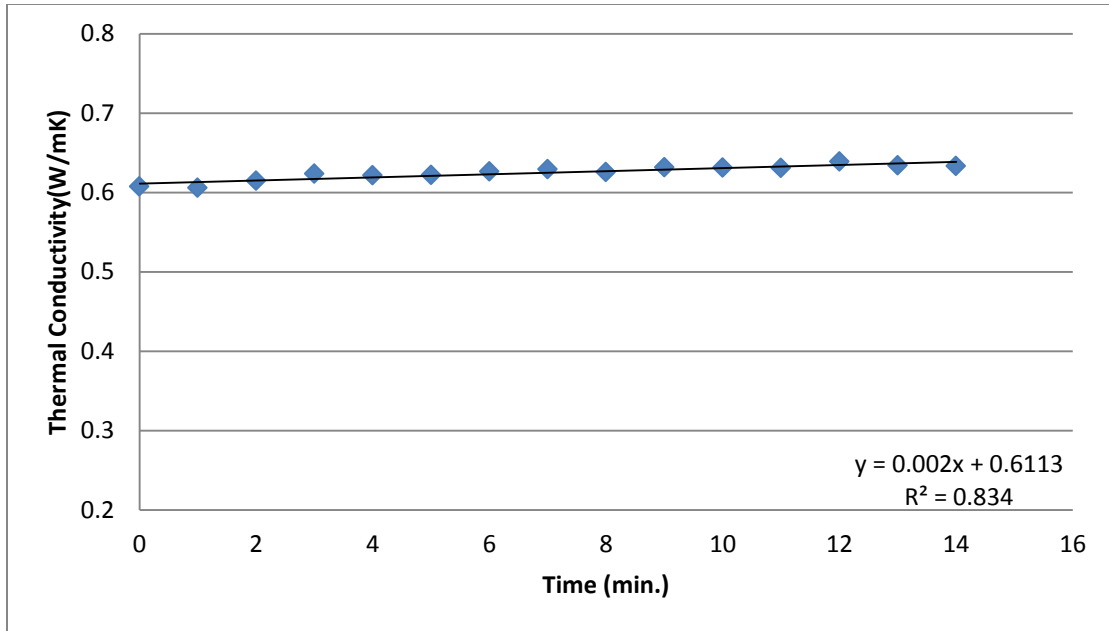


**Figure 26.** Al<sub>2</sub>O<sub>3</sub>/Water, 10 nm, 0.2% vol. concentration, thermophoresis and gravity in opposite directions.

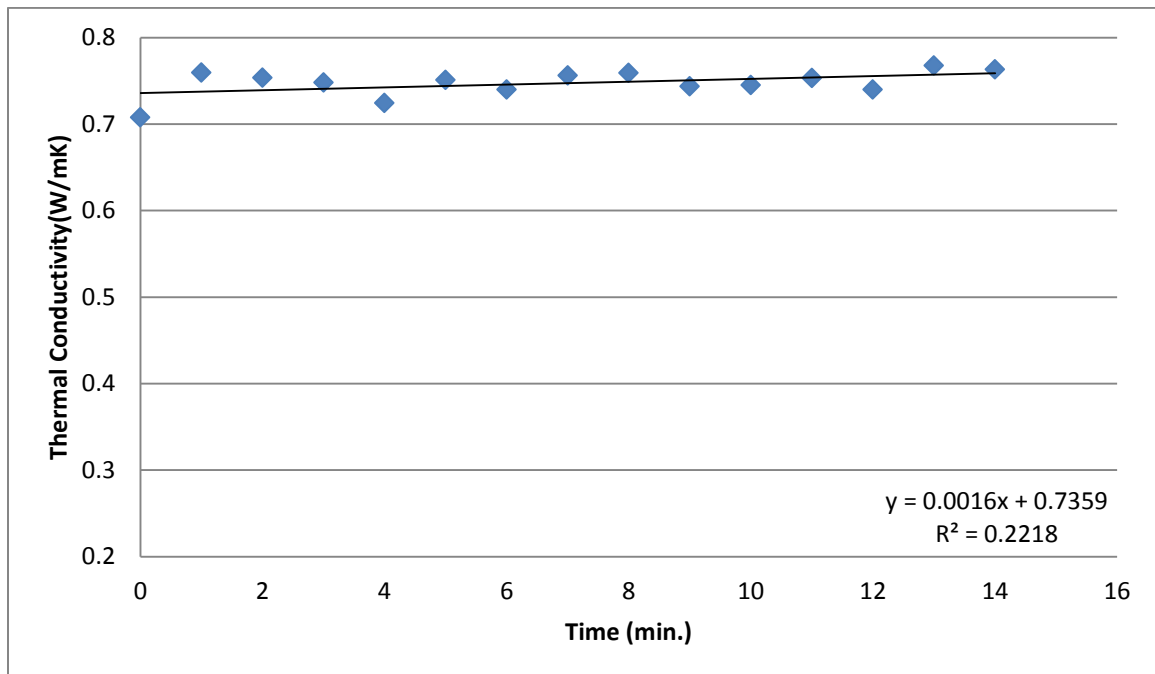


**Figure 27.** Al<sub>2</sub>O<sub>3</sub>/Water, 10 nm, 0.2% vol. concentration, thermophoresis and gravity in same directions.

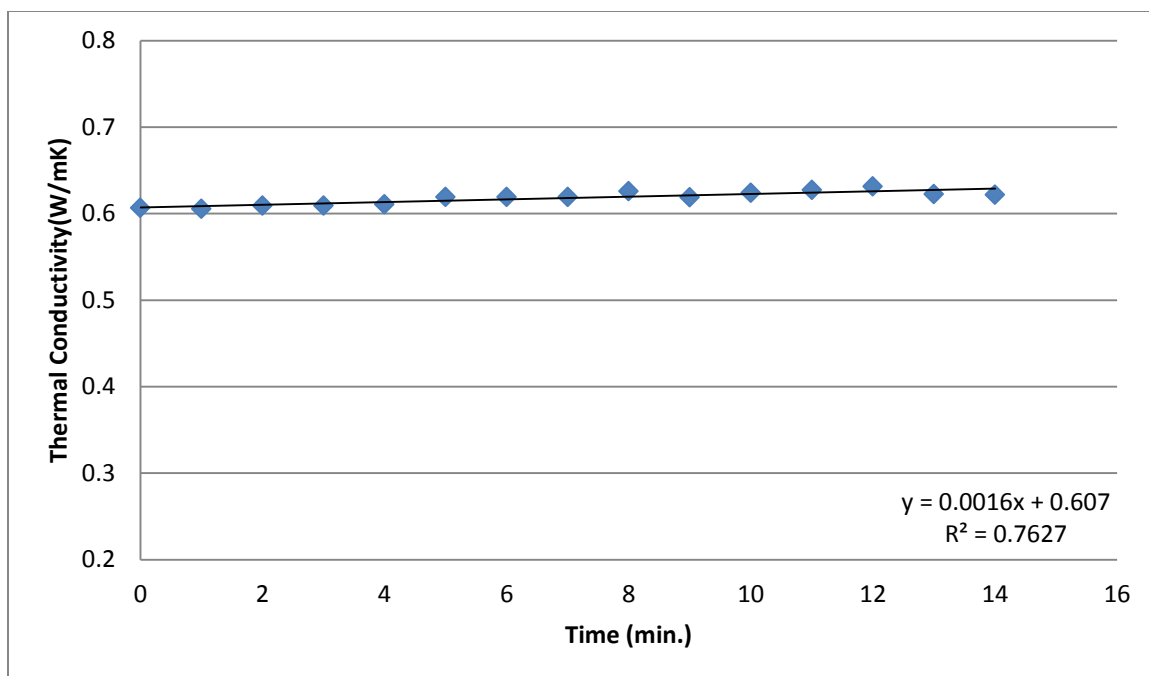


**Figure 28.** Al<sub>2</sub>O<sub>3</sub>/Water, 10 nm, 0.5% vol. concentration, thermophoresis and gravity in opposite directions.

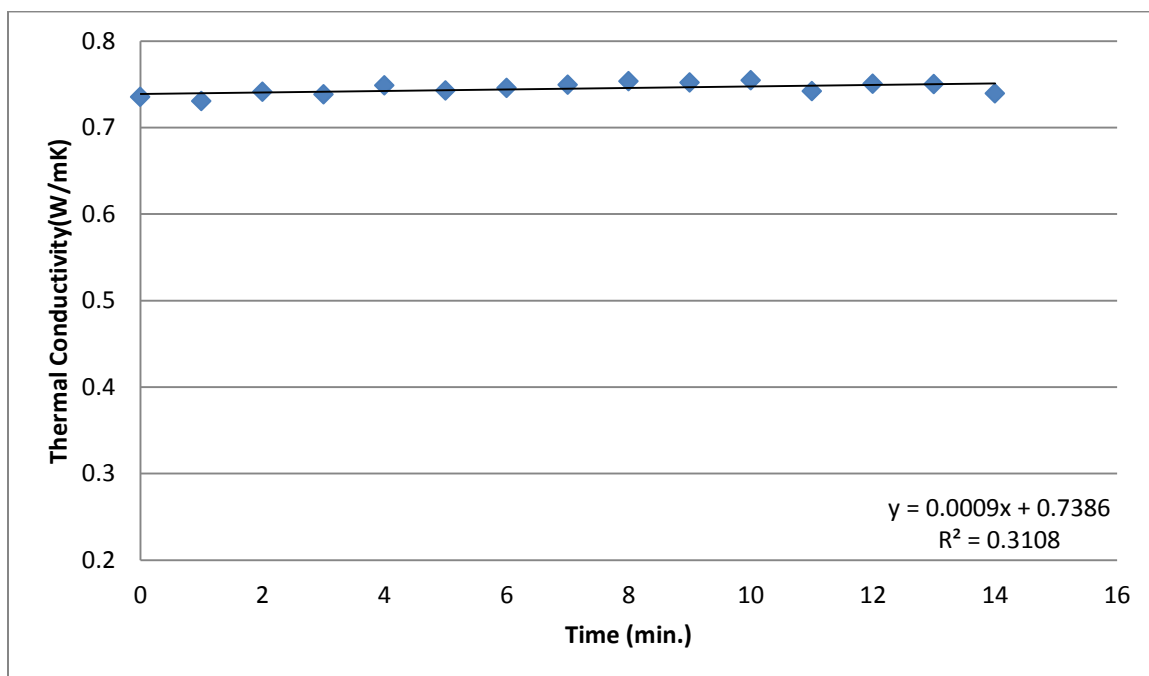


**Figure 29.** Al<sub>2</sub>O<sub>3</sub>/Water, 10 nm, 0.5% vol. concentration, thermophoresis and gravity in same directions.

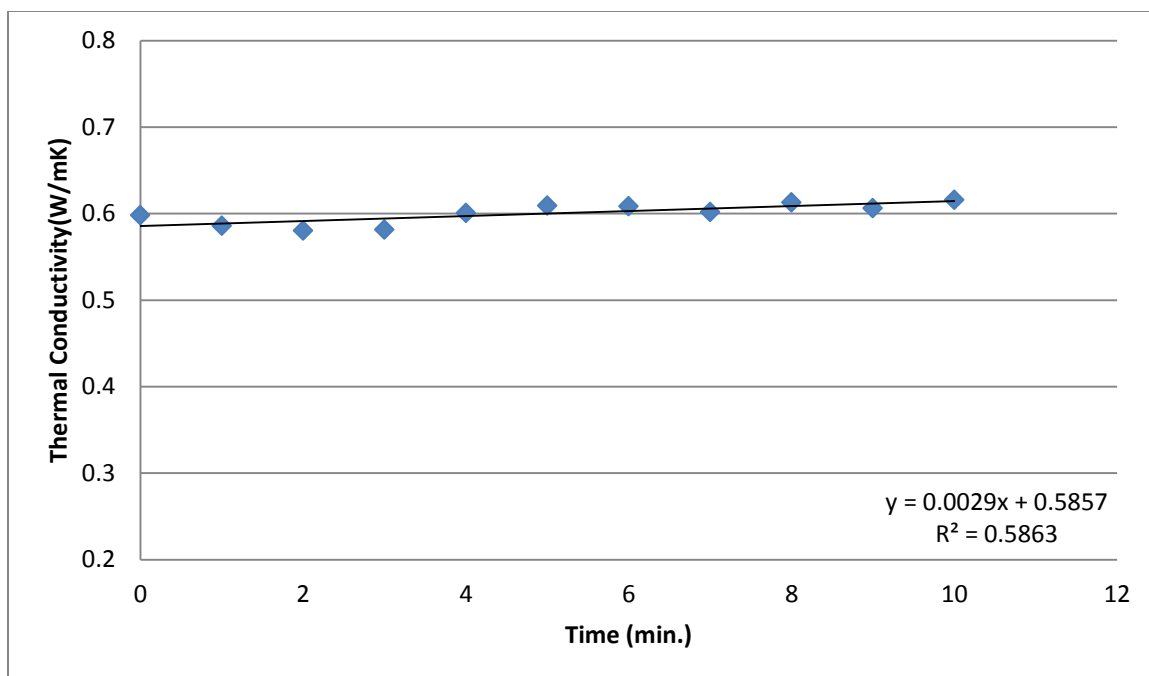


**Figure 30.** Al<sub>2</sub>O<sub>3</sub>/Water, 10 nm, 0.7% vol. concentration, thermophoresis and gravity in opposite directions.

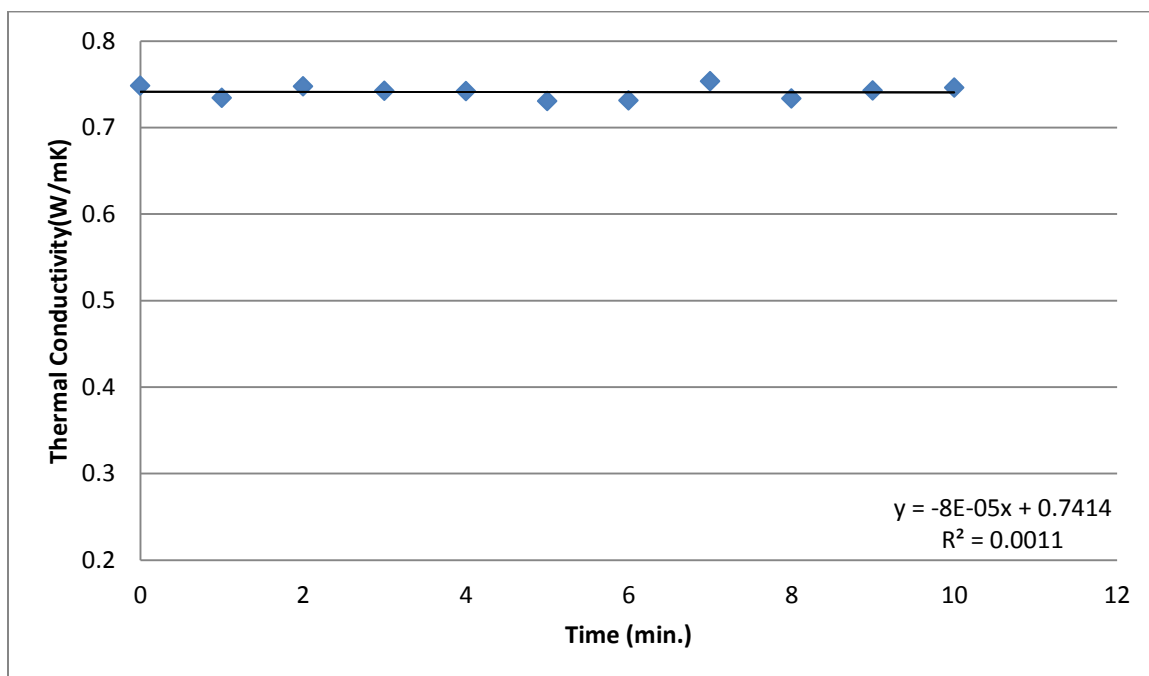


**Figure 31.** Al<sub>2</sub>O<sub>3</sub>/Water, 10 nm, 0.7% vol. concentration, thermophoresis and gravity in same directions.

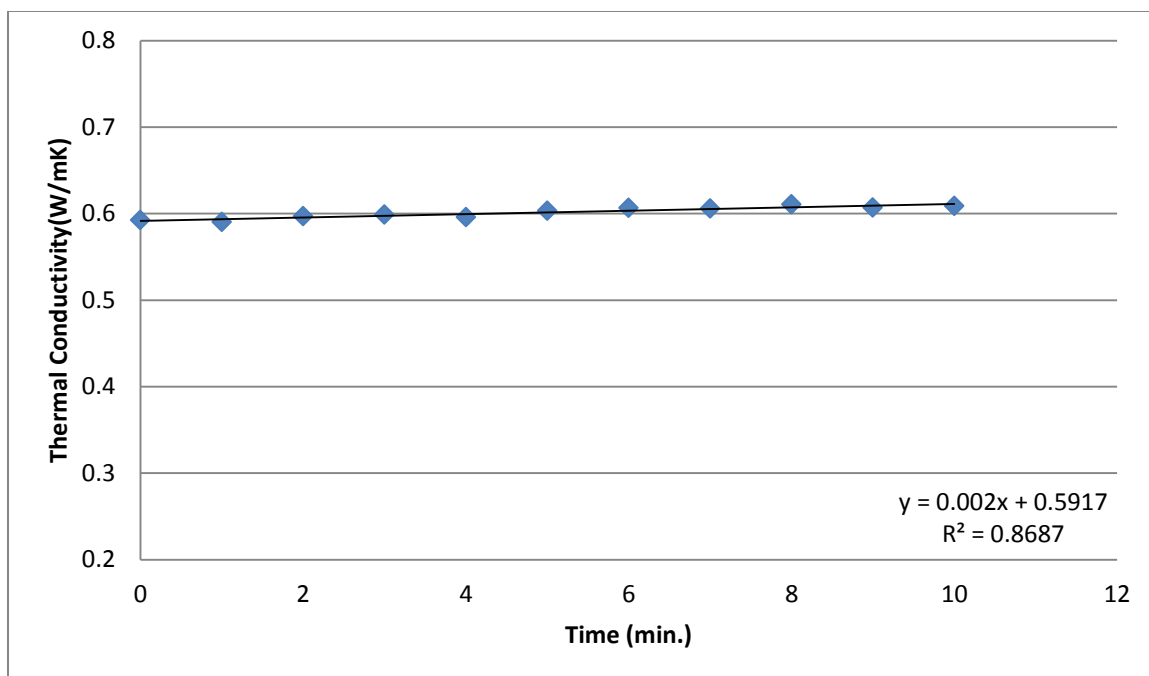


**Figure 32.** Al<sub>2</sub>O<sub>3</sub>/Water, 10 nm, 1% vol. concentration, thermophoresis and gravity in opposite directions.

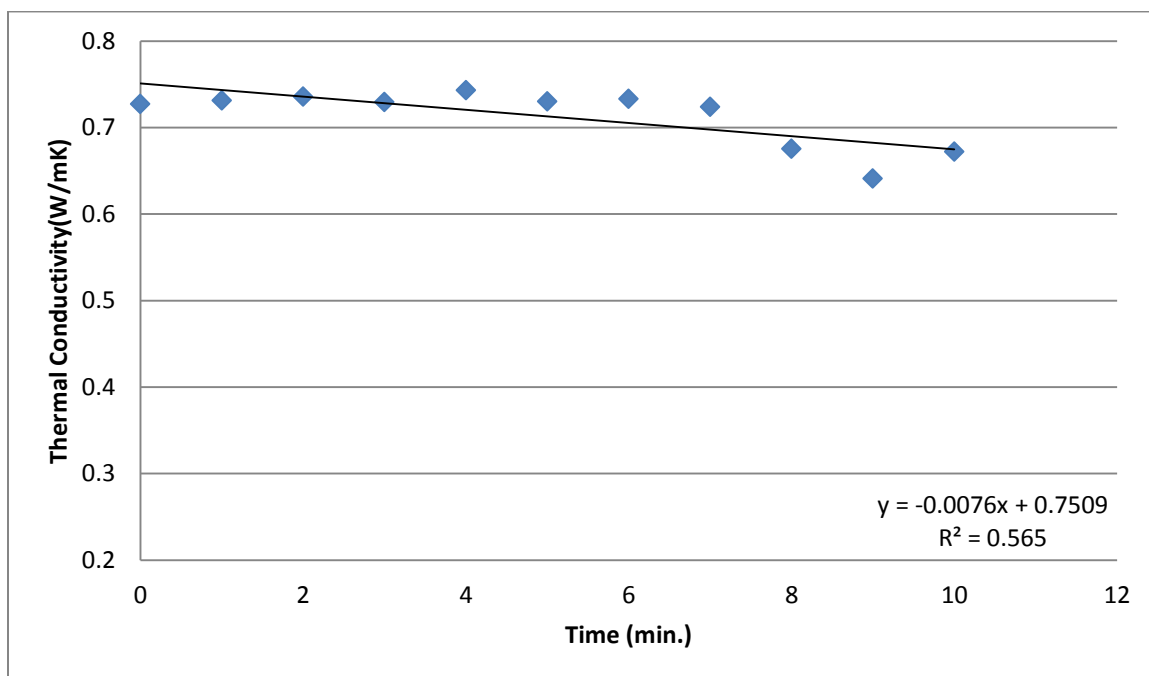


**Figure 33.** Al<sub>2</sub>O<sub>3</sub>/Water, 10 nm, 1% vol. concentration, thermophoresis and gravity in same directions.

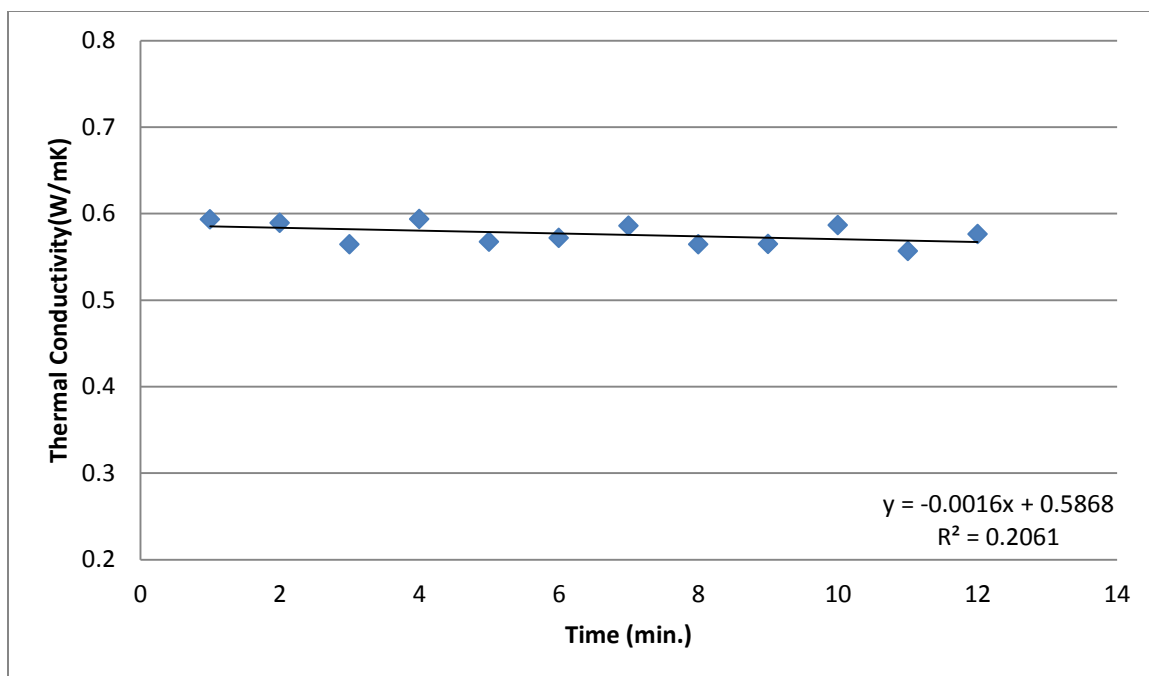


**Figure 34.** Al<sub>2</sub>O<sub>3</sub>/Water, 10 nm, 2% vol. concentration, thermophoresis and gravity in opposite directions.

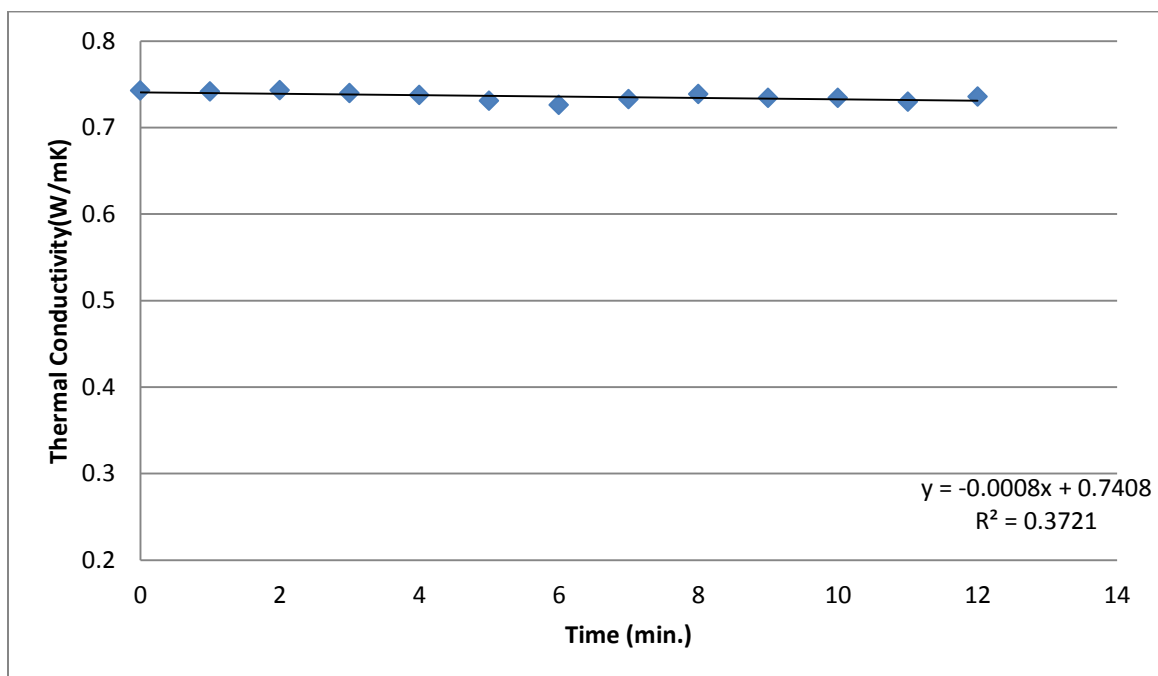


**Figure 35.** Al<sub>2</sub>O<sub>3</sub>/Water, 10 nm, 2% vol. concentration, thermophoresis and gravity in same directions.

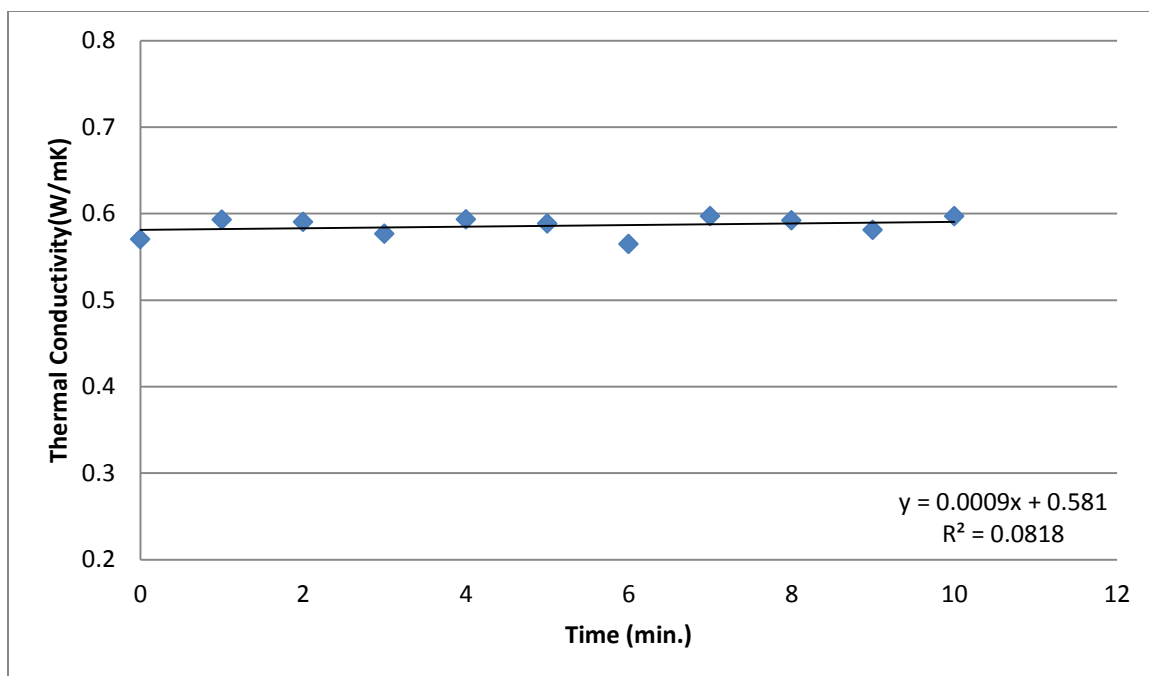


**Figure 36.** Al<sub>2</sub>O<sub>3</sub>/Water, 10 nm, 3% vol. concentration, thermophoresis and gravity in opposite directions.

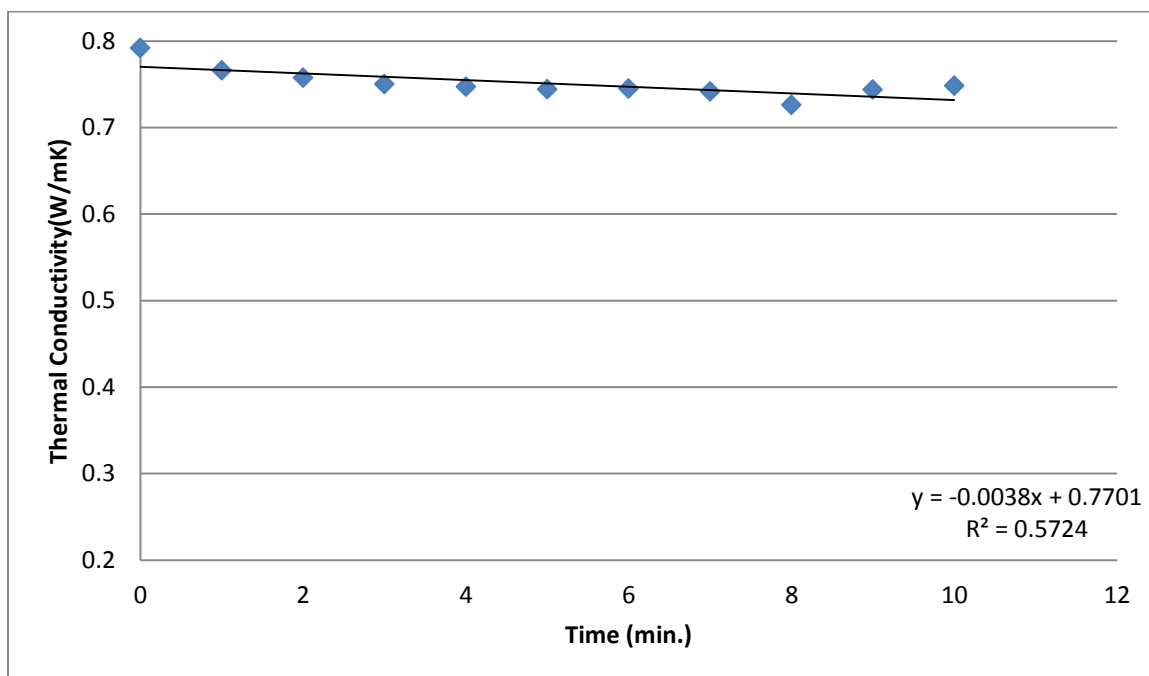


**Figure 37.** Al<sub>2</sub>O<sub>3</sub>/Water, 10 nm, 3% vol. concentration, thermophoresis and gravity in same directions.



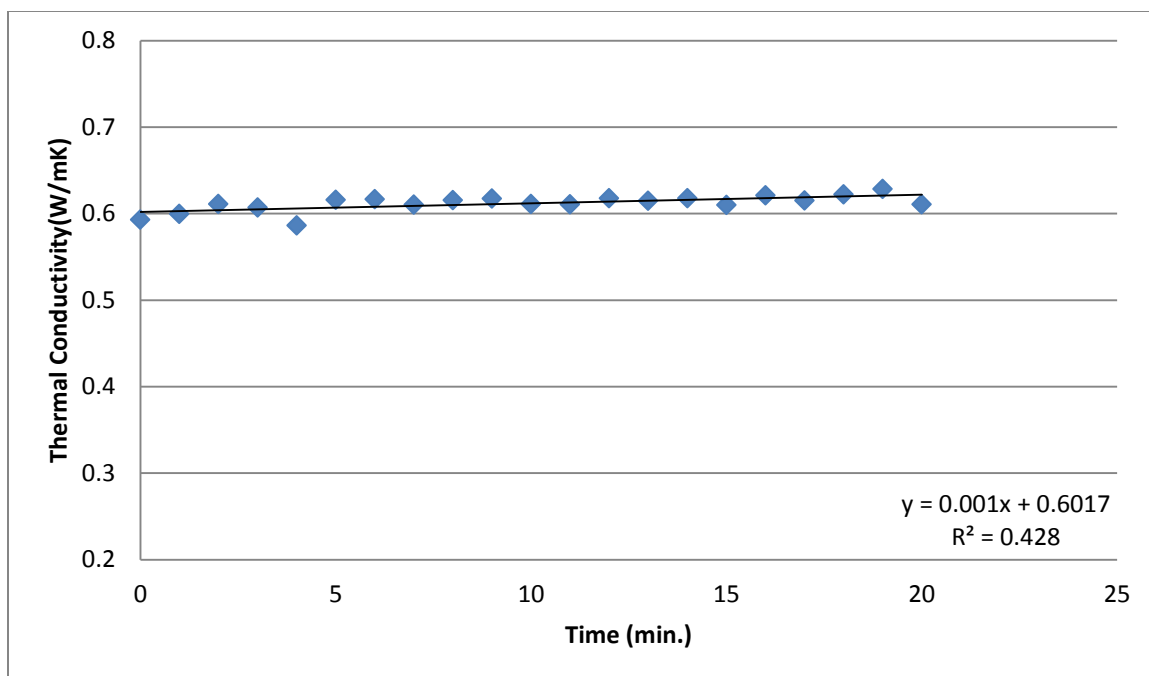


**Figure 38.** Al<sub>2</sub>O<sub>3</sub>/Water, 150 nm, 0.2% vol. concentration, thermophoresis and gravity in opposite directions.

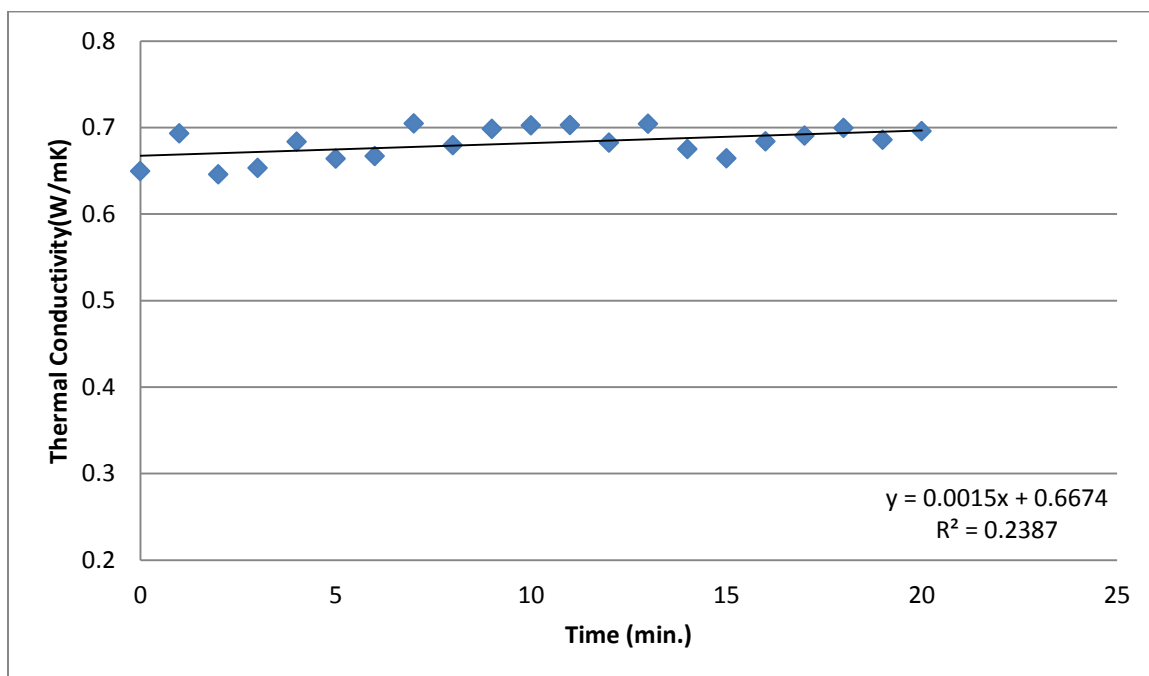


**Figure 39.** Al<sub>2</sub>O<sub>3</sub>/Water, 150 nm, 0.2% vol. concentration, thermophoresis and gravity in same directions.

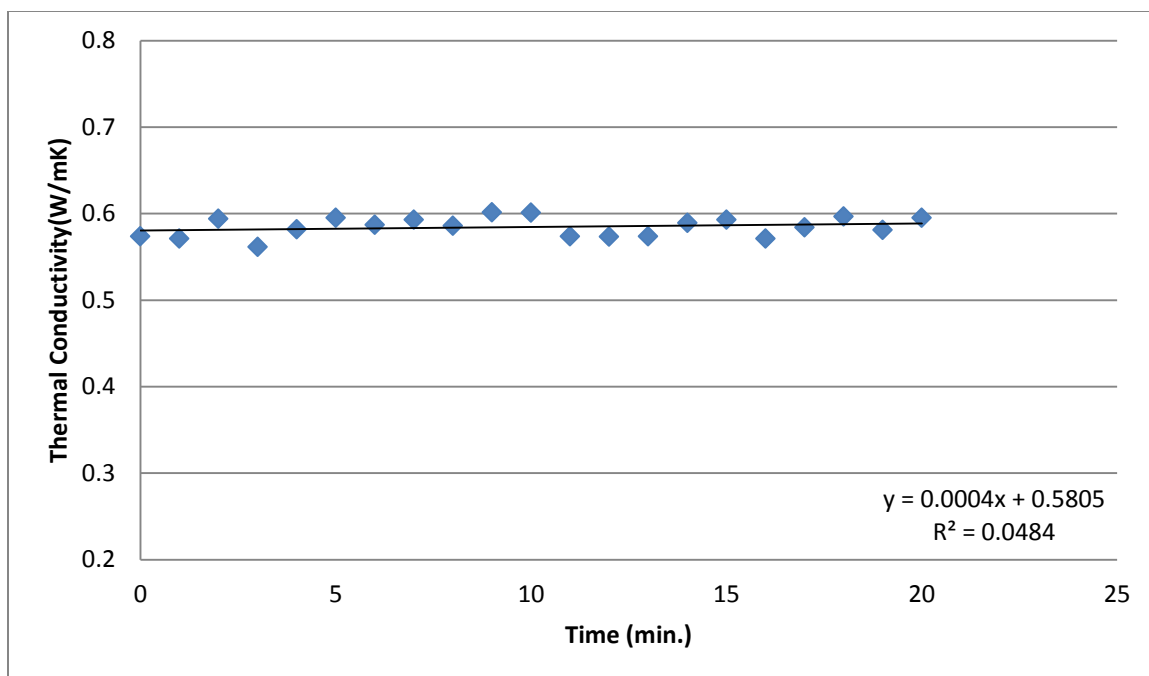


**Figure 40.** Al<sub>2</sub>O<sub>3</sub>/Water, 150 nm, 0.5% vol. concentration, thermophoresis and gravity in opposite directions.

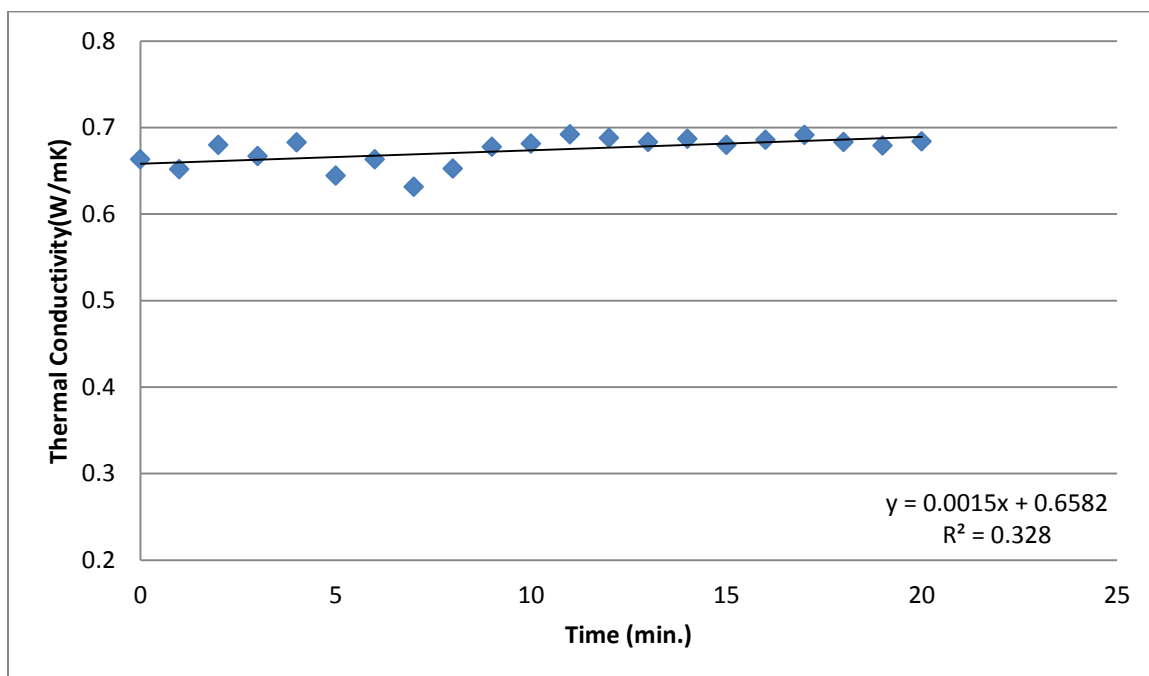


**Figure 41.** Al<sub>2</sub>O<sub>3</sub>/Water, 150 nm, 0.5% vol. concentration, thermophoresis and gravity in same directions.

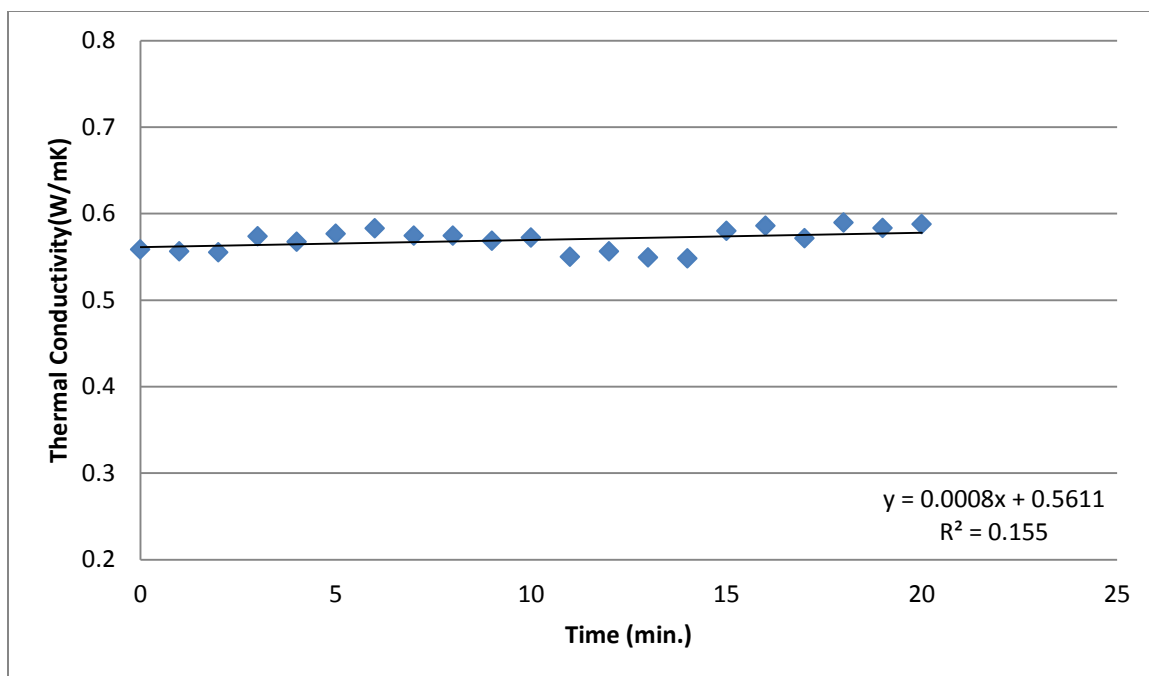


**Figure 42.** Al<sub>2</sub>O<sub>3</sub>/Water, 150 nm, 0.7% vol. concentration, thermophoresis and gravity in opposite directions.

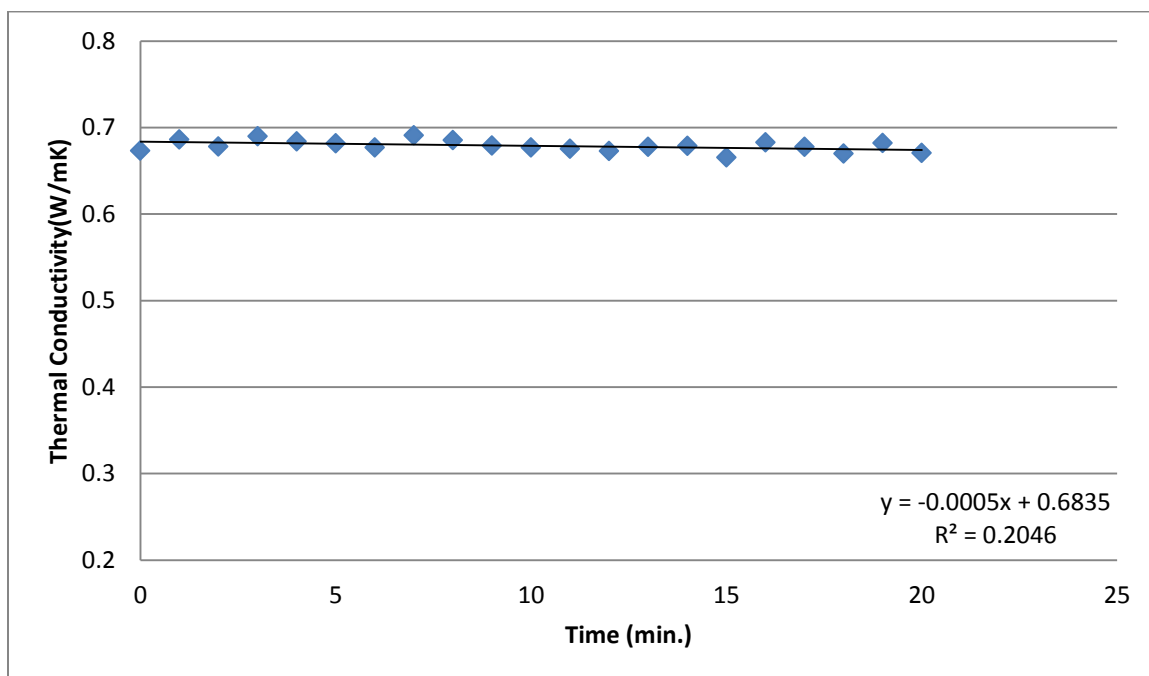


**Figure 43.** Al<sub>2</sub>O<sub>3</sub>/Water, 150 nm, 0.7% vol. concentration, thermophoresis and gravity in same directions.

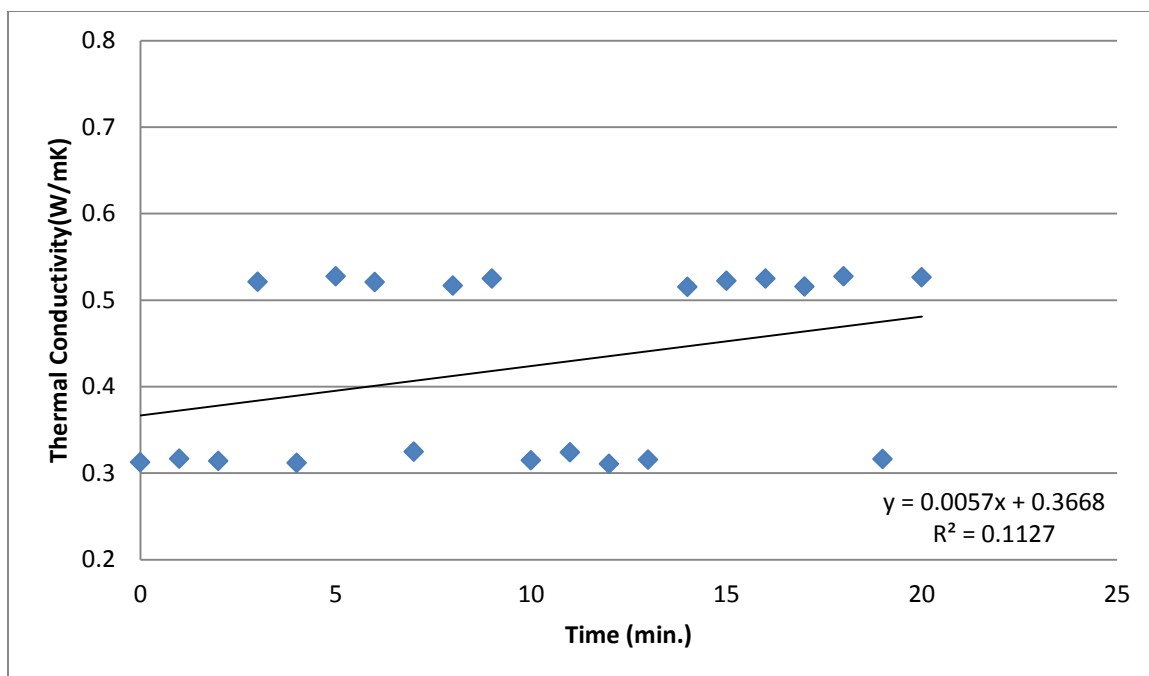


**Figure 44.** Al<sub>2</sub>O<sub>3</sub>/Water, 150 nm, 1% vol. concentration, thermophoresis and gravity in opposite directions.

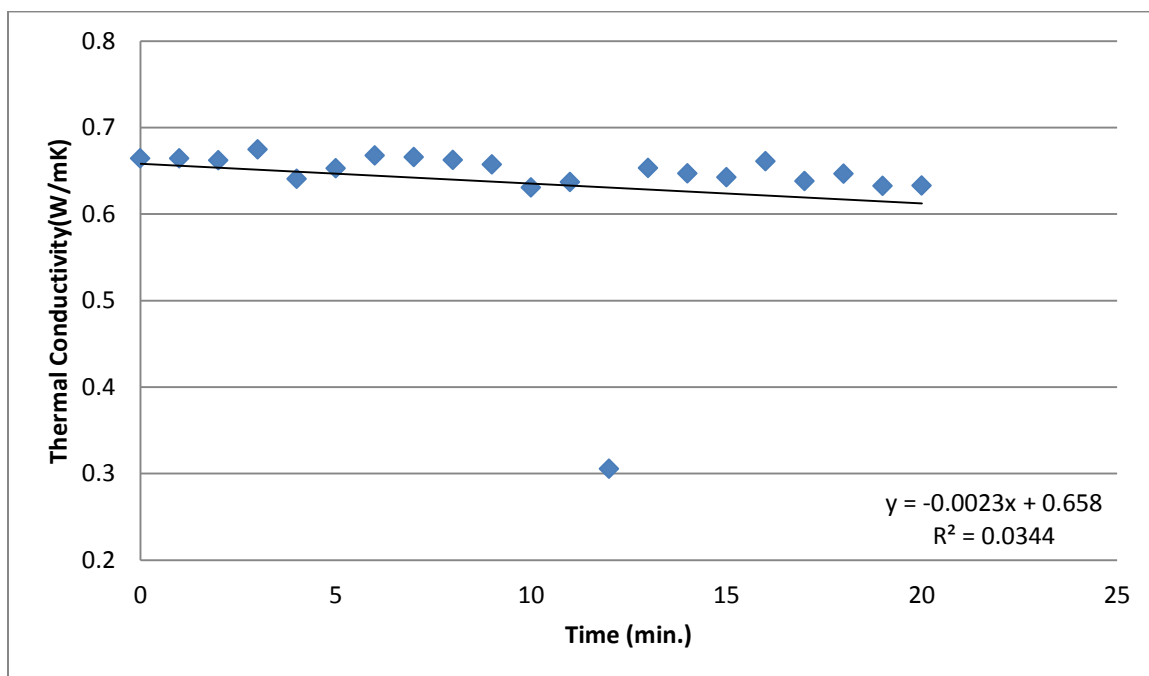


**Figure 45.** Al<sub>2</sub>O<sub>3</sub>/Water, 150 nm, 1% vol. concentration, thermophoresis and gravity in same directions.

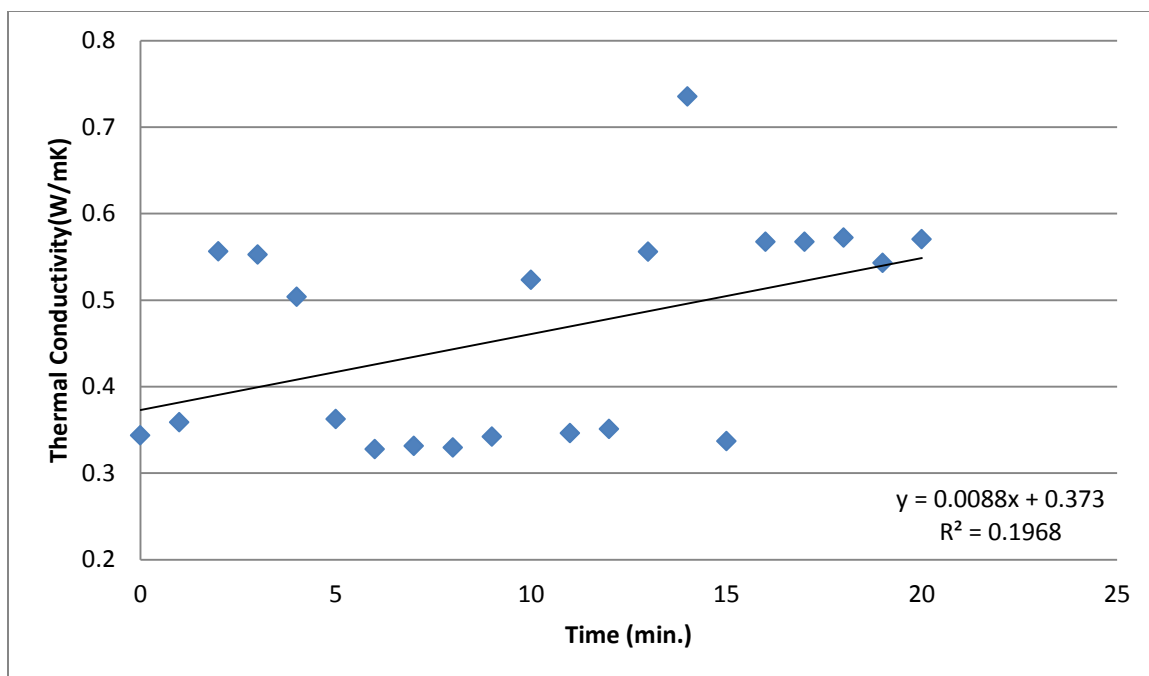


**Figure 46.** Al<sub>2</sub>O<sub>3</sub>/Water, 150 nm, 2% vol. concentration, thermophoresis and gravity in opposite directions.

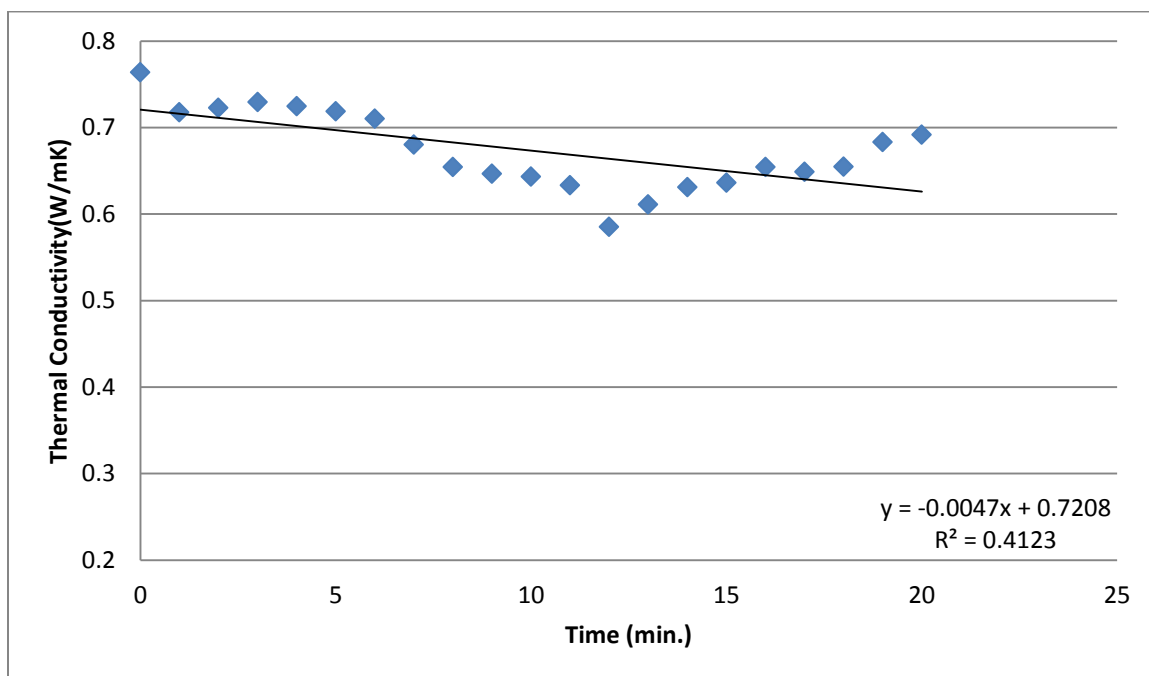


**Figure 47.** Al<sub>2</sub>O<sub>3</sub>/Water, 150 nm, 2% vol. concentration, thermophoresis and gravity in same directions.

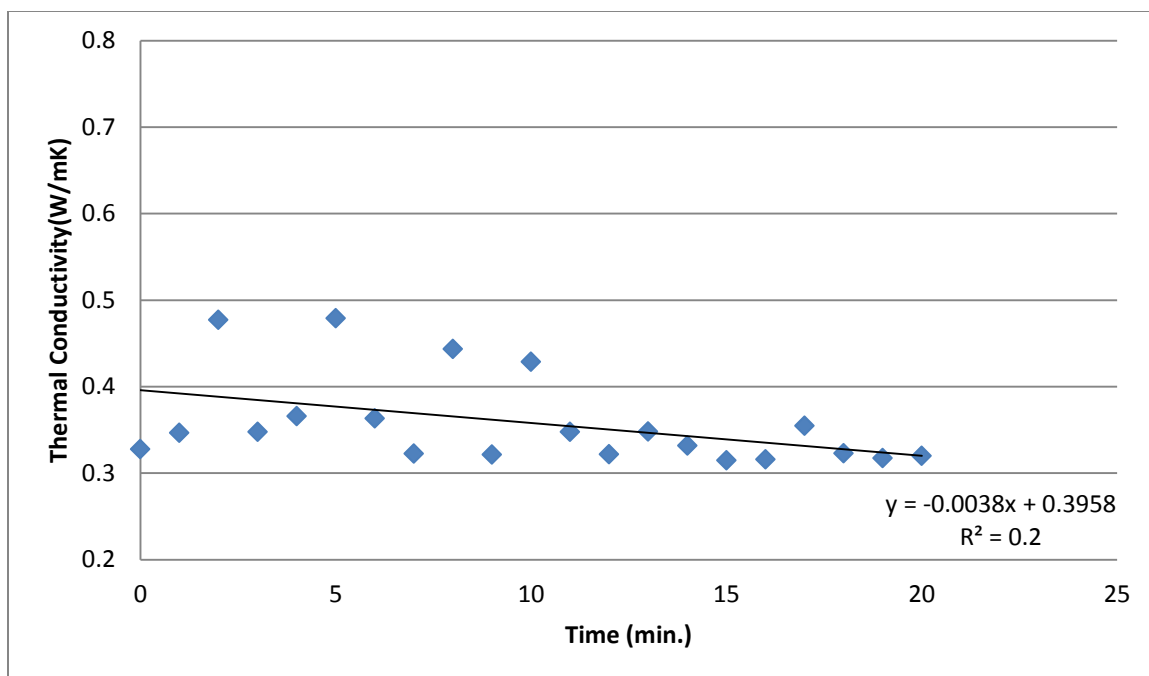


**Figure 48.** Al<sub>2</sub>O<sub>3</sub>/Water, 150 nm, 3% vol. concentration, thermophoresis and gravity in opposite directions.

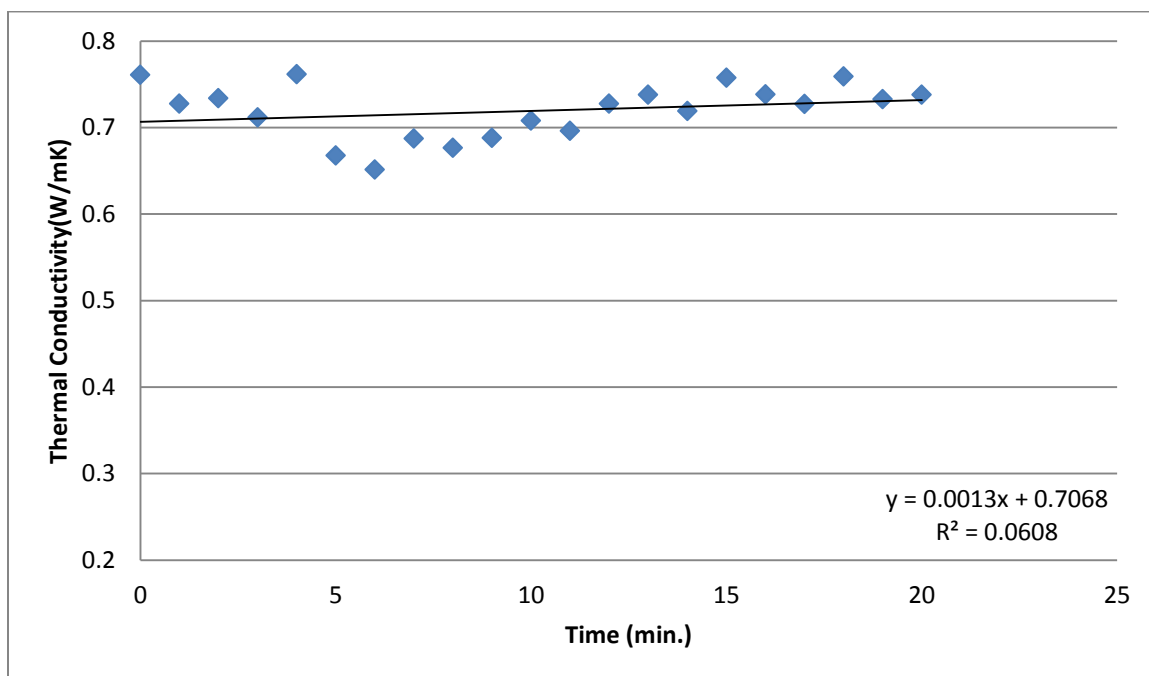


**Figure 49.** Al<sub>2</sub>O<sub>3</sub>/Water, 150 nm, 3% vol. concentration, thermophoresis and gravity in same directions.

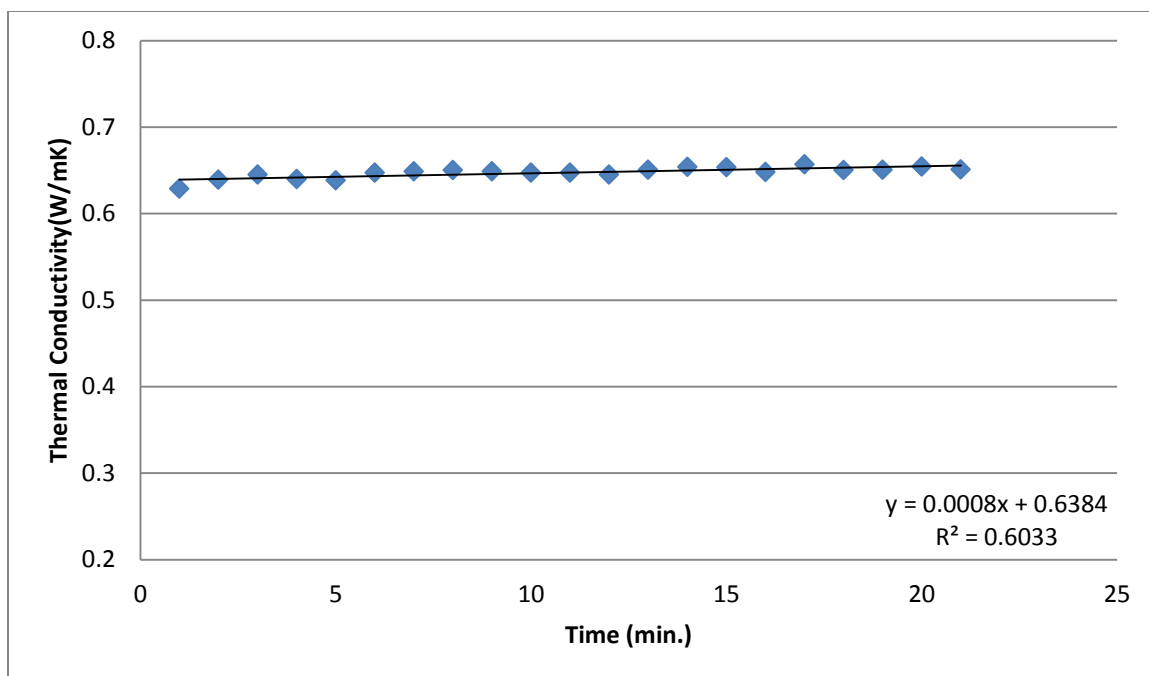


**Figure 50.** SiO<sub>2</sub>/Water, 15 nm, 0.2% vol. concentration, thermophoresis and gravity in opposite directions.

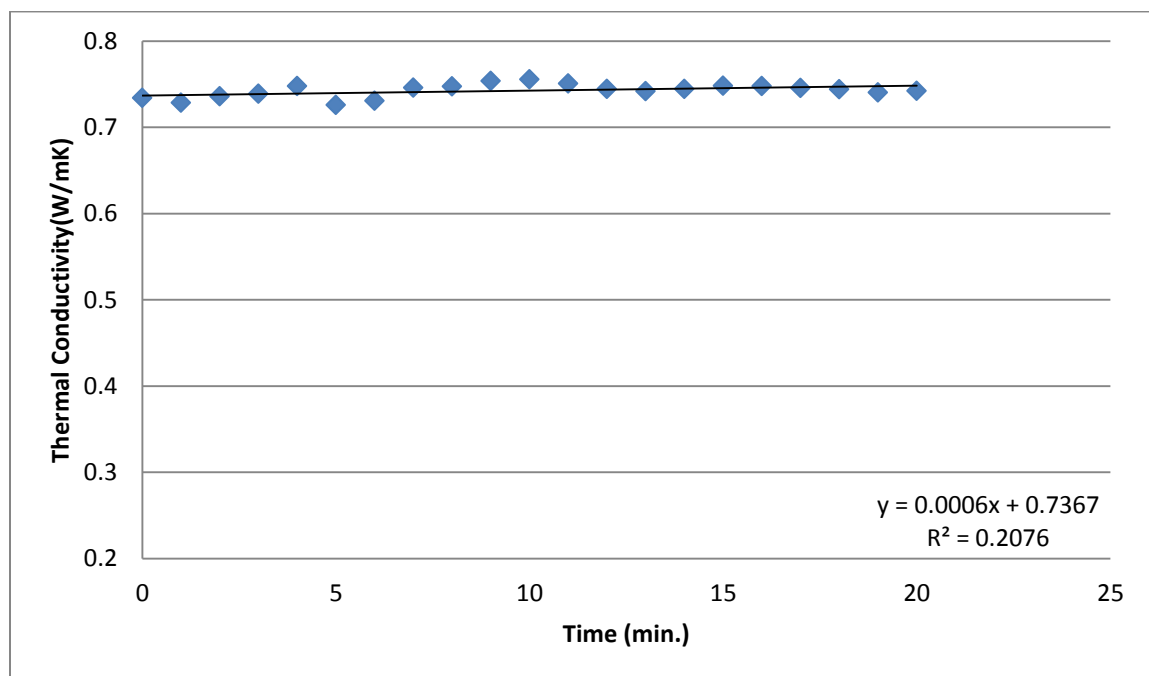


**Figure 51.** SiO<sub>2</sub>/Water, 15 nm, 0.2% vol. concentration, thermophoresis and gravity in same directions.

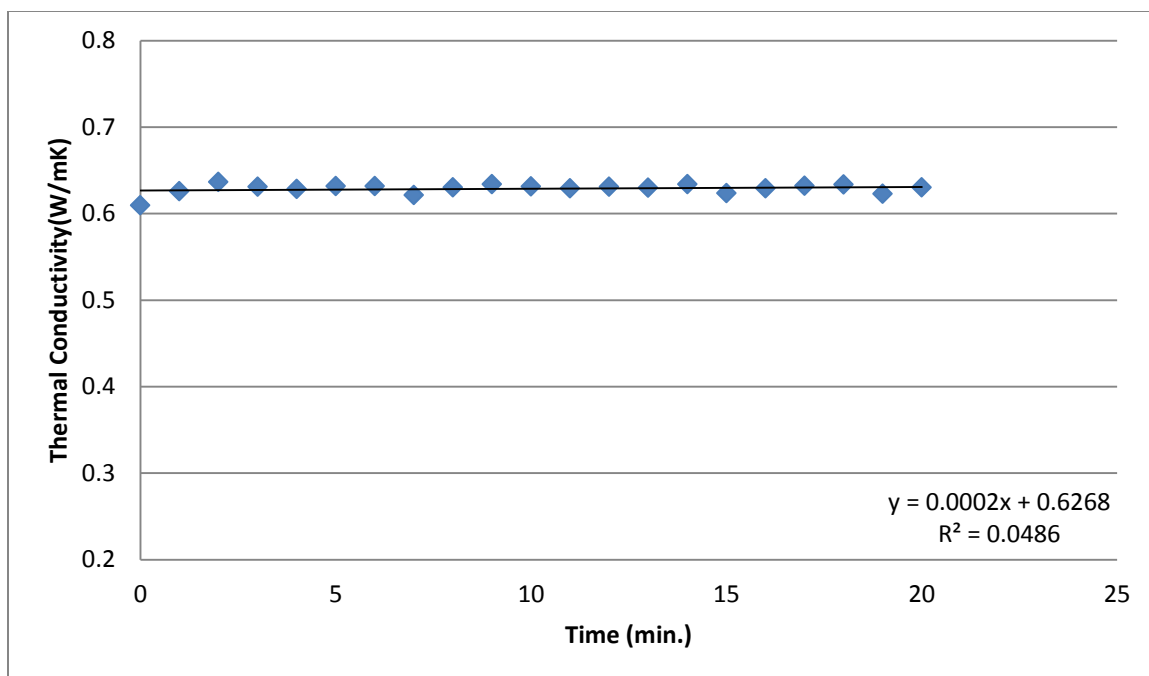


**Figure 52.** SiO<sub>2</sub>/Water, 15 nm, 0.5% vol. concentration, thermophoresis and gravity in opposite directions.

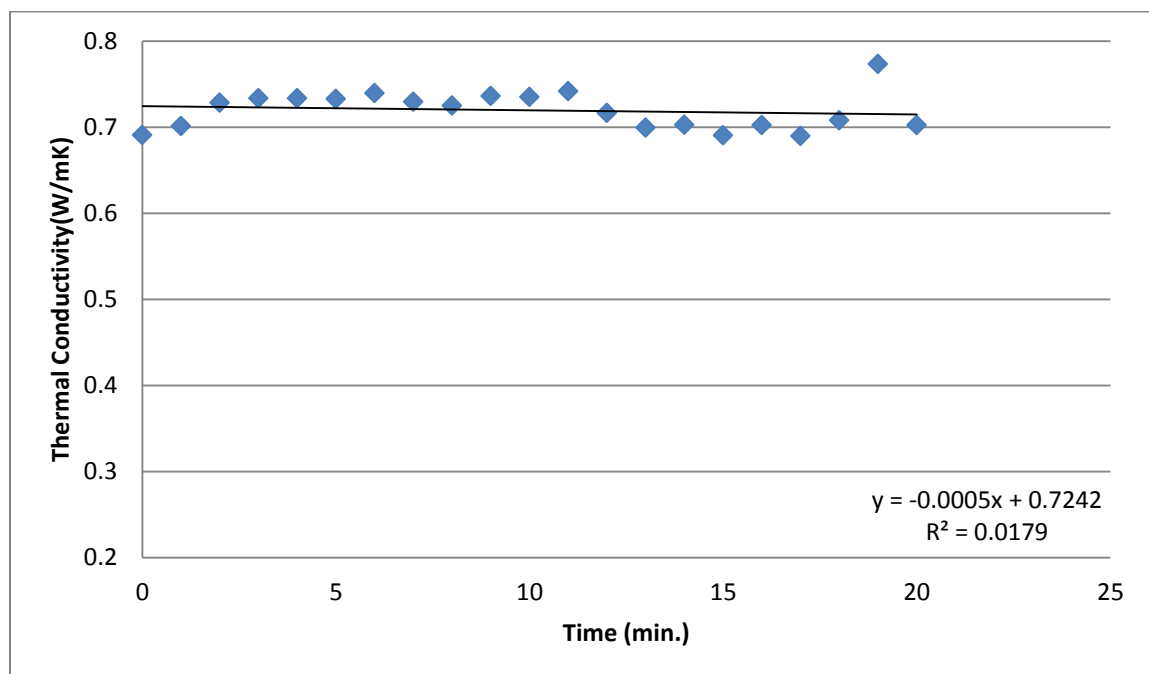


**Figure 53.** SiO<sub>2</sub>/Water, 15 nm, 0.5% vol. concentration, thermophoresis and gravity in same directions.



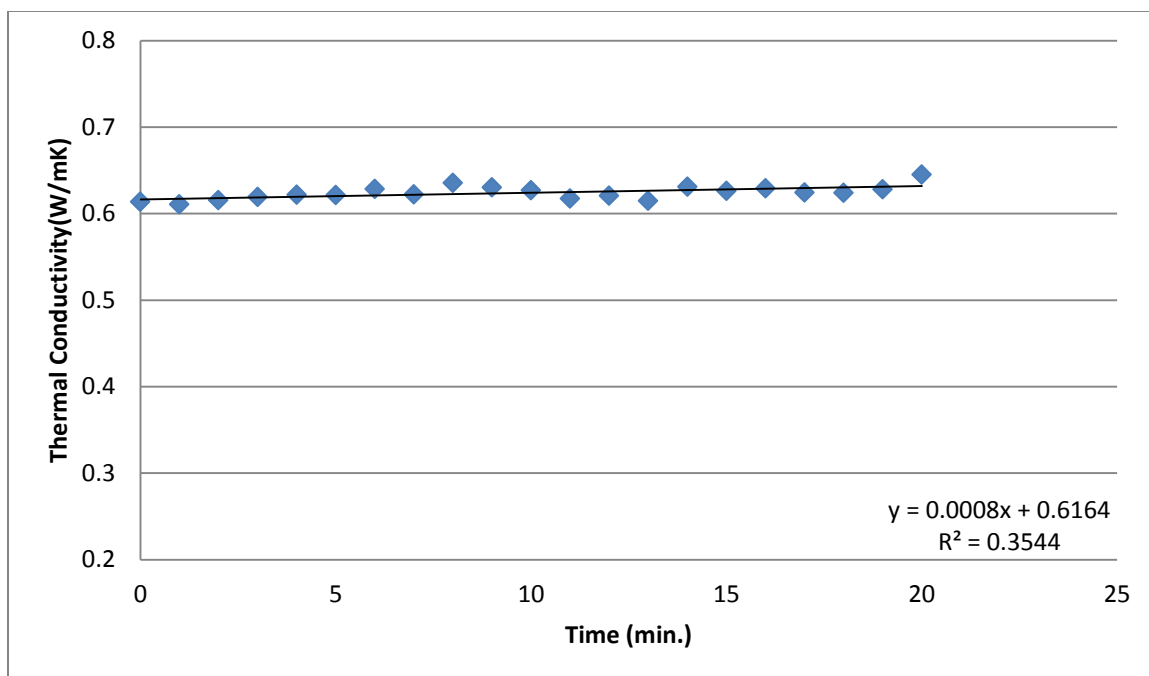


**Figure 54.** SiO<sub>2</sub>/Water, 15 nm, 0.7% vol. concentration, thermophoresis and gravity in opposite directions.

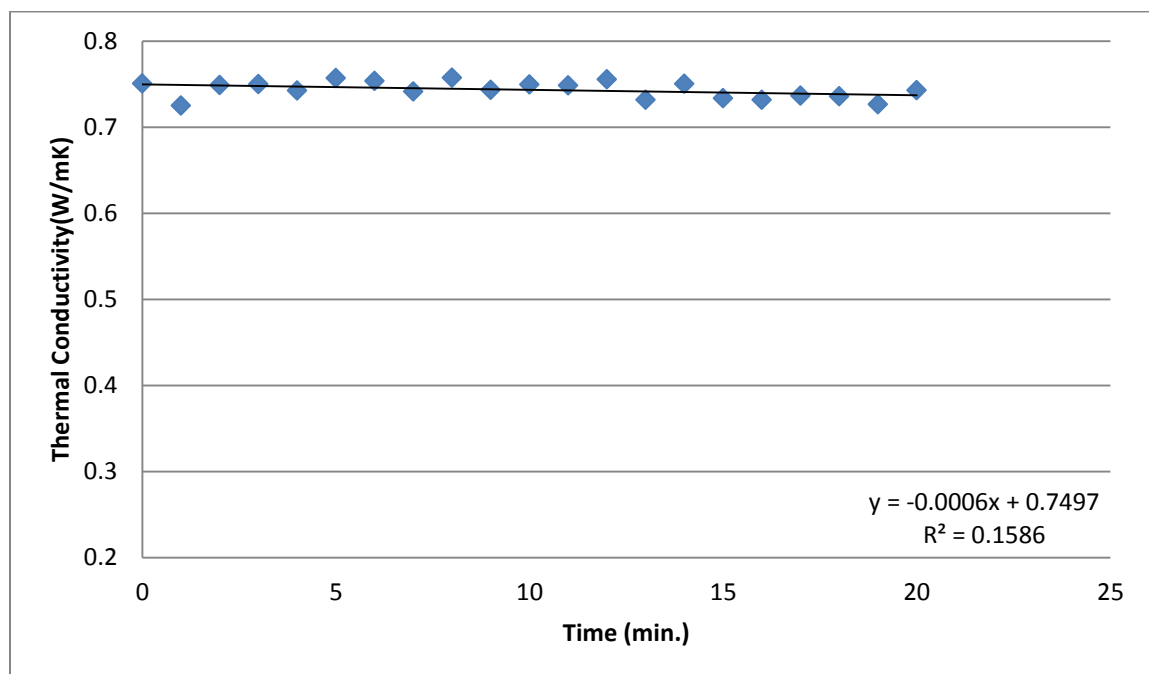


**Figure 55.** SiO<sub>2</sub>/Water, 15 nm, 0.7% vol. concentration, thermophoresis and gravity in same directions.

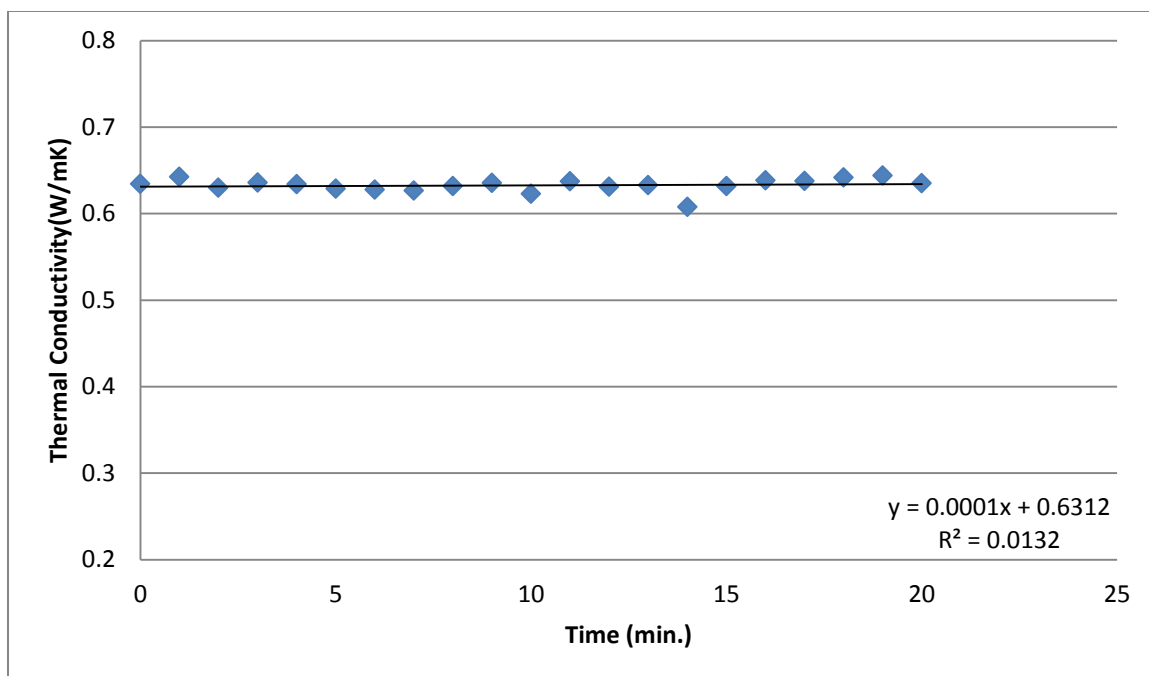


**Figure 56.** SiO<sub>2</sub>/Water, 15 nm, 1% vol. concentration, thermophoresis and gravity in opposite directions.

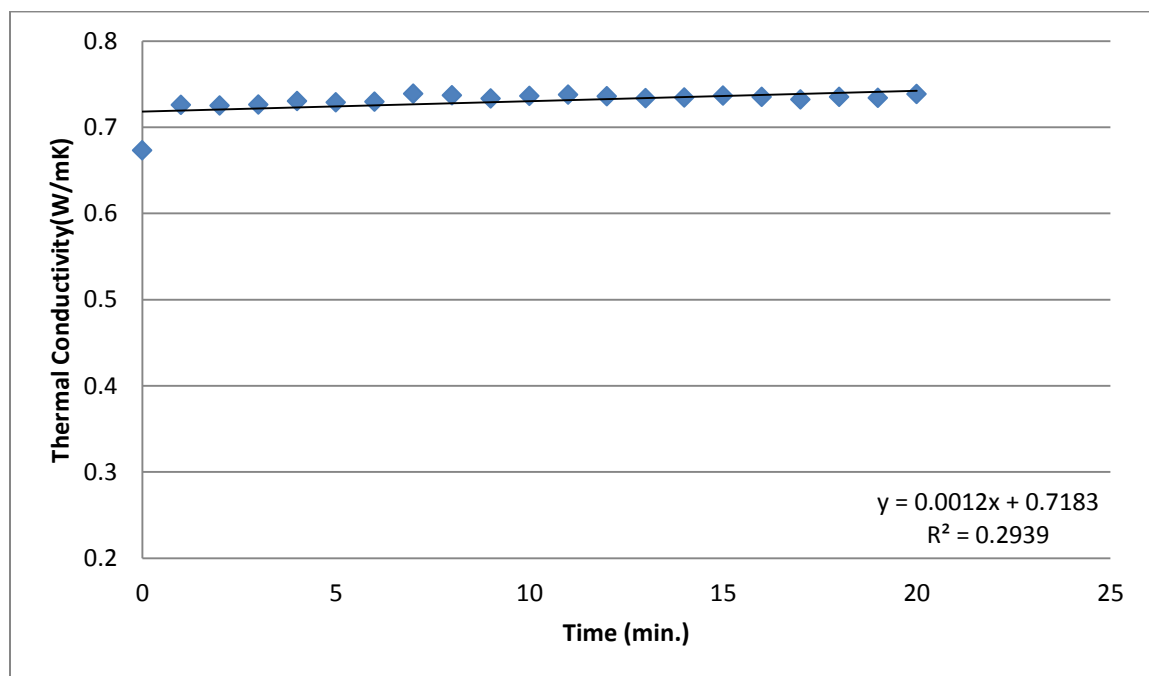


**Figure 57.** SiO<sub>2</sub>/Water, 15 nm, 1% vol. concentration, thermophoresis and gravity in same directions.

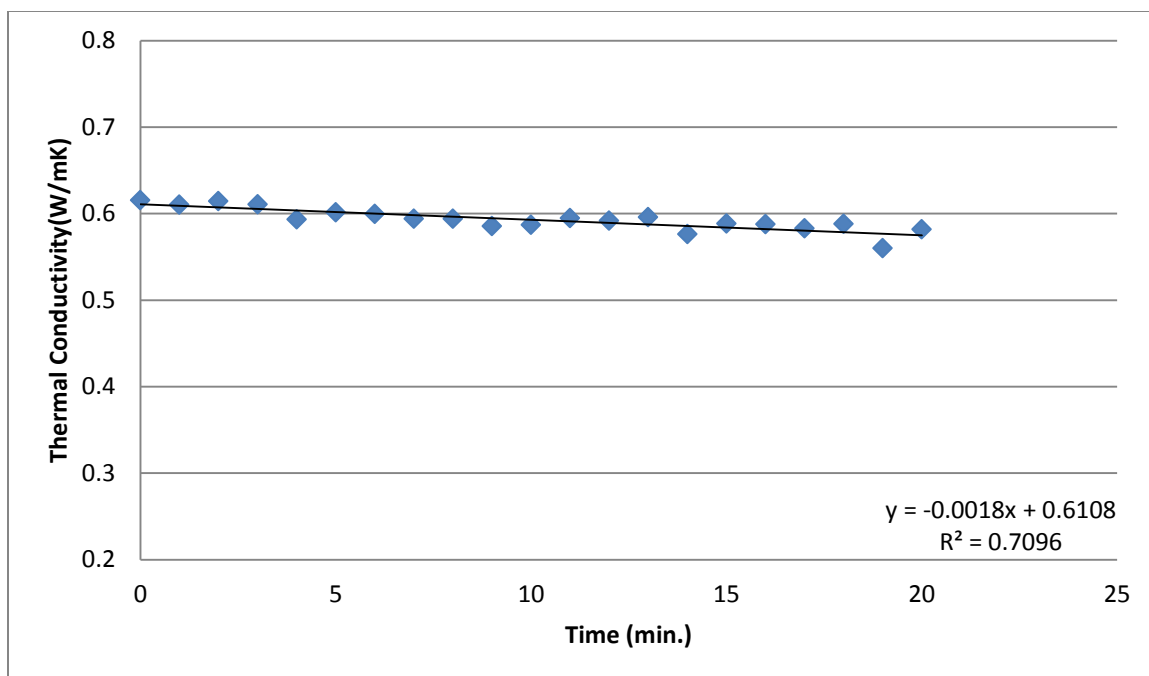


**Figure 58.** SiO<sub>2</sub>/Water, 15 nm, 2% vol. concentration, thermophoresis and gravity in opposite directions.

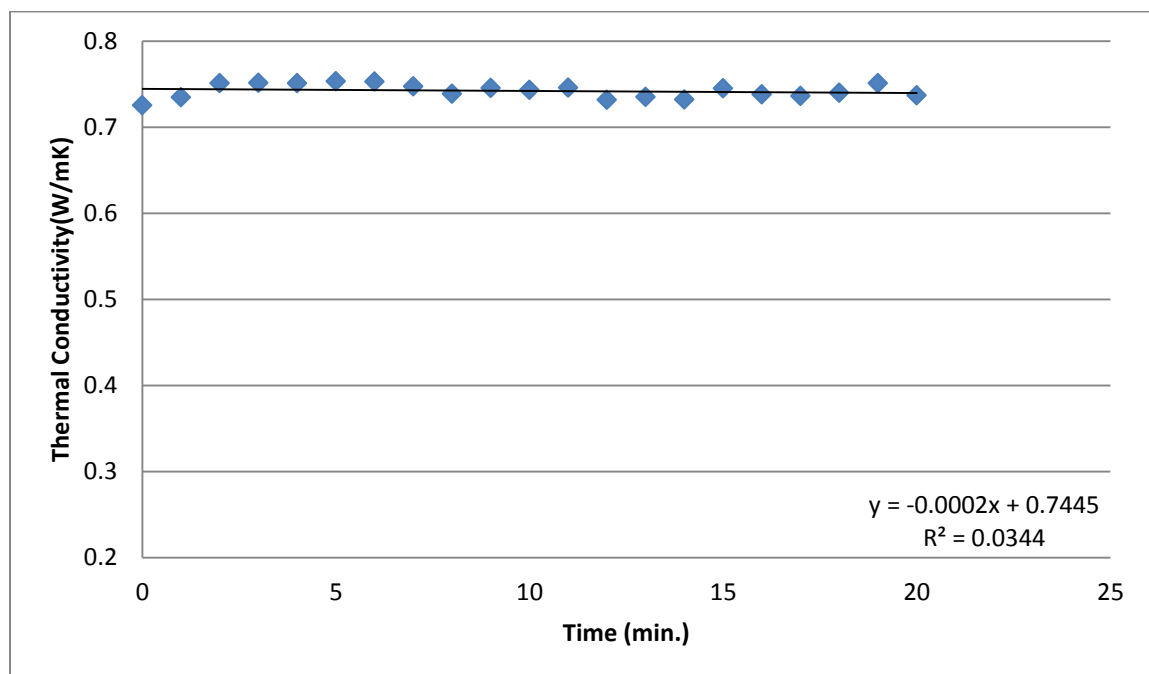


**Figure 59.** SiO<sub>2</sub>/Water, 15 nm, 2% vol. concentration, thermophoresis and gravity in same directions.

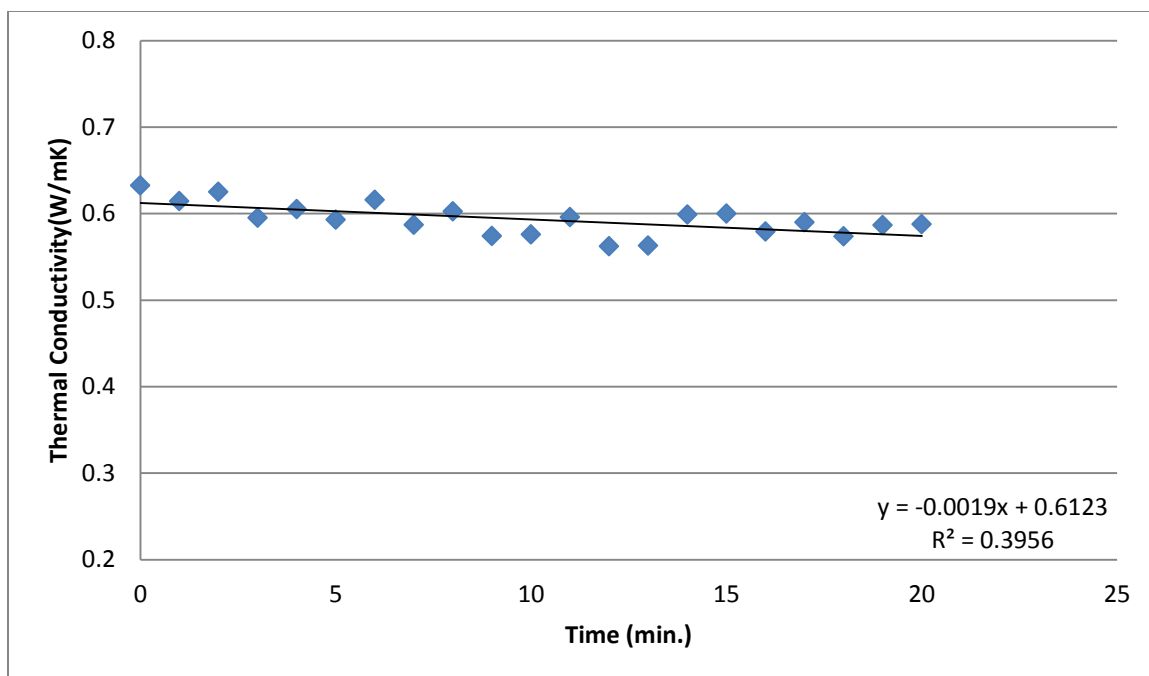


**Figure 60.** SiO<sub>2</sub>/Water, 15 nm, 3% vol. concentration, thermophoresis and gravity in opposite directions.

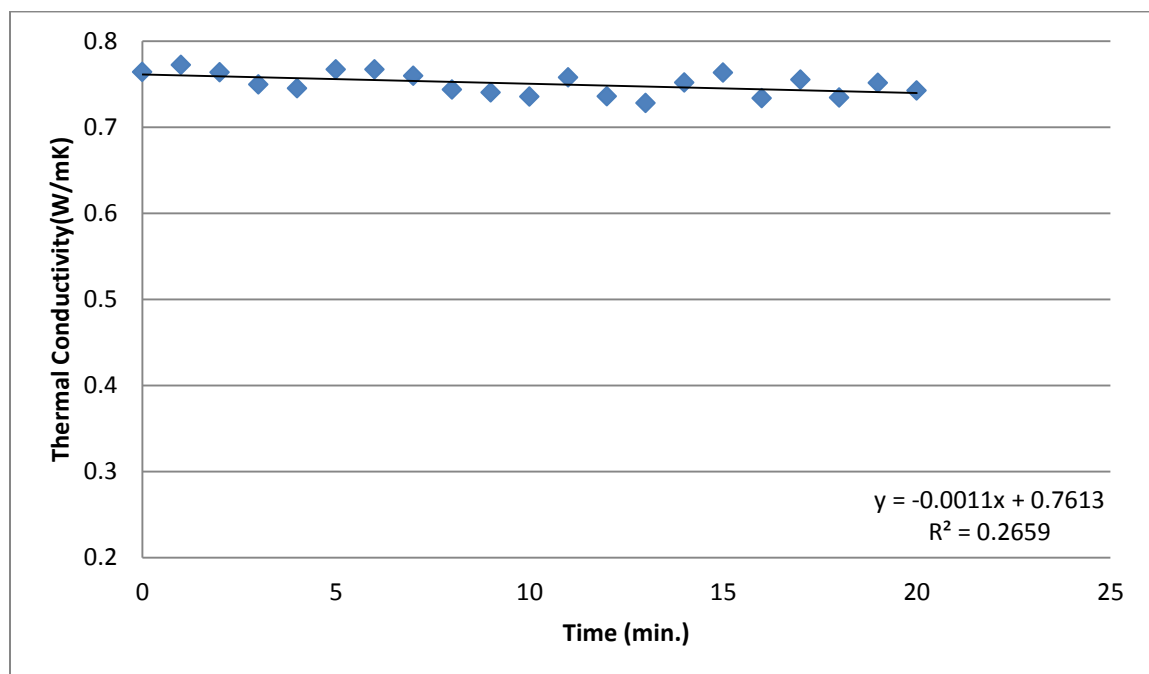


**Figure 61.** SiO<sub>2</sub>/Water, 15 nm, 3% vol. concentration, thermophoresis and gravity in same directions.

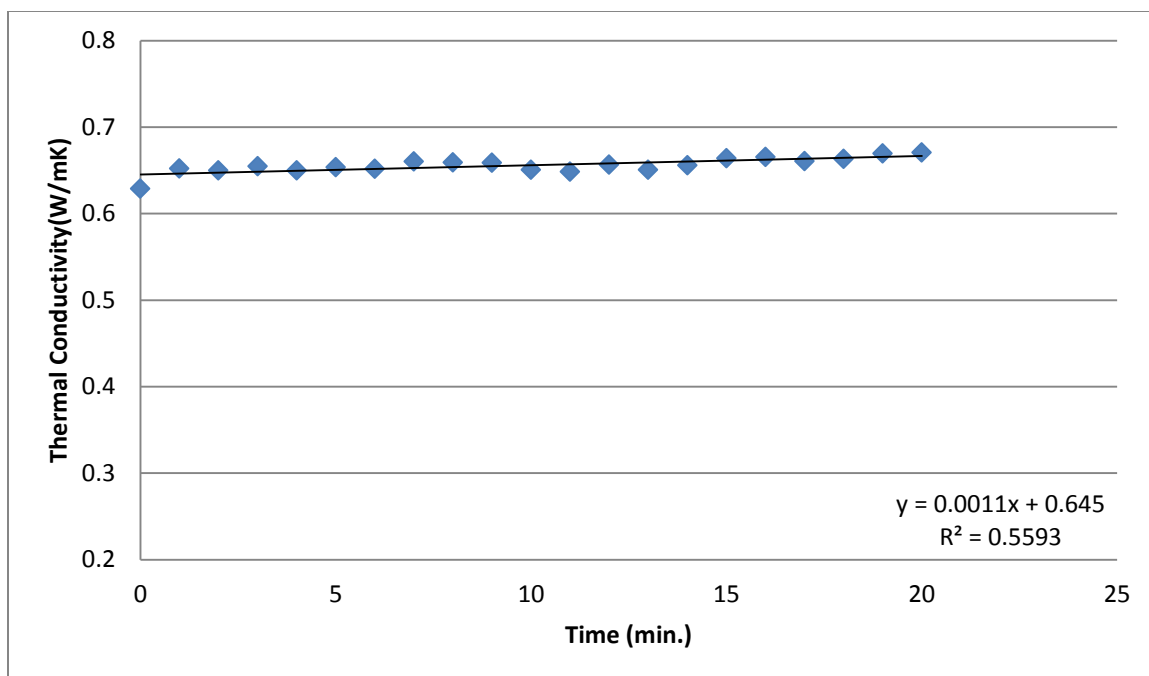


**Figure 62.** SiO<sub>2</sub>/Water, 80 nm, 0.2% vol. concentration, thermophoresis and gravity in opposite directions.

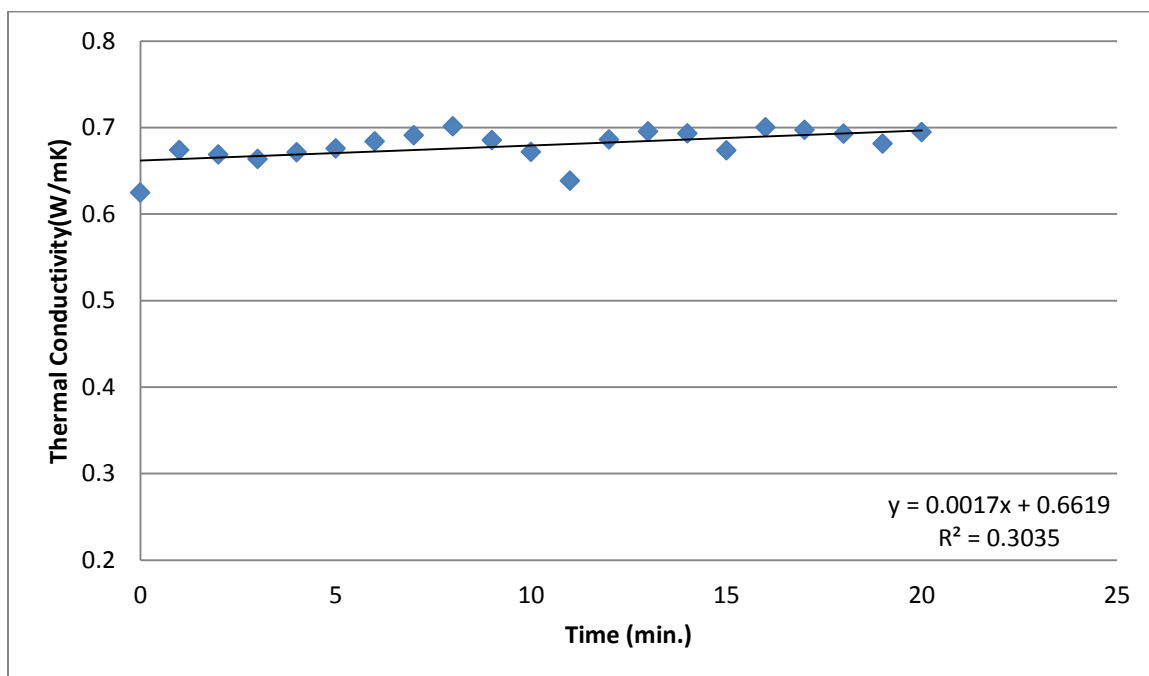


**Figure 63.** SiO<sub>2</sub>/Water, 80 nm, 0.2% vol. concentration, thermophoresis and gravity in same directions.

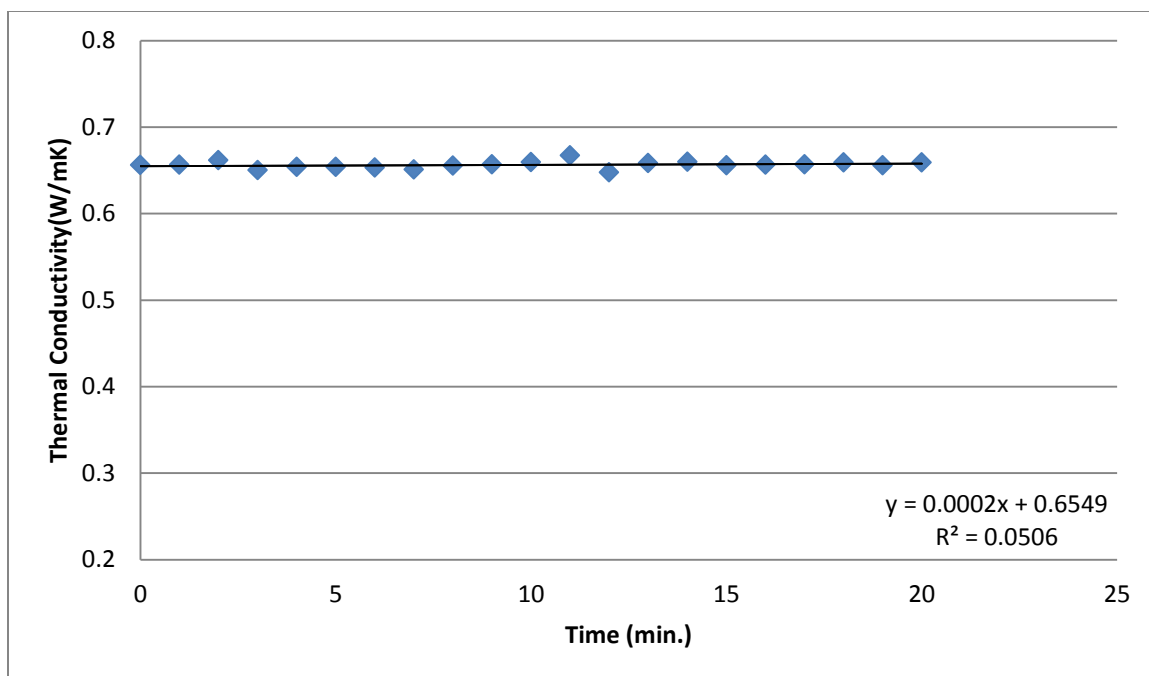


**Figure 64.** SiO<sub>2</sub>/Water, 80 nm, 0.5% vol. concentration, thermophoresis and gravity in opposite directions.

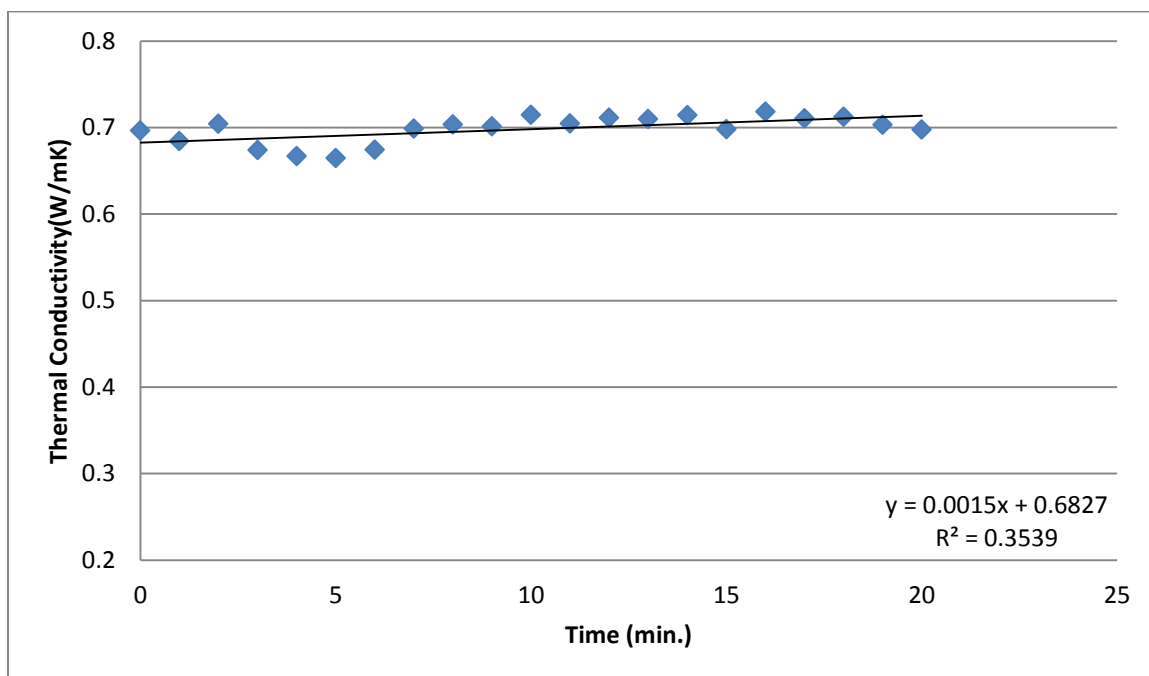


**Figure 65.** SiO<sub>2</sub>/Water, 80 nm, 0.5% vol. concentration, thermophoresis and gravity in same directions.

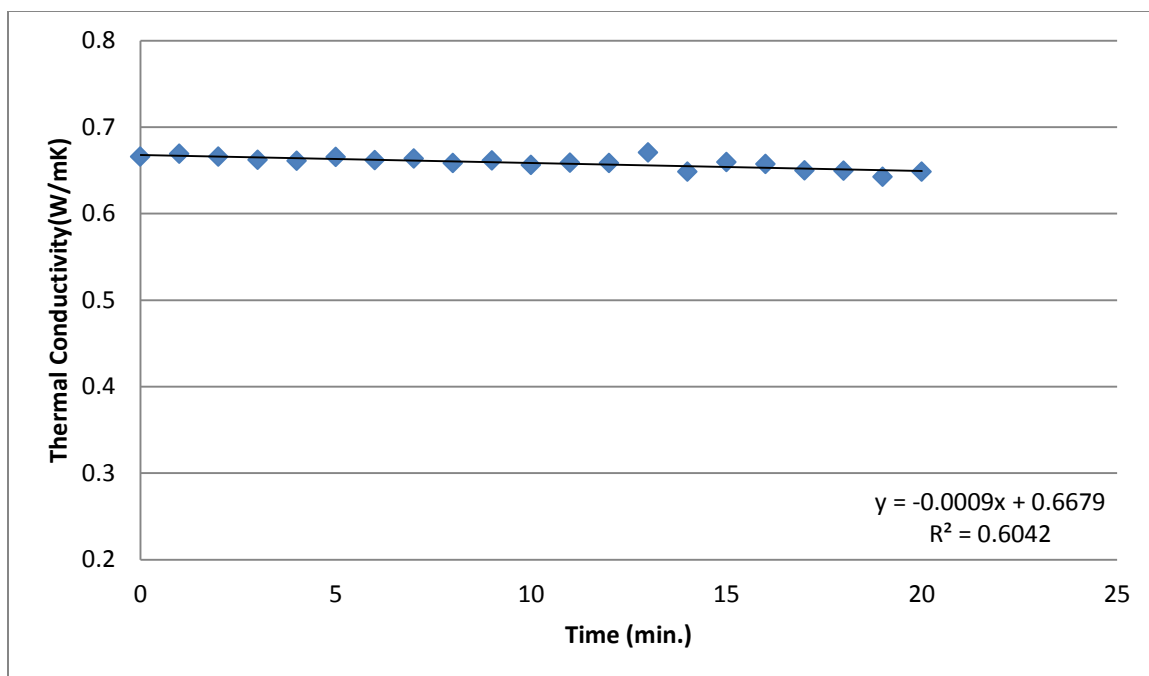


**Figure 66.** SiO<sub>2</sub>/Water, 80 nm, 0.7% vol. concentration, thermophoresis and gravity in opposite directions.

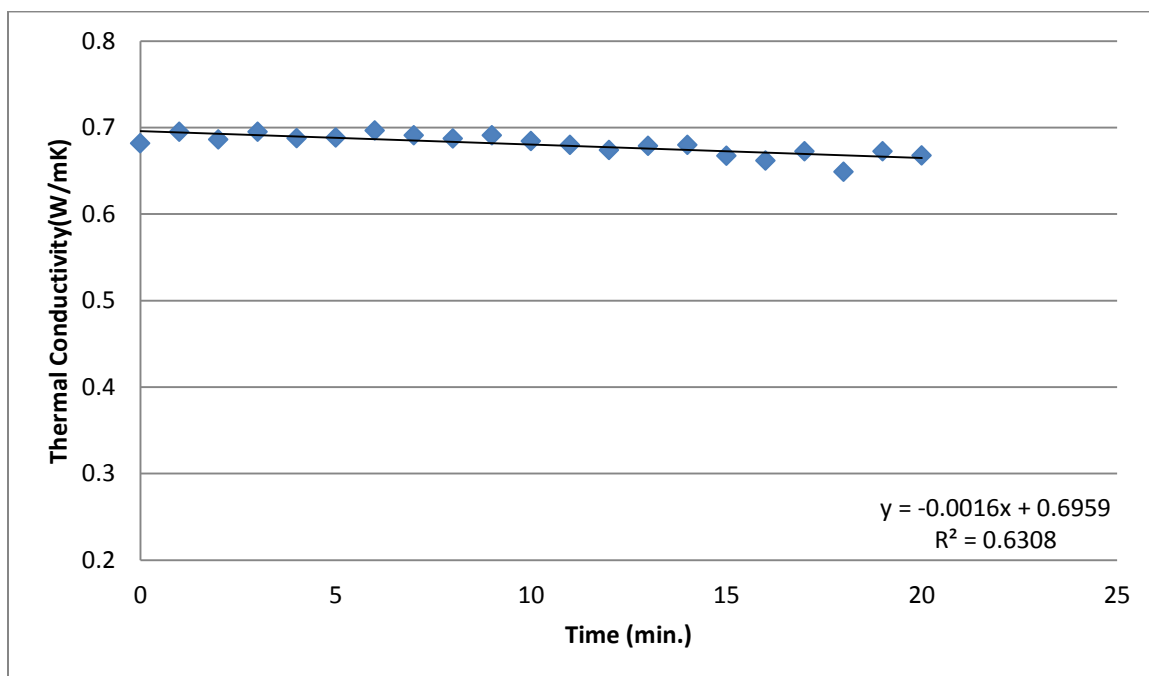


**Figure 67.** SiO<sub>2</sub>/Water, 80 nm, 0.7% vol. concentration, thermophoresis and gravity in same directions.

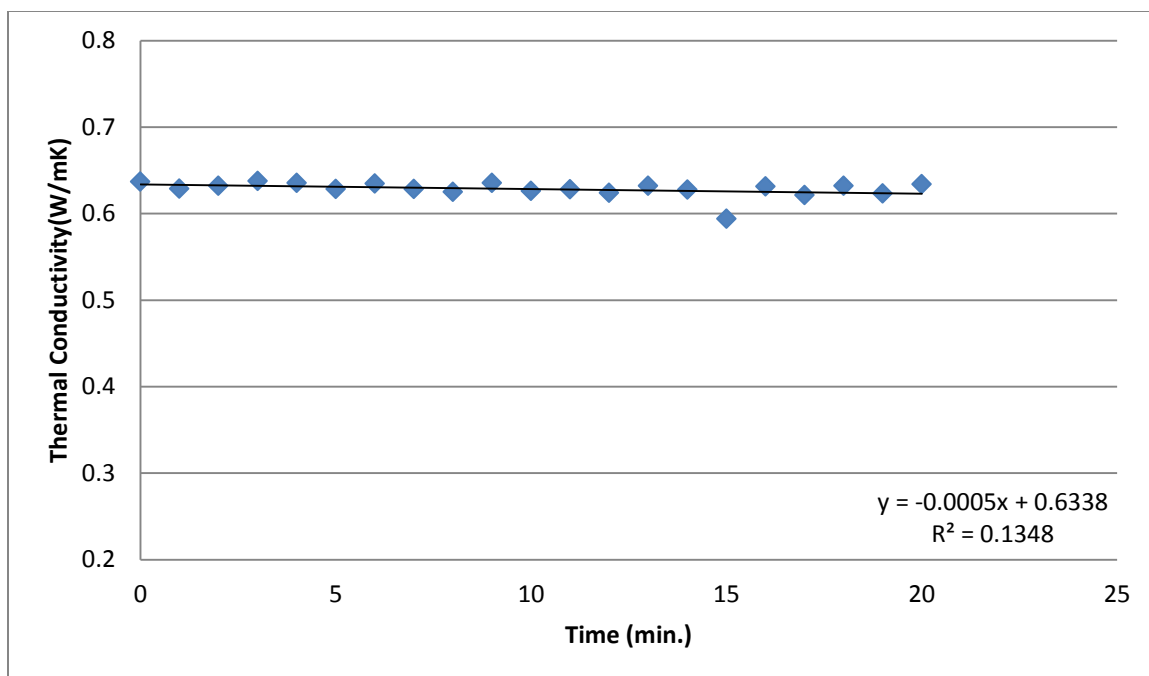


**Figure 68.** SiO<sub>2</sub>/Water, 80 nm, 1% vol. concentration, thermophoresis and gravity in opposite directions.

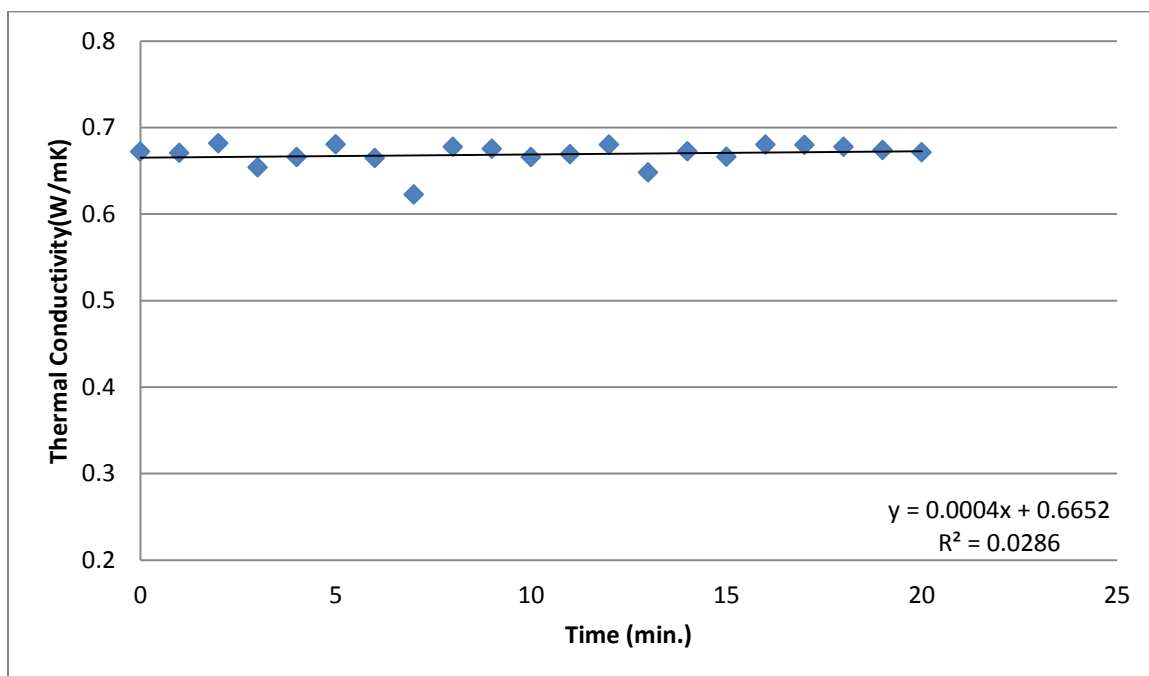


**Figure 69.** SiO<sub>2</sub>/Water, 80 nm, 1% vol. concentration, thermophoresis and gravity in same directions.



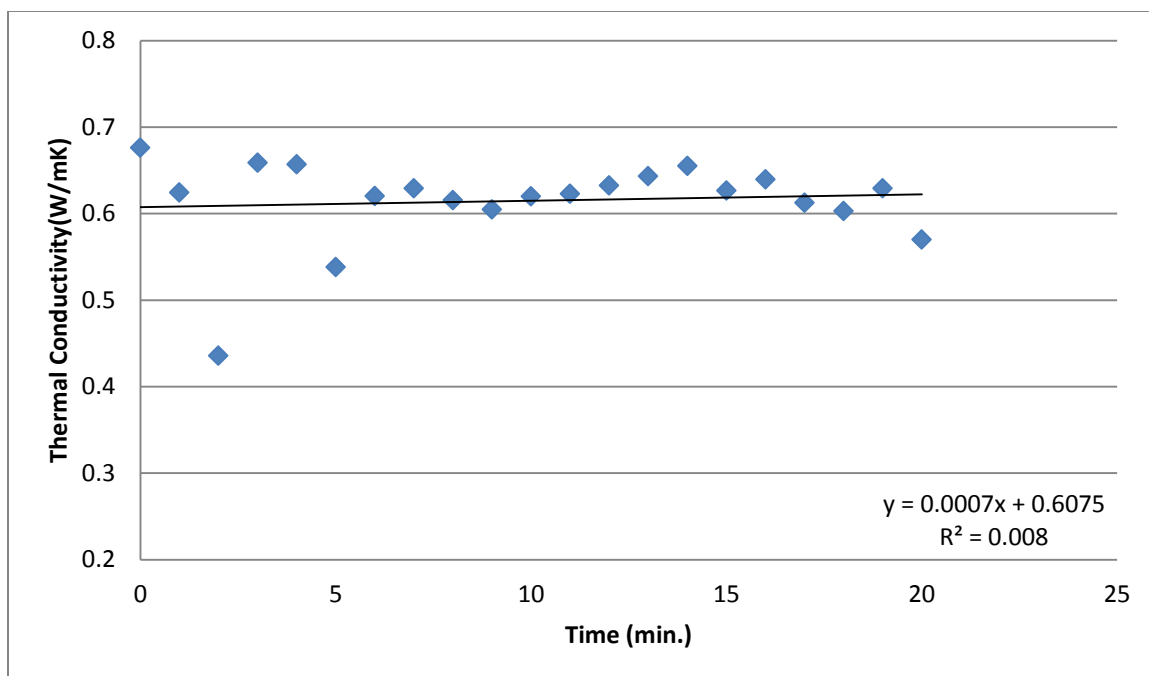


**Figure 70.** SiO<sub>2</sub>/Water, 80 nm, 2% vol. concentration, thermophoresis and gravity in opposite directions.

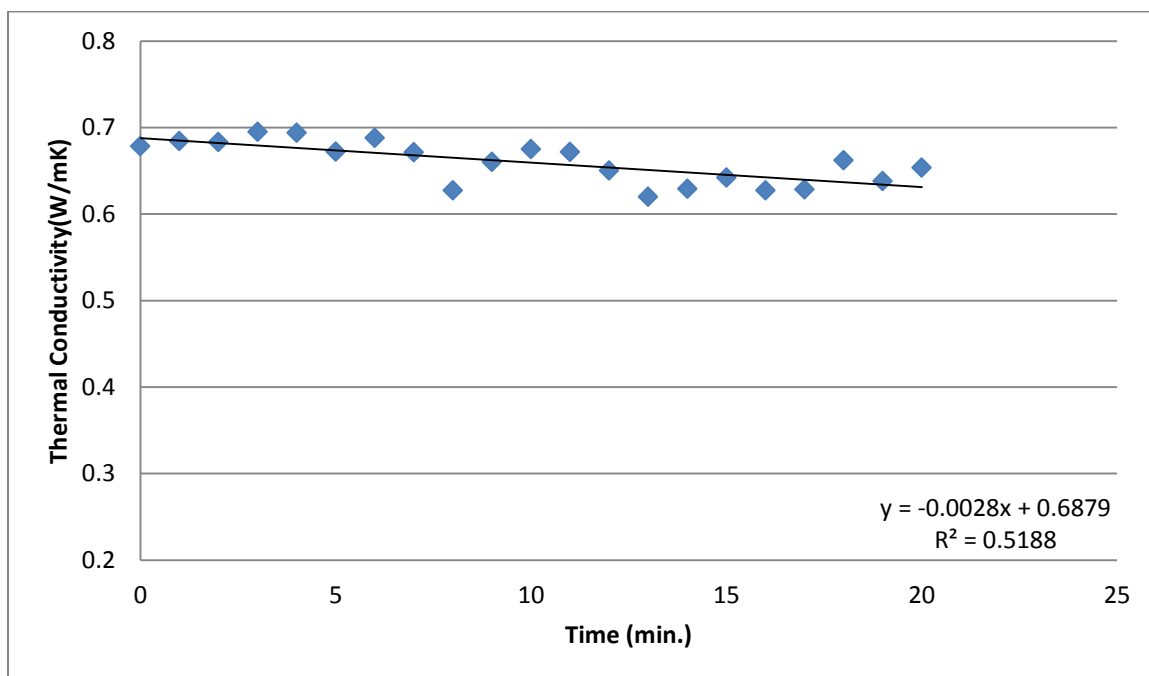


**Figure 71.** SiO<sub>2</sub>/Water, 80 nm, 2% vol. concentration, thermophoresis and gravity in same directions.

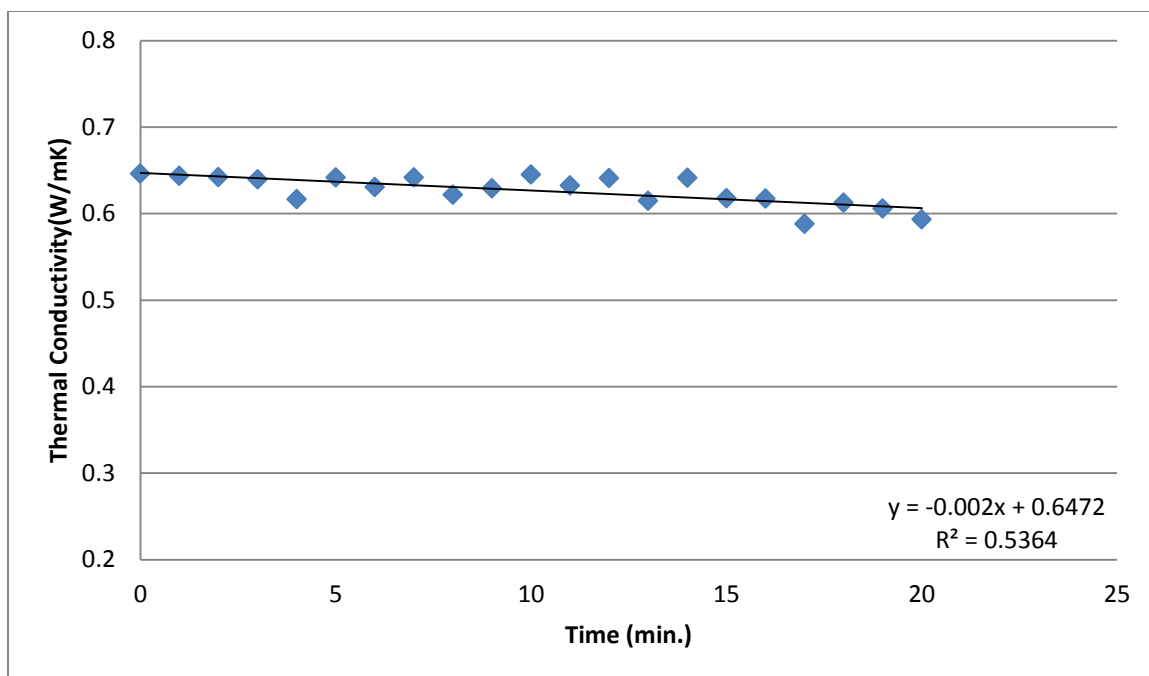


**Figure 72.** SiO<sub>2</sub>/Water, 80 nm, 3% vol. concentration, thermophoresis and gravity in opposite directions.

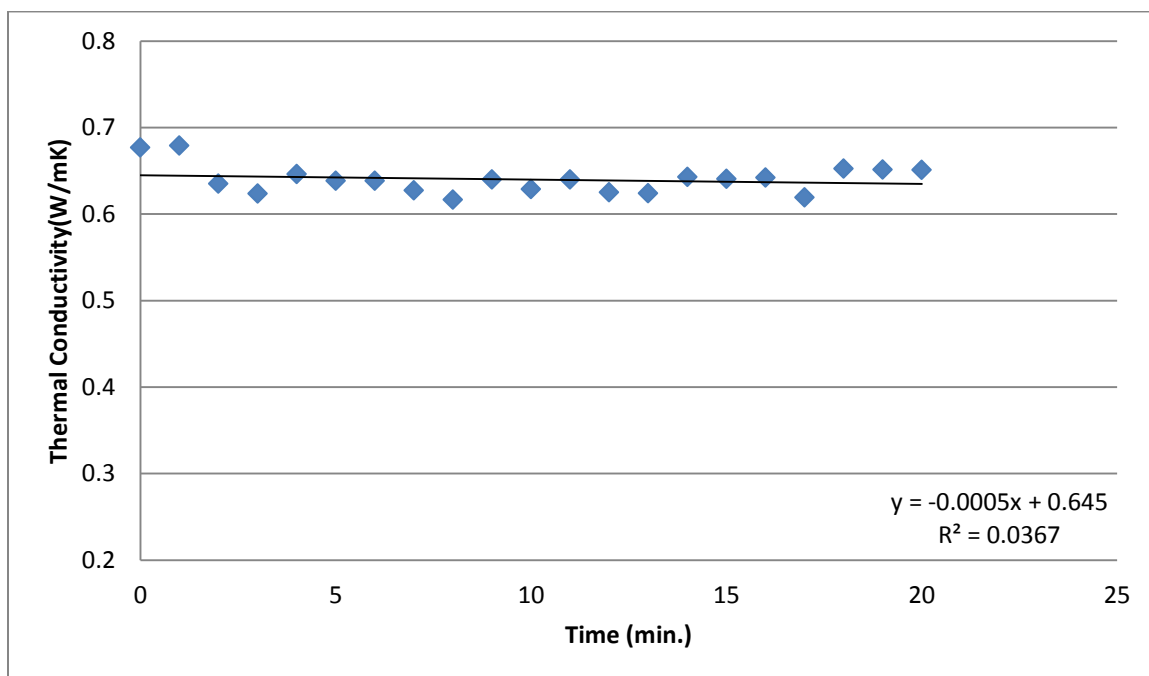


**Figure 73.** SiO<sub>2</sub>/Water, 80 nm, 3% vol. concentration, thermophoresis and gravity in same directions.

## Appendix C: Statistical Analysis

The statistical analysis suggested by R.S. Figliola and D.E. Beasley in Theory and Design for Mechanical Measurements was followed for all measurements. The accuracy of Thermtest Transient Plane Source TPS 500S was calculated using eq. 47 and eq. 48.

$$\epsilon = \text{True value} - \text{indicated value} \quad (47)$$

$$A = \left(1 - \frac{|\epsilon|}{\text{true value}}\right) \times 100 \quad (48)$$

A stainless steel sample, used to calibrate the instrument, was used. The absolute error was found to be 0.25 resulting in a 98.15% accuracy.

Next, the sample mean value, eq. 49, and the sample variance, eq. 50, were estimated for all the samples tested.

$$\bar{x} = \frac{1}{N} \sum_{i=1}^N x_i \quad (49)$$

$$S_x^2 = \frac{1}{N-1} \sum_{i=1}^N (x_i - \bar{x})^2 \quad (50)$$

Finally, the precision interval was calculated using eq. 51. A 95% probability was used.

$$x_i = \bar{x} \pm t_{v,P} S_x \quad (P\%) \quad (51)$$

All the results are presented in the following appendixes.

## Appendix D: Base fluid data

All thermal conductivity readings in W/mK

**Table 18.** Water/Al<sub>2</sub>O<sub>3</sub>, 10 nm, 0.1% vol. concentration.

Vol. Concentration	Sample	Thermal Conductivity	Z <sub>o</sub>
0.1%	0	0.6081	0.00
	1	0.6089	0.03
	2	0.5891	0.78
	3	0.6165	0.34
	4	0.6109	0.11
	5	0.6153	0.30

Outliers ( $Z \geq 2.13$ ): 0

N = 5

$\bar{x} = 0.6081$

$S_x = 0.010$

$x_i = 0.6081 \pm 0.0243$

**Table 19.** Water/Al<sub>2</sub>O<sub>3</sub>, 10 nm, 1% vol. concentration.

Vol. Concentration	Sample	Thermal Conductivity	Z <sub>o</sub>
1%	0	0.5998	0.30
	1	0.5702	0.47
	2	0.6041	0.41
	3	0.5964	0.21
	4	0.592	0.10
	5	0.5671	0.55

Outliers ( $Z \geq 2.13$ ): 0

N = 5

$\bar{x} = 0.5883$

$S_x = 0.0157$

$x_i = 0.5883 \pm 0.0385$

**Table 20.** Water/Al<sub>2</sub>O<sub>3</sub>, 10 nm, 10% vol. concentration.

Vol. Concentration	Sample	Thermal Conductivity	Z <sub>o</sub>
10%	0	0.6957	0.14
	1	0.6686	0.01
	2	0.8032	0.74
	3	0.641	0.17
	4	0.6099	0.34
	5	0.6067	0.36

Outliers ( $Z \geq 2.13$ ): 0

N = 5

$\bar{x} = 0.6709$

$S_x = 0.0733$

$x_i = 0.6709 \pm 0.1793$

**Table 21.** EG/Al<sub>2</sub>O<sub>3</sub>, 10 nm, 0.1% vol. concentration.

Vol. Concentration	Sample	Thermal Conductivity	Z <sub>o</sub>
0.1%	0	0.2121	0.40
	1	0.2078	0.14
	2	0.2076	0.16
	3	0.2137	0.60
	4	0.2068	0.26
	5	0.2053	0.45

Outliers ( $Z \geq 2.13$ ): 0

N = 5

$$S_x = 0.0033$$

$$x_i = 0.2089 \pm 0.080$$

$$\bar{x} = 0.2089$$

**Table 22.** EG/Al<sub>2</sub>O<sub>3</sub>, 10 nm, 1% vol. concentration.

Vol. Concentration	Sample	Thermal Conductivity	Z <sub>o</sub>
1%	0	0.2045	0.50
	1	0.209	0.12
	2	0.2045	0.50
	3	0.2092	0.15
	4	0.2116	0.48
	5	0.2099	0.25

Outliers ( $Z \geq 2.13$ ): 0

N = 5

$$\bar{x} = 0.2081$$

$$S_x = 0.0026$$

$$x_i = 0.2081 \pm 0.0072$$

**Table 23.** EG/Al<sub>2</sub>O<sub>3</sub>, 10 nm, 10% vol. concentration.

Vol. Concentration	Sample	Thermal Conductivity	Z <sub>o</sub>
10%	0	0.2175	0.56
	1	0.1873	0.01
	2	0.1684	0.33
	3	0.2096	0.42
	4	0.1749	0.21
	5	0.1623	0.44

Outliers ( $Z \geq 2.13$ ): 0

N = 5

$$\bar{x} = 0.1867$$

$$S_x = 0.0226$$

$$x_i = 0.1867 \pm 0.0552$$

75%EG-25% Water/Al<sub>2</sub>O<sub>3</sub> - 10nm:

**Table 24.** 75%EG-25% Water /Al<sub>2</sub>O<sub>3</sub>, 10 nm, 0.1% vol. concentration.

Vol. Concentration	Sample	Thermal Conductivity	Z <sub>o</sub>
0.1%	0	0.2885	0.22
	1	0.2813	0.34
	2	0.3308	0.47
	3	0.3368	0.57
	4	0.2861	0.26
	5	0.2874	0.24

Outliers ( $Z \geq 2.13$ ): 0

N = 5

$$\bar{x} = 0.3018$$

$$S_x = 0.0250$$

$$x_i = 0.3018 \pm 0.0611$$

**Table 25.** 75%EG-25% Water /Al<sub>2</sub>O<sub>3</sub>, 10 nm, 1% vol. concentration.

Vol. Concentration	Sample	Thermal Conductivity	Z <sub>o</sub>
1%	0	0.2843	0.09
	1	0.2845	0.11
	2	0.2749	0.75
	3	0.2884	0.46
	4	0.2853	0.18
	5	0.2823	0.09

Outliers ( $Z \geq 2.13$ ): 0

N = 5

$$\bar{x} = 0.2833$$

$$S_x = 0.0046$$

$$x_i = 0.2833 \pm 0.0112$$

**Table 26.** 75%EG-25% Water /Al<sub>2</sub>O<sub>3</sub>, 10 nm, 10% vol. concentration.

Vol. Concentration	Sample	Thermal Conductivity	Z <sub>o</sub>
10%	0	0.1918	0.27
	1	0.1922	0.26
	2	0.2233	0.62
	3	0.1855	0.45
	4	0.213	0.33
	5	0.2016	0.01

Outliers ( $Z \geq 2.13$ ): 0

N = 5

$$\bar{x} = 0.2012$$

$$S_x = 0.0145$$

$$x_i = 0.2012 \pm 0.0354$$

**Table 27.** 50%EG-50% Water /Al<sub>2</sub>O<sub>3</sub>, 10 nm, 0.1% vol. concentration.

Vol. Concentration	Sample	Thermal Conductivity	Z <sub>o</sub>
0.1%	0	0.3931	0.08
	1	0.3837	0.41
	2	0.3861	0.33
	3	0.4141	0.65
	4	0.4049	0.33
	5	0.3913	0.15

Outliers ( $Z \geq 2.13$ ): 0

N = 5

$$\bar{x} = 0.3955$$

$$S_x = 0.0117$$

$$x_i = 0.3955 \pm 0.0287$$

**Table 28.** 50%EG-50% Water /Al<sub>2</sub>O<sub>3</sub>, 10 nm, 1% vol. concentration.

Vol. Concentration	Sample	Thermal Conductivity	Z <sub>o</sub>
1%	0	0.3855	0.57
	1	0.3791	0.25
	2	0.3769	0.14
	3	0.3725	0.07
	4	0.3628	0.55
	5	0.3671	0.34

Outliers ( $Z \geq 2.13$ ): 0

N = 5

$$\bar{x} = 0.3740$$

$$S_x = 0.0202$$

$$x_i = 0.3740 \pm 0.0202$$

**Table 29.** 50%EG-50% Water /Al<sub>2</sub>O<sub>3</sub>, 10 nm, 10% vol. concentration.

Vol. Concentration	Sample	Thermal Conductivity	Z <sub>o</sub>
10%	0	0.3288	0.15
	1	0.3552	0.34
	2	0.3593	0.37
	3	0.2369	0.54
	4	0.2445	0.48
	5	0.3308	0.16

Outliers ( $Z \geq 2.13$ ): 0

N = 5

$$\bar{x} = 0.3093$$

$$S_x = 0.0546$$

$$x_i = 0.3093 \pm 0.134$$

**Table 30.** 25%EG-75% Water /Al<sub>2</sub>O<sub>3</sub>, 10 nm, 0.1% vol. concentration.

Vol. Concentration	Sample	Thermal Conductivity	Z <sub>o</sub>
0.1%	0	0.496	0.17
	1	0.4925	0.13
	2	0.4951	0.09
	3	0.4946	0.05
	4	0.4856	0.71
	5	0.5002	0.52

Outliers ( $Z \geq 2.13$ ): 0

$$N = 5$$

$$\bar{x} = 0.4940$$

$$S_x = 0.0048$$

$$x_i = 0.4940 \pm 0.0118$$

**Table 31.** 25%EG-75% Water /Al<sub>2</sub>O<sub>3</sub>, 10 nm, 1% vol. concentration.

Vol. Concentration	Sample	Thermal Conductivity	Z <sub>o</sub>
1%	0	0.4833	0.13
	1	0.4835	0.14
	2	0.4854	0.19
	3	0.4893	0.29
	4	0.481	0.07
	5	0.446	0.82

Outliers ( $Z \geq 2.13$ ): 0

$$N = 5$$

$$\bar{x} = 0.4781$$

$$S_x = 0.0160$$

$$x_i = 0.4781 \pm 0.0391$$

**Table 32.** 25%EG-75% Water /Al<sub>2</sub>O<sub>3</sub>, 10 nm, 10% vol. concentration.

Vol. Concentration	Sample	Thermal Conductivity	Z <sub>o</sub>
10%	0	0.5172	0.46
	1	0.5083	0.20
	2	0.5095	0.23
	3	0.4772	0.72
	4	0.4991	0.07
	5	0.4985	0.09

Outliers ( $Z \geq 2.13$ ): 0

$$N = 5$$

$$\bar{x} = 0.5016$$

$$S_x = 0.139$$

$$x_i = 0.5016 \pm 0.03394$$



## Appendix E: Volumetric concentration and particle size data

All thermal conductivity readings in W/mK

**Table 33.** SiO<sub>2</sub>/Water, 80 nm, 0.2% vol. concentration, thermophoresis and gravity in same directions.

Vol. Concentration	Sample	Thermal Conductivity	Z <sub>0</sub>
0.20%	0	0.6246	2.74
	1	0.6739	0.26
	2	0.6686	0.53
	3	0.6635	0.79
	4	0.6713	0.39
	5	0.6758	0.17
	6	0.6839	0.24
	7	0.6907	0.58
	8	0.7012	1.1
	9	0.6855	0.32
	10	0.6716	0.38
	11	0.6384	2.04
	12	0.6862	0.35
	13	0.6952	0.8
	14	0.6931	0.7
	15	0.6735	0.28
	16	0.7	1.04
	17	0.6973	0.91
	18	0.6928	0.68
	19	0.6813	0.11
	20	0.6944	0.76

Outliers ( $Z \geq 2.58$ ): 1 (sample # 0)

$$N = 19$$

$$\bar{x} = 0.6819$$

$$S_x = 0.0153$$

$$x_i = 0.6819 \pm 0.0320$$

**Table 34.** SiO<sub>2</sub>/Water, 80 nm, 0.5% vol. concentration, thermophoresis and gravity in same directions.

Vol. Concentration	Sample	Thermal Conductivity	Z <sub>0</sub>
0.50%	0	0.6964	0.11
	1	0.6842	0.84
	2	0.7043	0.37
	3	0.6738	1.47
	4	0.6667	1.9
	5	0.6647	2.02
	6	0.6743	1.44
	7	0.6986	0.03
	8	0.7034	0.32
	9	0.7013	0.19
	10	0.7145	0.99
	11	0.7046	0.39
	12	0.7111	0.78
	13	0.7096	0.69
	14	0.7141	0.96
	15	0.698	0.01
	16	0.7182	1.21
	17	0.7105	0.75
	18	0.7125	0.87
	19	0.703	0.29
	20	0.6975	0.04

Outliers ( $Z \geq 2.58$ ): 0

$$N = 20$$

$$\bar{x} = 0.6982$$

$$S_x = 0.0161$$

$$x_i = 0.6982 \pm 0.0336$$

**Table 35.** SiO<sub>2</sub>/Water, 80 nm, 0.7% vol. concentration, thermophoresis and gravity in same directions.

Vol. Concentration	Sample	Thermal Conductivity	Z <sub>o</sub>
0.70%	0	0.6818	0.13
	1	0.6948	1.19
	2	0.6862	0.49
	3	0.6951	1.22
	4	0.6874	0.58
	5	0.6882	0.65
	6	0.6965	1.33
	7	0.6909	0.87
	8	0.6873	0.58
	9	0.6909	0.87
	10	0.6844	0.34
	11	0.6799	0.03
	12	0.6738	0.53
	13	0.6785	0.14
	14	0.6798	0.04
	15	0.6671	1.08
	16	0.6617	1.52
	17	0.6725	0.64
	18	0.6487	2.58
	19	0.6725	0.64
	20	0.6675	1.05

Outliers ( $Z \geq 2.58$ ): 1 (sample 18)

$$N = 19$$

$$\bar{x} = 0.6818$$

$$S_x = 0.0101$$

$$x_i = 0.6818 \pm 0.0211$$

**Table 36.** SiO<sub>2</sub>/Water, 80 nm, 1% vol. concentration, thermophoresis and gravity in same directions.

Vol. Concentration	Sample	Thermal Conductivity	Z <sub>o</sub>
1%	0	0.6722	0.24
	1	0.6706	0.12
	2	0.6816	0.92
	3	0.6538	1.1
	4	0.6658	0.23
	5	0.6805	0.84
	6	0.6646	0.32
	7	0.6223	3.39
	8	0.6776	0.63
	9	0.6754	0.47
	10	0.6657	0.24
	11	0.6689	0
	12	0.6801	0.81
	13	0.6481	1.52
	14	0.6723	0.24
	15	0.6662	0.2
	16	0.68	0.8
	17	0.6797	0.78
	18	0.6775	0.62
	19	0.6738	0.35
	20	0.6713	0.17

Outliers ( $Z \geq 2.58$ ): 1 (sample # 7)

$$N = 19$$

$$\bar{x} = 0.6713$$

$$S_x = 0.0089$$

$$x_i = 0.6713 \pm 0.0186$$

**Table 37.** SiO<sub>2</sub>/Water, 80 nm, 2% vol. concentration, thermophoresis and gravity in same directions.

Vol. Concentration	Sample	Thermal Conductivity	Z <sub>o</sub>
2%	0	0.6784	0.77
	1	0.6844	1.02
	2	0.6831	0.97
	3	0.6948	1.44
	4	0.694	1.41
	5	0.6719	0.51
	6	0.688	1.17
	7	0.6714	0.49
	8	0.6272	1.33
	9	0.6602	0.03
	10	0.675	0.63
	11	0.6716	0.49
	12	0.6503	0.38
	13	0.6199	1.63
	14	0.629	1.25
	15	0.6419	0.72
	16	0.6274	1.32
	17	0.6283	1.28
	18	0.662	0.10
	19	0.6381	0.88
	20	0.6537	0.24

Outliers ( $Z \geq 2.58$ ): 0

N = 20

$\bar{x} = 0.6596$

$S_x = 0.0244$

$x_i = 0.6596 \pm 0.0510$

**Table 38.** SiO<sub>2</sub>/Water, 80 nm, 3% vol. concentration, thermophoresis and gravity in same directions.

Vol. Concentration	Sample	Thermal Conductivity	Z <sub>o</sub>
3%	0	0.677	2.26
	1	0.6789	2.38
	2	0.6352	0.29
	3	0.6234	1.00
	4	0.6462	0.38
	5	0.6383	0.10
	6	0.6383	0.10
	7	0.6274	0.76
	8	0.6165	1.43
	9	0.6397	0.01
	10	0.6289	0.67
	11	0.64	0.01
	12	0.6251	0.90
	13	0.6239	0.97
	14	0.6427	0.17
	15	0.6406	0.04
	16	0.642	0.13
	17	0.6191	1.27
	18	0.6524	0.76
	19	0.6514	0.70
	20	0.6509	0.67

Outliers ( $Z \geq 2.58$ ): 0

N = 20

$\bar{x} = 0.6399$

$S_x = 0.0164$

$x_i = 0.6399 \pm 0.0342$

**Table 39.** SiO<sub>2</sub>/Water, 15 nm, 0.2% vol. concentration, thermophoresis and gravity in same directions.

Vol. Concentration	Sample	Thermal Conductivity	Z <sub>o</sub>
0.2%	0	0.7339	1.06
	1	0.7285	1.72
	2	0.7357	0.84
	3	0.7388	0.45
	4	0.7476	0.63
	5	0.7259	2.04
	6	0.7305	1.48
	7	0.7459	0.42
	8	0.7472	0.58
	9	0.7537	1.38
	10	0.7554	1.59
	11	0.7508	1.03
	12	0.7445	0.25
	13	0.7418	0.08
	14	0.7443	0.22
	15	0.748	0.68
	16	0.7477	0.64
	17	0.7455	0.37
	18	0.744	0.19
	19	0.7403	0.27
	20	0.7421	0.05

Outliers ( $Z \geq 2.58$ ): 0

N = 20

$\bar{x} = 0.7425$

$S_x = 0.0079$

$x_i = 0.7425 \pm 0.0165$

**Table 40.** SiO<sub>2</sub>/Water, 15 nm, 0.5% vol. concentration, thermophoresis and gravity in same directions.

Vol. Concentration	Sample	Thermal Conductivity	Z <sub>o</sub>
0.5%	0	0.6908	1.33
	1	0.7013	0.84
	2	0.7283	0.40
	3	0.7335	0.65
	4	0.7336	0.65
	5	0.7329	0.62
	6	0.7394	0.92
	7	0.7294	0.46
	8	0.7248	0.24
	9	0.736	0.76
	10	0.7348	0.71
	11	0.7416	1.02
	12	0.7165	0.14
	13	0.6993	0.94
	14	0.7027	0.78
	15	0.6905	1.34
	16	0.7021	0.81
	17	0.6896	1.38
	18	0.7078	0.54
	19	0.7731	2.48
	20	0.7023	0.80

Outliers ( $Z \geq 2.58$ ): 0

N = 20

$\bar{x} = 0.7195$

$S_x = 0.0216$

$x_i = 0.7195 \pm 0.0451$

**Table 41.** SiO<sub>2</sub>/Water, 15 nm, 0.7% vol. concentration, thermophoresis and gravity in same directions.

Vol. Concentration	Sample	Thermal Conductivity	Z <sub>0</sub>
0.7%	0	0.7506	0.73
	1	0.7251	1.84
	2	0.7486	0.53
	3	0.7499	0.66
	4	0.7425	0.08
	5	0.7568	1.36
	6	0.7537	1.05
	7	0.7413	0.20
	8	0.7574	1.42
	9	0.7431	0.02
	10	0.7494	0.61
	11	0.7482	0.49
	12	0.7553	1.21
	13	0.7315	1.19
	14	0.7502	0.69
	15	0.7335	0.99
	16	0.7316	1.18
	17	0.7363	0.71
	18	0.7356	0.78
	19	0.7265	1.70
	20	0.7427	0.06

Outliers ( $Z \geq 2.58$ ): 0

N = 20

$\bar{x} = 0.7433$

$S_x = 0.0099$

$x_i = 0.7433 \pm 0.0207$

**Table 42.** SiO<sub>2</sub>/Water, 15 nm, 1% vol. concentration, thermophoresis and gravity in same directions.

Vol. Concentration	Sample	Thermal Conductivity	Z <sub>0</sub>
1%	0	0.6732	4.16
	1	0.7257	0.33
	2	0.725	0.39
	3	0.7262	0.30
	4	0.7301	0.01
	5	0.7289	0.10
	6	0.7295	0.06
	7	0.7387	0.61
	8	0.737	0.49
	9	0.733	0.20
	10	0.7362	0.43
	11	0.7376	0.53
	12	0.7359	0.41
	13	0.7334	0.23
	14	0.7344	0.30
	15	0.7366	0.46
	16	0.7352	0.36
	17	0.7321	0.13
	18	0.735	0.34
	19	0.7341	0.28
	20	0.7383	0.58

Outliers ( $Z \geq 2.58$ ): 1 (sample # 0)

N = 19

$\bar{x} = 0.7331$

$S_x = 0.0042$

$x_i = 0.7331 \pm 0.0089$

**Table 43.** SiO<sub>2</sub>/Water, 15 nm, 2% vol. concentration, thermophoresis and gravity in same directions.

Vol. Concentration	Sample	Thermal Conductivity	Z <sub>o</sub>
2%	0	0.7253	2.07
	1	0.7347	0.91
	2	0.751	1.10
	3	0.7513	1.13
	4	0.7511	1.11
	5	0.7531	1.35
	6	0.7527	1.31
	7	0.7471	0.62
	8	0.7386	0.43
	9	0.7455	0.42
	10	0.743	0.11
	11	0.7458	0.46
	12	0.7315	1.31
	13	0.7348	0.90
	14	0.7318	1.27
	15	0.7449	0.34
	16	0.7381	0.49
	17	0.7362	0.73
	18	0.7398	0.28
	19	0.7509	1.08
	20	0.7369	0.64

Outliers ( $Z \geq 2.58$ ): 0

N = 20

$\bar{x} = 0.7421$

$S_x = 0.0081$

$x_i = 0.7421 \pm 0.0169$

**Table 44.** SiO<sub>2</sub>/Water, 15 nm, 3% vol. concentration, thermophoresis and gravity in same directions.

Vol. Concentration	Sample	Thermal Conductivity	Z <sub>o</sub>
3%	0	0.7639	1.03
	1	0.7721	1.65
	2	0.7636	1.00
	3	0.7494	0.08
	4	0.745	0.41
	5	0.767	1.26
	6	0.7669	1.25
	7	0.7595	0.69
	8	0.7436	0.52
	9	0.74	0.79
	10	0.7352	1.15
	11	0.7575	0.54
	12	0.7357	1.12
	13	0.7278	1.72
	14	0.7516	0.09
	15	0.7633	0.98
	16	0.7333	1.30
	17	0.7552	0.37
	18	0.7342	1.23
	19	0.7512	0.06
	20	0.7423	0.62

Outliers ( $Z \geq 2.58$ ): 0

N = 20

$\bar{x} = 0.7504$

$S_x = 0.0132$

$x_i = 0.7504 \pm 0.0274$

**Table 45.** Al<sub>2</sub>O<sub>3</sub>/Water, 150 nm, 0.2% vol. concentration, thermophoresis and gravity in same directions.

Vol. Concentration	Sample	Thermal Conductivity	Z <sub>0</sub>
0.2%	0	0.6495	1.75
	1	0.693	0.59
	2	0.6459	1.94
	3	0.653	1.56
	4	0.6835	0.08
	5	0.6639	0.98
	6	0.6669	0.82
	7	0.7044	1.20
	8	0.6796	0.13
	9	0.6983	0.87
	10	0.7025	1.10
	11	0.7029	1.12
	12	0.6825	0.02
	13	0.7041	1.18
	14	0.6748	0.39
	15	0.6643	0.96
	16	0.6839	0.10
	17	0.6904	0.45
	18	0.6993	0.92
	19	0.6856	0.19
	20	0.6956	0.73

Outliers ( $Z \geq 2.58$ ): 0

N = 20

$$\bar{x} = 0.6821$$

$$S_x = 0.0186$$

$$x_i = 0.6821 \pm 0.0388$$

**Table 46.** Al<sub>2</sub>O<sub>3</sub>/Water, 150 nm, 0.5% vol. concentration, thermophoresis and gravity in same directions.

Vol. Concentration	Sample	Thermal Conductivity	Z <sub>0</sub>
0.5%	0	0.6631	0.63
	1	0.6518	1.31
	2	0.6797	0.36
	3	0.6667	0.42
	4	0.6826	0.54
	5	0.6441	1.77
	6	0.6631	0.63
	7	0.6314	2.53
	8	0.6524	1.27
	9	0.6776	0.24
	10	0.6813	0.46
	11	0.6919	1.09
	12	0.6881	0.87
	13	0.6832	0.57
	14	0.6868	0.79
	15	0.6797	0.36
	16	0.6856	0.72
	17	0.6912	1.05
	18	0.6832	0.57
	19	0.6791	0.33
	20	0.684	0.62

Outliers ( $Z \geq 2.58$ ): 0

N = 20

$$\bar{x} = 0.6736$$

$$S_x = 0.0167$$

$$x_i = 0.6736 \pm 0.0348$$

**Table 47.** Al<sub>2</sub>O<sub>3</sub>/Water, 150 nm, 0.7% vol. concentration, thermophoresis and gravity in same directions.

Vol. Concentration	Sample	Thermal Conductivity	Z <sub>0</sub>
0.7%	0	0.6732	0.85
	1	0.6861	1.13
	2	0.6778	0.15
	3	0.6899	1.71
	4	0.684	0.81
	5	0.6816	0.44
	6	0.6768	0.30
	7	0.6908	1.85
	8	0.6852	0.99
	9	0.6792	0.07
	10	0.6769	0.28
	11	0.6755	0.50
	12	0.6726	0.94
	13	0.6776	0.18
	14	0.6788	0.01
	15	0.6652	2.08
	16	0.6826	0.59
	17	0.6777	0.16
	18	0.6699	1.36
	19	0.6819	0.48
	20	0.6704	1.28

Outliers ( $Z \geq 2.58$ ): 0

N = 20

$$\bar{x} = 0.6787$$

$$S_x = 0.0065$$

$$x_i = 0.6787 \pm 0.0136$$

**Table 48.** Al<sub>2</sub>O<sub>3</sub>/Water, 150 nm, 1% vol. concentration, thermophoresis and gravity in same directions.

Vol. Concentration	Sample	Thermal Conductivity	Z <sub>0</sub>
1%	0	0.6641	0.38
	1	0.6641	0.38
	2	0.6621	0.35
	3	0.6747	0.52
	4	0.6407	0.07
	5	0.6528	0.23
	6	0.6675	0.42
	7	0.6658	0.40
	8	0.6623	0.35
	9	0.6571	0.29
	10	0.6305	0.06
	11	0.637	0.02
	12	0.3053	4.30
	13	0.6532	0.24
	14	0.6468	0.15
	15	0.6423	0.09
	16	0.6611	0.34
	17	0.6379	0.04
	18	0.6466	0.15
	19	0.6323	0.04
	20	0.6327	0.03

Outliers ( $Z \geq 2.58$ ): 1 (sample # 12)

N = 19

$$\bar{x} = 0.6516$$

$$S_x = 0.0135$$

$$x_i = 0.6516 \pm 0.0283$$



**Table 49.** Al<sub>2</sub>O<sub>3</sub>/Water, 150 nm, 2% vol. concentration, thermophoresis and gravity in same directions.

Vol. Concentration	Sample	Thermal Conductivity	Z <sub>0</sub>
2%	0	0.7638	1.97
	1	0.7176	0.97
	2	0.7227	1.08
	3	0.7293	1.22
	4	0.7246	1.12
	5	0.7187	0.99
	6	0.7102	0.80
	7	0.6802	0.15
	8	0.6543	0.41
	9	0.6466	0.58
	10	0.6431	0.66
	11	0.6332	0.88
	12	0.585	1.93
	13	0.6108	1.36
	14	0.6311	0.92
	15	0.6363	0.81
	16	0.6541	0.42
	17	0.6488	0.53
	18	0.6545	0.41
	19	0.683	0.21
	20	0.6917	0.40

Outliers ( $Z \geq 2.58$ ): 0

N = 20

$$\bar{x} = 0.6733$$

$$S_x = 0.0458$$

$$x_i = 0.6733 \pm 0.0956$$

**Table 50.** Al<sub>2</sub>O<sub>3</sub>/Water, 150 nm, 3% vol. concentration, thermophoresis and gravity in same directions.

Vol. Concentration	Sample	Thermal Conductivity	Z <sub>0</sub>
3%	0	0.7609	1.31
	1	0.7275	0.26
	2	0.7338	0.46
	3	0.7116	0.24
	4	0.7616	1.33
	5	0.6676	1.63
	6	0.6514	2.15
	7	0.6873	1.01
	8	0.6763	1.36
	9	0.6879	0.99
	10	0.7079	0.36
	11	0.6959	0.74
	12	0.7274	0.25
	13	0.738	0.59
	14	0.719	0.01
	15	0.7573	1.20
	16	0.7384	0.60
	17	0.7271	0.24
	18	0.759	1.25
	19	0.7327	0.42
	20	0.7379	0.59

Outliers ( $Z \geq 2.58$ ): 0

N = 20

$$\bar{x} = 0.7194$$

$$S_x = 0.0317$$

$$x_i = 0.7194 \pm 0.0317$$

**Table 51.** Al<sub>2</sub>O<sub>3</sub>/Water, 10 nm, 0.2% vol. concentration, thermophoresis and gravity in same directions.

Vol. Concentration	Sample	Thermal Conductivity	Z <sub>0</sub>
0.2%	0	0.7077	2.99
	1	0.7593	0.63
	2	0.7534	0.22
	3	0.7478	0.18
	4	0.724	1.85
	5	0.7509	0.04
	6	0.7398	0.74
	7	0.756	0.40
	8	0.7588	0.60
	9	0.7434	0.49
	10	0.7448	0.39
	11	0.7531	0.20
	12	0.7397	0.75
	13	0.7676	1.22
	14	0.7629	0.89
	15	0.7457	0.32
	16	0.7661	1.11
	17	0.7592	0.63
	18	0.7567	0.45
	19	0.7612	0.77
	20	0.7582	0.56

Outliers ( $Z \geq 2.58$ ): 1 ( sample # 0)

$$N = 19$$

$$\bar{x} = 0.7524$$

$$S_x = 0.0106$$

$$x_i = 0.7524 \pm 0.0222$$

**Table 52.** Al<sub>2</sub>O<sub>3</sub>/Water, 10 nm, 0.5% vol. concentration, thermophoresis and gravity in same directions.

Vol. Concentration	Sample	Thermal Conductivity	Z <sub>0</sub>
0.5%	0	0.7351	1.64
	1	0.7305	2.26
	2	0.7413	0.81
	3	0.7384	1.20
	4	0.7486	0.17
	5	0.7425	0.65
	6	0.7458	0.21
	7	0.7495	0.29
	8	0.7535	0.82
	9	0.7519	0.61
	10	0.7545	0.96
	11	0.7419	0.73
	12	0.7503	0.39
	13	0.75	0.35
	14	0.7392	1.09
	15	0.7586	1.50
	16	0.7527	0.71
	17	0.7472	0.02
	18	0.7563	1.20
	19	0.752	0.62
	20	0.7548	1.00

Outliers ( $Z \geq 2.58$ ): 0

$$N = 20$$

$$\bar{x} = 0.7474$$

$$S_x = 0.0075$$

$$x_i = 0.7474 \pm 0.0156$$

**Table 53.** Al<sub>2</sub>O<sub>3</sub>/Water, 10 nm, 0.7% vol. concentration, thermophoresis and gravity in same directions.

Vol. Concentration	Sample	Thermal Conductivity	Z <sub>0</sub>
0.7%	0	0.7484	0.45
	1	0.7343	1.46
	2	0.7473	0.31
	3	0.7424	0.36
	4	0.7419	0.43
	5	0.7303	2.00
	6	0.7311	1.89
	7	0.7533	1.12
	8	0.7336	1.55
	9	0.7427	0.32
	10	0.746	0.13
	11	0.7408	0.58
	12	0.7498	0.64
	13	0.7494	0.59
	14	0.7502	0.70
	15	0.7463	0.17
	16	0.7502	0.70
	17	0.7545	1.28
	18	0.7499	0.66
	19	0.7529	1.07
	20	0.7507	0.77

Outliers ( $Z \geq 2.58$ ): 0

N = 20

$$\bar{x} = 0.7450$$

$$S_x = 0.0074$$

$$x_i = 0.7450 \pm 0.0154$$

**Table 54.** Al<sub>2</sub>O<sub>3</sub>/Water, 10 nm, 1% vol. concentration, thermophoresis and gravity in same directions.

Vol. Concentration	Sample	Thermal Conductivity	Z <sub>0</sub>
1%	0	0.727	0.4
	1	0.7312	0.61
	2	0.7355	0.78
	3	0.7293	0.54
	4	0.7432	1.08
	5	0.73	0.56
	6	0.733	0.68
	7	0.7237	0.32
	8	0.6755	1.57
	9	0.6411	2.91
	10	0.6719	1.71
	11	0.6986	0.66
	12	0.7001	0.61
	13	0.7144	0.05
	14	0.7259	0.40
	15	0.7343	0.73
	16	0.7342	0.73
	17	0.7133	0.09
	18	0.7094	0.24
	19	0.7337	0.71
	20	0.7223	0.26

Outliers ( $Z \geq 2.58$ ): 1 (sample # 9)

N = 19

$$\bar{x} = 0.7193$$

$$S_x = 0.0196$$

$$x_i = 0.7193 \pm 0.0410$$

**Table 55.** Al<sub>2</sub>O<sub>3</sub>/Water, 10 nm, 2% vol. concentration, thermophoresis and gravity in same directions.

Vol. Concentration	Sample	Thermal Conductivity	Z <sub>0</sub>
2%	0	0.7428	1.33
	1	0.7414	1.19
	2	0.7429	1.34
	3	0.7398	1.03
	4	0.7376	0.81
	5	0.7309	0.15
	6	0.726	0.33
	7	0.7327	0.33
	8	0.7387	0.92
	9	0.7341	0.47
	10	0.734	0.46
	11	0.7297	0.04
	12	0.7357	0.63
	13	0.7145	1.46
	14	0.7157	1.34
	15	0.7143	1.48
	16	0.7203	0.89
	17	0.7219	0.73
	18	0.7293	0.00
	19	0.7101	1.90
	20	0.7237	0.56

Outliers ( $Z \geq 2.58$ ): 0

N = 20

$$\bar{x} = 0.6736$$

$$S_x = 0.0167$$

$$x_i = 0.6736 \pm 0.0348$$

**Table 56.** Al<sub>2</sub>O<sub>3</sub>/Water, 10 nm, 3% vol. concentration, thermophoresis and gravity in same directions.

Vol. Concentration	Sample	Thermal Conductivity	Z <sub>0</sub>
3%	0	0.792	3.35
	1	0.7658	1.40
	2	0.7576	0.80
	3	0.75	0.23
	4	0.747	0.01
	5	0.744	0.21
	6	0.7449	0.15
	7	0.7415	0.40
	8	0.7262	1.53
	9	0.7438	0.23
	10	0.7481	0.09
	11	0.748	0.08
	12	0.7462	0.05
	13	0.7513	0.33
	14	0.7471	0.02
	15	0.7414	0.41
	16	0.7438	0.23
	17	0.7449	0.15
	18	0.737	0.73
	19	0.7351	0.87
	20	0.7287	1.35

Outliers ( $Z \geq 2.58$ ): 0

N = 20

$$\bar{x} = 0.6787$$

$$S_x = 0.0065$$

$$x_i = 0.6787 \pm 0.0136$$

**Table 57.** SiO<sub>2</sub>/Water, 15 nm, 0.2% vol. concentration, thermophoresis and gravity in opposite directions.

Vol. Concentration	Sample	Thermal Conductivity	Z <sub>0</sub>
0.2%	0	0.6287	2.88
	1	0.6392	1.26
	2	0.645	0.36
	3	0.6397	1.18
	4	0.6384	1.38
	5	0.6471	0.04
	6	0.6487	0.21
	7	0.6503	0.46
	8	0.6487	0.21
	9	0.6471	0.04
	10	0.6473	0.01
	11	0.6449	0.38
	12	0.6507	0.52
	13	0.654	1.03
	14	0.6534	0.93
	15	0.648	0.10
	16	0.6568	1.46
	17	0.6503	0.46
	18	0.6506	0.50
	19	0.6543	1.07
	20	0.651	0.56

Outliers ( $Z \geq 2.58$ ): 1 (sample # 0)

N = 19

$$\bar{x} = 0.6483$$

$$S_x = 0.0050$$

$$x_i = 0.6483 \pm 0.0105$$

**Table 58.** SiO<sub>2</sub>/Water, 15 nm, 0.5% vol. concentration, thermophoresis and gravity in opposite directions.

Vol. Concentration	Sample	Thermal Conductivity	Z <sub>0</sub>
0.5%	0	0.6096	3.31
	1	0.6257	0.54
	2	0.6364	1.30
	3	0.631	0.37
	4	0.6283	0.09
	5	0.6316	0.47
	6	0.6317	0.49
	7	0.6213	1.30
	8	0.6303	0.25
	9	0.6338	0.85
	10	0.6314	0.44
	11	0.629	0.03
	12	0.6308	0.34
	13	0.6297	0.15
	14	0.6339	0.87
	15	0.6236	0.90
	16	0.629	0.03
	17	0.6321	0.56
	18	0.6334	0.78
	19	0.6228	1.04
	20	0.6303	0.25

Outliers ( $Z \geq 2.58$ ): 1 (sample # 0)

N = 19

$$\bar{x} = 0.6298$$

$$S_x = 0.0039$$

$$x_i = 0.6298 \pm 0.0081$$

**Table 59.** SiO<sub>2</sub>/Water, 15 nm, 0.7% vol. concentration, thermophoresis and gravity in opposite directions.

Vol. Concentration	Sample	Thermal Conductivity	Z <sub>0</sub>
0.7%	0	0.6136	1.30
	1	0.6106	1.68
	2	0.6155	1.07
	3	0.619	0.63
	4	0.6218	0.28
	5	0.6213	0.34
	6	0.6283	0.53
	7	0.622	0.25
	8	0.6354	1.42
	9	0.6302	0.77
	10	0.627	0.37
	11	0.6173	0.84
	12	0.6205	0.44
	13	0.6146	1.18
	14	0.6309	0.86
	15	0.6261	0.26
	16	0.6291	0.63
	17	0.6244	0.05
	18	0.624	0.00
	19	0.6281	0.51
	20	0.6451	2.63

Outliers ( $Z \geq 2.58$ ): 1 (sample # 20)

$$N = 19$$

$$\bar{x} = 0.6230$$

$$S_x = 0.0066$$

$$x_i = 0.6230 \pm 0.0137$$

**Table 60.** SiO<sub>2</sub>/Water, 15 nm, 1% vol. concentration, thermophoresis and gravity in opposite directions.

Vol. Concentration	Sample	Thermal Conductivity	Z <sub>0</sub>
1%	0	0.6342	0.2
	1	0.6423	1.24
	2	0.6299	0.36
	3	0.6357	0.39
	4	0.6339	0.16
	5	0.6287	0.51
	6	0.6278	0.63
	7	0.6266	0.78
	8	0.6317	0.12
	9	0.6353	0.34
	10	0.6229	1.26
	11	0.6373	0.60
	12	0.6309	0.23
	13	0.6329	0.03
	14	0.6078	3.20
	15	0.6317	0.12
	16	0.6385	0.75
	17	0.6377	0.65
	18	0.6416	1.15
	19	0.6439	1.45
	20	0.6349	0.29

Outliers ( $Z \geq 2.58$ ): 1 (sample # 14)

$$N = 19$$

$$\bar{x} = 0.6339$$

$$S_x = 0.0054$$

$$x_i = 0.6339 \pm 0.0113$$

**Table 61.** SiO<sub>2</sub>/Water, 15 nm, 2% vol. concentration, thermophoresis and gravity in opposite directions.

Vol. Concentration	Sample	Thermal Conductivity	Z <sub>0</sub>
2%	0	0.6153	1.70
	1	0.6102	1.31
	2	0.6142	1.61
	3	0.6106	1.34
	4	0.5933	0.03
	5	0.6015	0.65
	6	0.5997	0.51
	7	0.5939	0.07
	8	0.594	0.08
	9	0.5853	0.58
	10	0.587	0.45
	11	0.5946	0.13
	12	0.5917	0.09
	13	0.5959	0.22
	14	0.5761	1.28
	15	0.5884	0.34
	16	0.5876	0.41
	17	0.583	0.75
	18	0.5879	0.38
	19	0.5598	2.51
	20	0.5816	0.86

Outliers ( $Z \geq 2.58$ ): 0

N = 20

$$\bar{x} = 0.5929$$

$$S_x = 0.0132$$

$$x_i = 0.5929 \pm 0.0275$$

**Table 62.** SiO<sub>2</sub>/Water, 15 nm, 3% vol. concentration, thermophoresis and gravity in opposite directions.

Vol. Concentration	Sample	Thermal Conductivity	Z <sub>0</sub>
3%	0	0.6325	2.09
	1	0.6144	1.13
	2	0.6251	1.69
	3	0.5952	0.11
	4	0.6052	0.64
	5	0.5929	0.02
	6	0.6159	1.21
	7	0.5869	0.33
	8	0.6026	0.50
	9	0.574	1.02
	10	0.5759	0.92
	11	0.5959	0.14
	12	0.5622	1.65
	13	0.563	1.60
	14	0.5988	0.30
	15	0.5998	0.35
	16	0.5792	0.74
	17	0.5898	0.18
	18	0.5735	1.05
	19	0.5866	0.35
	20	0.5876	0.30

Outliers ( $Z \geq 2.58$ ): 0

N = 20

$$\bar{x} = 0.5932$$

$$S_x = 0.0188$$

$$x_i = 0.5932 \pm 0.0393$$

**Table 63.** Al<sub>2</sub>O<sub>3</sub>/Water, 150 nm, 0.2% vol. concentration, thermophoresis and gravity in opposite directions.

Vol. Concentration	Sample	Thermal Conductivity	Z <sub>0</sub>
0.2%	0	0.5928	1.99
	1	0.5994	1.30
	2	0.6111	0.08
	3	0.6068	0.53
	4	0.5861	2.68
	5	0.6159	0.42
	6	0.6164	0.47
	7	0.6103	0.16
	8	0.6153	0.36
	9	0.6171	0.54
	10	0.6108	0.11
	11	0.6105	0.14
	12	0.6175	0.59
	13	0.6145	0.27
	14	0.6178	0.62
	15	0.6099	0.21
	16	0.621	0.95
	17	0.615	0.33
	18	0.6221	1.07
	19	0.6285	1.73
	20	0.6105	0.14

Outliers ( $Z \geq 2.58$ ): 1 (sample # 4)

N = 19

$$\bar{x} = 0.6132$$

$$S_x = 0.0078$$

$$x_i = 0.6132 \pm 0.0163$$

**Table 64.** Al<sub>2</sub>O<sub>3</sub>/Water, 150 nm, 0.5% vol. concentration, thermophoresis and gravity in opposite directions.

Vol. Concentration	Sample	Thermal Conductivity	Z <sub>0</sub>
0.5%	0	0.5735	0.97
	1	0.5709	1.20
	2	0.594	0.83
	3	0.5614	2.03
	4	0.5816	0.26
	5	0.5952	0.94
	6	0.5871	0.23
	7	0.5929	0.74
	8	0.5857	0.10
	9	0.6012	1.47
	10	0.6009	1.44
	11	0.5736	0.96
	12	0.5731	1.00
	13	0.5735	0.97
	14	0.5893	0.42
	15	0.5929	0.74
	16	0.5712	1.17
	17	0.5841	0.04
	18	0.5965	1.05
	19	0.5812	0.29
	20	0.595	0.92

Outliers ( $Z \geq 2.58$ ): 0

N = 20

$$\bar{x} = 0.5845$$

$$S_x = 0.0114$$

$$x_i = 0.5845 \pm 0.0237$$



**Table 65.** Al<sub>2</sub>O<sub>3</sub>/Water, 150 nm, 0.7% vol. concentration, thermophoresis and gravity in opposite directions.

Vol. Concentration	Sample	Thermal Conductivity	Z <sub>0</sub>
0.7%	0	0.5586	0.8
	1	0.5561	1.01
	2	0.5553	1.07
	3	0.5736	0.30
	4	0.5675	0.16
	5	0.5764	0.51
	6	0.583	1.01
	7	0.5742	0.35
	8	0.5743	0.36
	9	0.5684	0.09
	10	0.572	0.18
	11	0.5498	1.49
	12	0.5564	0.99
	13	0.5492	1.53
	14	0.548	1.62
	15	0.58	0.79
	16	0.586	1.24
	17	0.5713	0.13
	18	0.5894	1.49
	19	0.5832	1.03
	20	0.5875	1.35

Outliers ( $Z \geq 2.58$ ): 0

N = 20

$\bar{x} = 0.5696$

$S_x = 0.0133$

$x_i = 0.5696 \pm 0.0277$

**Table 66.** Al<sub>2</sub>O<sub>3</sub>/Water, 150 nm, 1% vol. concentration, thermophoresis and gravity in opposite directions.

Vol. Concentration	Sample	Thermal Conductivity	Z <sub>0</sub>
1%	0	0.3126	1.1
	1	0.3165	1.02
	2	0.3138	1.04
	3	0.5212	0.92
	4	0.3117	1.06
	5	0.5272	0.98
	6	0.5206	0.92
	7	0.3246	0.94
	8	0.5167	0.88
	9	0.5249	0.96
	10	0.3145	1.04
	11	0.3239	0.95
	12	0.3107	1.07
	13	0.3156	1.03
	14	0.515	0.9
	15	0.5223	0.93
	16	0.5247	0.96
	17	0.5155	0.87
	18	0.5274	0.98
	19	0.3163	1.02
	20	0.5263	0.97

Outliers ( $Z \geq 2.58$ ):0

N = 20

$\bar{x} = 0.4239$

$S_x = 0.1055$

$x_i = 0.4239 \pm 0.2201$

**Table 67.** Al<sub>2</sub>O<sub>3</sub>/Water, 150 nm, 2% vol. concentration, thermophoresis and gravity in opposite directions.

Vol. Concentration	Sample	Thermal Conductivity	Z <sub>0</sub>
2%	0	0.3436	0.95
	1	0.3588	0.83
	2	0.5563	0.78
	3	0.5525	0.75
	4	0.5036	0.35
	5	0.3625	0.80
	6	0.3277	1.08
	7	0.3315	1.05
	8	0.3293	1.07
	9	0.3422	0.97
	10	0.5234	0.51
	11	0.3463	0.93
	12	0.3508	0.90
	13	0.5557	0.77
	14	0.7353	2.24
	15	0.3369	1.01
	16	0.5675	0.87
	17	0.5673	0.87
	18	0.5721	0.91
	19	0.5431	0.67
	20	0.5703	0.89

Outliers ( $Z \geq 2.58$ ): 0

N = 20

$\bar{x} = 0.4608$

$S_x = 0.1228$

$x_i = 0.4608 \pm 0.2562$

**Table 68.** Al<sub>2</sub>O<sub>3</sub>/Water, 150 nm, 3% vol. concentration, thermophoresis and gravity in opposite directions.

Vol. Concentration	Sample	Thermal Conductivity	Z <sub>0</sub>
3%	0	0.3277	0.57
	1	0.3465	0.22
	2	0.4771	2.27
	3	0.3475	0.20
	4	0.3659	0.15
	5	0.4791	2.31
	6	0.3631	0.10
	7	0.3224	0.68
	8	0.4433	1.62
	9	0.3212	0.70
	10	0.4288	1.35
	11	0.3475	0.20
	12	0.3216	0.69
	13	0.3478	0.19
	14	0.3317	0.50
	15	0.3146	0.82
	16	0.3157	0.80
	17	0.3545	0.06
	18	0.3228	0.67
	19	0.3171	0.78
	20	0.3199	0.72

Outliers ( $Z \geq 2.58$ ): 0

N = 20

$\bar{x} = 0.3579$

$S_x = 0.0526$

$x_i = 0.3579 \pm 0.1097$

**Table 69.** Al<sub>2</sub>O<sub>3</sub>/Water, 10 nm, 0.2% vol. concentration, thermophoresis and gravity in opposite directions.

Vol. Concentration	Sample	Thermal Conductivity	Z <sub>0</sub>
0.20%	0	0.6075	1.82
	1	0.6056	2.02
	2	0.6147	1.07
	3	0.6233	0.18
	4	0.6214	0.38
	5	0.6219	0.32
	6	0.6264	0.15
	7	0.6292	0.44
	8	0.6255	0.05
	9	0.6316	0.69
	10	0.6313	0.66
	11	0.6308	0.60
	12	0.6388	1.44
	13	0.6339	0.93
	14	0.6332	0.85

Outliers ( $Z \geq 2.45$ ): 0

N = 14

$\bar{x} = 0.6250$

$S_x = 0.0096$

$x_i = 0.6250 \pm 0.0206$

**Table 70.** Al<sub>2</sub>O<sub>3</sub>/Water, 10 nm, 0.5% vol. concentration, thermophoresis and gravity in opposite directions.

Vol. Concentration	Sample	Thermal Conductivity	Z <sub>0</sub>
0.50%	0	0.6065	1.39
	1	0.6053	1.54
	2	0.6093	1.05
	3	0.609	1.08
	4	0.6106	0.88
	5	0.619	0.16
	6	0.619	0.16
	7	0.619	0.16
	8	0.6257	1.00
	9	0.6188	0.14
	10	0.6238	0.76
	11	0.6274	1.21
	12	0.6314	1.71
	13	0.6224	0.59
	14	0.6217	0.50

Outliers ( $Z \geq 2.45$ ): 0

N = 14

$\bar{x} = 0.6177$

$S_x = 0.0080$

$x_i = 0.6177 \pm 0.0172$

**Table 71.** Al<sub>2</sub>O<sub>3</sub>/Water, 10 nm, 0.7% vol. concentration, thermophoresis and gravity in opposite directions.

Vol. Concentration	Sample	Thermal Conductivity	Z <sub>o</sub>
0.70%	0	0.598	0.16
	1	0.5858	1.14
	2	0.5802	1.59
	3	0.5815	1.49
	4	0.6007	0.05
	5	0.6093	0.74
	6	0.6084	0.67
	7	0.6019	0.15
	8	0.6127	1.02
	9	0.606	0.48
	10	0.6159	1.27

Outliers ( $Z \geq 2.33$ ): 0

N = 10

$\bar{x} = 0.6001$

$S_x = 0.0124$

$x_i = 0.6001 \pm 0.0277$

**Table 72.** Al<sub>2</sub>O<sub>3</sub>/Water, 10 nm, 1% vol. concentration, thermophoresis and gravity in opposite directions.

Vol. Concentration	Sample	Thermal Conductivity	Z <sub>o</sub>
1%	0	0.5924	1.30
	1	0.5903	1.60
	2	0.597	0.63
	3	0.5986	0.40
	4	0.5958	0.81
	5	0.6033	0.27
	6	0.6065	0.73
	7	0.6058	0.63
	8	0.6106	1.32
	9	0.6069	0.79
	10	0.6089	1.08

Outliers ( $Z \geq 2.33$ ):0

N = 10

$\bar{x} = 0.6014$

$S_x = 0.0069$

$x_i = 0.6014 \pm 0.0155$

**Table 73.** Al<sub>2</sub>O<sub>3</sub>/Water, 10 nm, 2% vol. concentration, thermophoresis and gravity in opposite directions.

Vol. Concentration	Sample	Thermal Conductivity	Z <sub>0</sub>
2%	0	0.5934	1.27
	1	0.5891	0.95
	2	0.5645	0.86
	3	0.5937	1.29
	4	0.5674	0.65
	5	0.5718	0.32
	6	0.5858	0.71
	7	0.5645	0.86
	8	0.5649	0.83
	9	0.5864	0.75
	10	0.5567	1.44

Outliers ( $Z \geq 2.33$ ): 0

N = 10

$\bar{x} = 0.5762$

$S_x = 0.0136$

$x_i = 0.5762 \pm 0.0302$

**Table 74.** Al<sub>2</sub>O<sub>3</sub>/Water, 10 nm, 3% vol. concentration, thermophoresis and gravity in opposite directions.

Vol. Concentration	Sample	Thermal Conductivity	Z <sub>0</sub>
3%	0	0.5703	1.40
	1	0.5928	0.64
	2	0.5902	0.41
	3	0.5767	0.82
	4	0.5933	0.69
	5	0.5885	0.25
	6	0.5646	1.92
	7	0.5968	1.01
	8	0.5923	0.60
	9	0.5812	0.41
	10	0.5969	1.02

Outliers ( $Z \geq 2.33$ ): 0

N = 10

$\bar{x} = 0.5857$

$S_x = 0.0110$

$x_i = 0.5857 \pm 0.0245$

**Table 75.** SiO<sub>2</sub>/Water, 80 nm, 0.2% vol. concentration, thermophoresis and gravity in opposite directions.

Vol. Concentration	Sample	Thermal Conductivity	Z <sub>0</sub>
0.2%	0	0.6289	2.91
	1	0.6519	0.97
	2	0.65	1.13
	3	0.6547	0.74
	4	0.6497	1.16
	5	0.6537	0.82
	6	0.6518	0.98
	7	0.6603	0.27
	8	0.6592	0.36
	9	0.6588	0.39
	10	0.6506	1.08
	11	0.6482	1.28
	12	0.6563	0.60
	13	0.6504	1.10
	14	0.6559	0.64
	15	0.6637	0.02
	16	0.6653	0.15
	17	0.6607	0.23
	18	0.6633	0.01
	19	0.6693	0.49
	20	0.6704	0.58

Outliers ( $Z \geq 2.58$ ): 1 (sample # 0)

N = 19

$$\bar{x} = 0.6572$$

$$S_x = 0.0067$$

$$x_i = 0.6572 \pm 0.0067$$

**Table 76.** SiO<sub>2</sub>/Water, 80 nm, 0.5% vol. concentration, thermophoresis and gravity in opposite directions.

Vol. Concentration	Sample	Thermal Conductivity	Z <sub>0</sub>
0.5%	0	0.6562	0.04
	1	0.6564	0.00
	2	0.6616	1.25
	3	0.6502	1.48
	4	0.654	0.57
	5	0.654	0.57
	6	0.6531	0.78
	7	0.651	1.28
	8	0.6555	0.21
	9	0.6568	0.10
	10	0.6594	0.72
	11	0.6672	2.58
	12	0.6477	2.07
	13	0.6585	0.51
	14	0.6599	0.84
	15	0.6558	0.14
	16	0.6566	0.05
	17	0.6569	0.12
	18	0.659	0.63
	19	0.6557	0.16
	20	0.659	0.63

Outliers ( $Z \geq 2.58$ ): 1 (sample # 11)

N = 19

$$\bar{x} = 0.6559$$

$$S_x = 0.0035$$

$$x_i = 0.6559 \pm 0.0073$$

**Table 77.** SiO<sub>2</sub>/Water, 80 nm, 0.7% vol. concentration, thermophoresis and gravity in opposite directions.

Vol. Concentration	Sample	Thermal Conductivity	Z <sub>0</sub>
0.7%	0	0.6656	1.09
	1	0.669	1.54
	2	0.6656	1.09
	3	0.662	0.61
	4	0.6611	0.49
	5	0.6652	1.04
	6	0.6616	0.55
	7	0.6634	0.80
	8	0.6582	0.10
	9	0.6613	0.51
	10	0.6562	0.17
	11	0.6588	0.18
	12	0.6583	0.11
	13	0.6704	1.73
	14	0.6484	1.21
	15	0.6596	0.29
	16	0.6573	0.02
	17	0.6497	1.04
	18	0.6495	1.06
	19	0.6424	2.01
	20	0.6484	1.21

Outliers ( $Z \geq 2.58$ ): 0

N = 20

$$\bar{x} = 0.6575$$

$$S_x = 0.0075$$

$$x_i = 0.6575 \pm 0.0156$$

**Table 78.** SiO<sub>2</sub>/Water, 80 nm, 1% vol. concentration, thermophoresis and gravity in opposite directions.

Vol. Concentration	Sample	Thermal Conductivity	Z <sub>0</sub>
1%	0	0.637	1
	1	0.6289	0.13
	2	0.632	0.47
	3	0.6376	1.08
	4	0.6354	0.84
	5	0.6282	0.06
	6	0.6346	0.75
	7	0.6282	0.06
	8	0.625	0.29
	9	0.6353	0.8
	10	0.626	0.18
	11	0.6279	0.02
	12	0.6238	0.42
	13	0.632	0.47
	14	0.6277	0.00
	15	0.5938	3.68
	16	0.6314	0.40
	17	0.6214	0.68
	18	0.632	0.47
	19	0.6233	0.48
	20	0.6338	0.67

Outliers ( $Z \geq 2.58$ ): 1 (sample # 15)

N = 19

$$\bar{x} = 0.6301$$

$$S_x = 0.0048$$

$$x_i = 0.6301 \pm 0.0099$$

**Table 79.** SiO<sub>2</sub>/Water, 80 nm, 2% vol. concentration, thermophoresis and gravity in opposite directions.

Vol. Concentration	Sample	Thermal Conductivity	Z <sub>0</sub>
2%	0	0.676	1.20
	1	0.6242	0.18
	2	0.4357	3.52
	3	0.6586	0.86
	4	0.657	0.83
	5	0.5382	1.51
	6	0.6204	0.11
	7	0.6292	0.28
	8	0.6153	0.01
	9	0.6046	0.20
	10	0.6199	0.10
	11	0.6228	0.16
	12	0.6324	0.34
	13	0.6432	0.56
	14	0.6549	0.79
	15	0.6266	0.23
	16	0.6393	0.48
	17	0.6123	0.05
	18	0.603	0.23
	19	0.6291	0.28
	20	0.5698	0.89

Outliers ( $Z \geq 2.58$ ): 1 (sample # 2)

N = 19

$$\bar{x} = 0.6238$$

$$S_x = 0.0308$$

$$x_i = 0.6238 \pm 0.0645$$

**Table 80.** SiO<sub>2</sub>/Water, 80 nm, 3% vol. concentration, thermophoresis and gravity in opposite directions.

Vol. Concentration	Sample	Thermal Conductivity	Z <sub>0</sub>
3%	0	0.6462	1.12
	1	0.6434	0.96
	2	0.6422	0.89
	3	0.6393	0.72
	4	0.6167	0.58
	5	0.6418	0.87
	6	0.6305	0.21
	7	0.6417	0.86
	8	0.6217	0.29
	9	0.6292	0.14
	10	0.645	1.05
	11	0.6324	0.32
	12	0.6411	0.83
	13	0.6148	0.69
	14	0.6415	0.85
	15	0.6177	0.53
	16	0.6174	0.54
	17	0.5882	2.23
	18	0.6124	0.83
	19	0.6059	1.21
	20	0.5934	1.93

Outliers ( $Z \geq 2.58$ ): 0

N = 20

$$\bar{x} = 0.6268$$

$$S_x = 0.0173$$

$$x_i = 0.6268 \pm 0.0361$$